

Later Life Consequences of Developmental Mitochondrial DNA Damage in *C. elegans*

by

John P. Rooney

Environment
Duke University

Date: _____

Approved:

Joel N. Meyer, Supervisor

William C. Copeland

Richard T. Di Giulio

David E. Hinton

Matthew D. Hirschey

Dissertation submitted in partial fulfillment of
the requirements for the degree of Doctor
of Philosophy in Environment
in the Graduate School
of Duke University

2015

ABSTRACT

Later Life Consequences of Developmental Mitochondrial DNA Damage in *C. elegans*

by

John P. Rooney

Environment
Duke University

Date: _____

Approved:

Joel N. Meyer, Supervisor

William C. Copeland

Richard T. Di Giulio

David E. Hinton

Matthew D. Hirschey

An abstract of a dissertation submitted in partial
fulfillment of the requirements for the degree
of Doctor of Philosophy in Environment
in the Graduate School of
Duke University

2015

Copyright by
John P. Rooney
2015

Abstract

Mitochondria are responsible for producing the vast majority of cellular ATP, and are therefore critical to organismal health [1]. They contain their own genomes (mtDNA) which encode 13 proteins that are all subunits of the mitochondrial respiratory chain (MRC) and are essential for oxidative phosphorylation [2]. mtDNA is present in multiple copies per cell, usually between 10^3 and 10^4 , though this number is reduced during certain developmental stages [3, 4]. The health of the mitochondrial genome is also important to the health of the organism, as mutations in mtDNA lead to human diseases that collectively affect approximately 1 in 4000 people [5, 6]. mtDNA is more susceptible than nuclear DNA (nucDNA) to damage by many environmental pollutants, for reasons including the absence of Nucleotide Excision Repair (NER) in the mitochondria [7]. NER is a highly functionally conserved DNA repair pathway that removes bulky, helix distorting lesions such as those caused by many environmental toxicants, including benzo[a]pyrene (BaP) and cyclobutane pyrimidine dimers caused by ultraviolet C (UVC) radiation [8]. While these lesions cannot be repaired, they are slowly removed through a process that involves mitochondrial dynamics and autophagy [9, 10]. However, when present during development in *C. elegans*, this damage reduces mtDNA copy number and ATP levels [11]. We hypothesize that this damage, when

present during development, will result in mitochondrial dysfunction and increase the potential for adverse outcomes later in life.

To test this hypothesis, 1st larval stage (L1) *C. elegans* are exposed to 3 doses of 7.5J/m² ultraviolet C radiation 24 hours apart, leading to the accumulation of mtDNA damage [9, 11]. After exposure, many mitochondrial endpoints are assessed at multiple time points later in life. mtDNA and nucDNA damage levels and genome copy numbers are measured via QPCR and real-time PCR, respectively, every 2 days for 10 days. Steady state ATP levels are measured via luciferase expressing reporter strains and traditional ATP extraction methods. Oxygen consumption is measured using a Seahorse XF^e24 extra cellular flux analyzer. Gene expression changes are measured via real time PCR and targeted metabolomics via LC-MS are used to investigate changes in organic acid, amino acid and acyl-carnitine levels. Lastly, nematode developmental delay is assessed as growth, and measured via imaging and COPAS biosort.

I have found that despite being removed, UVC induced mtDNA damage during development leads to persistent deficits in energy production later in life. mtDNA copy number is permanently reduced, as are ATP levels, though oxygen consumption is increased, indicating inefficient or uncoupled respiration. Metabolomic data and mutant sensitivity indicate a role for NADPH and oxidative stress in these results, and exposed nematodes are more sensitive to the mitochondrial poison rotenone later in life. These

results fit with the developmental origin of health and disease hypothesis, and show the potential for environmental exposures to have lasting effects on mitochondrial function.

Lastly, we are currently working to investigate the potential for irreparable mtDNA lesions to drive mutagenesis in mtDNA. Mutations in mtDNA lead to a wide range of diseases, yet we currently do not understand the environmental component of what causes them. *In vitro* evidence suggests that UVC induced thymine dimers can be mutagenic [12]. We are using duplex sequencing of *C. elegans* mtDNA to determine mutation rates in nematodes exposed to our serial UVC protocol. Furthermore, by including mutant strains deficient in mitochondrial fission and mitophagy, we hope to determine if deficiencies in these processes will further increase mtDNA mutation rates, as they are implicated in human diseases.

Dedication

This work is dedicated to my wife Cassie. Without you, I would not have found myself in the position for this to be possible. I love you, and I thank you for your patience and support. I could never have done this without you.

Contents

Abstract	iv
List of Tables.....	xii
List of Figures.....	xiii
Acknowledgements.....	xv
1. Introduction.....	1
1.1 Mitochondria	1
1.2 Oxidative phosphorylation (OXPHOS)	2
1.3 Mitochondrial DNA.....	5
1.4 Mitochondria and disease.....	5
1.5 mtDNA is an important target of environmental toxicants.....	7
1.6 mtDNA Damage reduces whole organism ATP levels	9
1.7 Metabolic rate and lifespan in <i>C. elegans</i>	10
1.8 The Developmental Origin of Health and Disease hypothesis (DOHaD).....	12
1.9 The <i>C. elegans</i> model.....	13
1.10 Dissertation objectives.....	14
2. Developmental mitochondrial DNA damage results in lifelong deficits in energy production in <i>C. elegans</i>	16
2.1 Introduction:	16
2.2 Results:.....	19
2.2.1 Mitochondrial DNA damage is removed.....	19
2.2.2 Mitochondrial DNA copy number is permanently reduced.....	20

2.2.3 Developmental mtDNA damage does not induce mito-nuclear protein imbalance	22
2.2.4 ATP levels are permanently reduced in response to developmental mtDNA damage	23
2.2.5 Oxygen consumption is increased.....	24
2.2.6 Expression of intermediary metabolic enzymes are unchanged	26
2.2.7 Targeted metabolomics reveals potential NADPH stress	26
2.2.8 Screening for sensitive and protected mutants	27
2.2.9 Stress resistance is decreased and lifespan unchanged.....	30
2.3 Discussion	31
2.3.1 mtDNA damage and removal.....	31
2.3.2 mtDNA copy number.....	34
2.3.3 ATP Levels and Oxygen Consumption.....	36
2.3.4 A role for reactive oxygen species.....	37
2.3.5 DOHaD or lifespan extension and stress resistance	39
2.3.6 Future directions	42
2.4 Methods.....	43
2.4.1 <i>C. elegans</i> Strains and Culture Conditions.....	43
2.4.2 UVC Exposure	44
2.4.3 DNA Damage Assay	44
2.4.4 Genome Copy number.....	46
2.4.5 ATP Levels.....	46
2.4.6 Oxygen Consumption	48

2.4.7 Gene Expression Assays	50
2.4.8 Targeted Metabolomics.....	51
2.4.9 Growth and Size Assays	51
2.4.10 Survival	52
2.4.11 Rescue Assays.....	53
3. Gene x Environment interactions in the origin of mitochondrial DNA mutations.....	80
3.1 Introduction	80
3.2 Experimental Design	82
3.3 Methods.....	83
3.4 Progress to Date	86
4. Conclusions	87
4.1 Summary	87
4.2 Broader Impacts	88
Appendix A - Effects of 5'-Fluoro-2-deoxyuridine on Mitochondrial Biology in <i>Caenorhabditis elegans</i>	90
A.1 Abstract	91
A.2 Introduction.....	93
A.3 Methods.....	96
A.3.1 Strains and culture conditions	96
A.3.2 Genome Copy Number Analysis	96
A.3.3 DNA Damage Analysis.....	97
A.3.4 Steady State ATP Level Analysis.....	97

A.3.5 Size Analysis.....	99
A.3.6 Mitochondrial Morphology.....	100
A.3.7 Lifespan Assay	100
A.3.8 mtDNA Half-life Analysis.....	100
A.4 Results.....	101
A.4.1 Genome Copy Number and Damage Analysis.....	101
A.4.2 Steady State ATP Levels	104
A.4.3 Nematode Size.....	106
A.4.4 Mitochondrial Morphology.....	107
A.4.5 Lifespan	107
A.4.6 mtDNA Half-life Analysis.....	108
A.5 Discussion	109
A.5.1 Use of Germ Line Deficient Strains.....	109
A.5.2 Copy number.....	110
A.5.3 ATP Levels.....	112
A.5.4 mtDNA Half-life	112
A.5.5 Strain differences	114
A.5.6 Lifespan	115
A.6 Conclusions.....	116
References.....	130
Biography.....	149

List of Tables

Table 1: Targets for Transcriptional Regulation of Intermediary Metabolism.....	53
Table 2: Primers for DNA Damage and Copy Number Assays in <i>C. elegans</i>	55
Table 3: Real Time PCR Primers for Gene Expression.....	56
Table 4: FUdR Induced DNA Damage.....	118

List of Figures

Figure 1: UVC induced mtDNA damage is removed, yet re-occurs later in life.	58
Figure 2: mtDNA damage during development permanently reduces mtDNA/nucDNA copy number ratio in JK1107 <i>glp-1(q224)</i> nematodes.	59
Figure 3: mtDNA damage during development permanently reduces mtDNA/nucDNA copy number ratio in PE255 <i>glp-4</i> nematodes.	60
Figure 4: UVC induced mtDNA damage does not change mitochondrial respiratory chain transcript levels	61
Figure 5: Complex II and Tfam Transcript Levels	62
Figure 6: Mitochondrial Unfolded Protein Response.....	63
Figure 7: ATP Levels are reduced, however oxygen consumption is increased.....	64
Figure 8: ATP levels are permanently reduced in PE255 <i>glp-4</i> nematodes.....	65
Figure 9: No evidence of transcriptional regulation of intermediary metabolism genes.	66
Figure 10: Organic Acid Levels.	67
Figure 11: Amino Acid Levels.	68
Figure 12: Long Chain acyl-Carnitine Levels	69
Figure 13: Absolute LCAC Levels	70
Figure 14: <i>sod-2</i> mutants are more sensitive to UVC exposure.....	71
Figure 15: <i>sod-2</i> and <i>sod-3</i> mutants are more sensitive to UVC induced growth delay 96 hours post exposure	72
Figure 16: Mitochondrial SOD mutants are more sensitive to UVC.....	73
Figure 17: MRC mutants are more sensitive to UVC	74
Figure 18: Skn-1 mutants are protected from UVC induced growth delay	75

Figure 19: Adult size is reduced in response to UVC induced developmental mtDNA damage.....	76
Figure 20: Lifespan is unchanged.....	77
Figure 21: Sensitivity to rotenone, but not paraquat, is increased in UVC exposed nematodes.....	78
Figure 22: Model for ROS Involvement.....	79
Figure 23: Effects of FUdR on mt and nuc DNA Copy Numbers in JK1107 <i>glp-1(q224)</i>	119
Figure 24: Effects of FUdR on mt and nuc DNA Copy Numbers in PE255 <i>glp-4(bn2)</i>	120
Figure 25: Steady State ATP Levels in JK1107 <i>glp-1(q224)</i>	121
Figure 26: <i>In vivo</i> Steady State ATP Levels in PE255 <i>glp-4(bn2)</i>	122
Figure 27: Steady State ATP Levels in PE255 <i>glp-4(bn2)</i>	123
Figure 28: Effects of FUdR on Area and Length in JK1107 <i>glp-1(q224)</i>	124
Figure 29: Effects of FUdR on Area and Length in PE255 <i>glp-4(bn2)</i>	125
Figure 30: Mitochondrial morphology.....	126
Figure 31: Lifespan.....	127
Figure 32: Determination of mtDNA Half-life in JK1107 <i>glp-1(q224)</i>	128
Figure 33: Determination of mtDNA Half-life in JK1107 <i>glp-1(q224)</i>	129

Acknowledgements

First, I would like to thank my advisor and friend, Joel Meyer, for your guidance, patience, and mentorship. It was truly a pleasure to work with you for these past years, and I doubt I will ever have a better boss! Our one on one meetings were the first meetings that I have ever looked forward too, and I will always appreciate the many and long discussions we had. You've done an excellent job guiding me along the way without telling me what to do, even if sometimes I wished you would! Most importantly I know that I have become a better scientist, and person, because of you.

To my committee, Rich Di Giulio, David Hinton, Bill Copeland and Matt Hirschey, thank you for the guidance and support, and for helping me see my work from other perspectives.

To the Meyer Lab, past and present, you are the best bunch of lab-mates anyone could ask for! I'm pretty sure the only reason I survived this process is because of you all. Claudia, thanks for being a great friend and colleague, and for the rides to school and the nickname. You're next! Ian, thanks for all the hard work these past few years, you've done more than you're fair share to help me out along the way. Good luck with Babcock, and sorry about Kessel. Let's go Buffalo. Tony, thanks for your tireless work ethic and help with all these last minute experiments. Try not to make everyone else look bad! Laura, thanks for listening to me complain these last few months, and for the

writing and job advice. It was great to have someone to chat with who still remembers this whole process.

To my family, mom, dad and Matt, thanks for always supporting me, listening to me, and helping me make the tough decisions. Love you guys.

To Cassie, again thanks for the love and support these past years. I know it hasn't always been easy, and I'm sure I didn't help all of the time. If there's anything I've done that I'm more proud of than this it's marrying you. You mean the world to me and without you this would not have been possible.

1. Introduction

1.1 Mitochondria

Mitochondria are dynamic, networked organelles best known for their role in ATP production via oxidative phosphorylation (OXPHOS) [1]. They consist of 2 phospholipid bilayers, creating an outer and inner membrane (OMM and IMM, respectively), an intermembrane space between them, and the mitochondrial matrix interior to the inner membrane. The inner membrane houses the 5 complexes of the electron transport chain (ETC) that carry out the process of OXPHOS [13]. Mitochondria contain their own, circular genomes (discussed in further detail below) that encode 12 or 13 proteins, which are all essential subunits of OXPHOS complexes, as well as 22 tRNAs and 2 ribosomal RNAs [2]. The vast majority of the proteins found in the mitochondria however, are encoded in the nuclear genome [14]. In addition to OXPHOS, mitochondria are also the site of many other metabolic processes, including the TCA cycle, amino acid oxidation and fatty acid beta-oxidation. Furthermore, they are responsible for the synthesis of iron-sulfur complexes, some steroid hormones and nucleotides, and are the major source of endogenous reactive oxygen species (ROS) [15]. They also play a central role in apoptosis (Reviewed in [16]). Considering their diverse and essential functions, it is no surprise that mitochondrial health is critical to cellular and organismal health.

1.2 Oxidative phosphorylation (OXPHOS)

OXPHOS is the process of transferring electrons via a series of redox reactions through protein complexes in the inner membrane to create a proton gradient that provides the energy required for ATP synthesis [17]. Complexes I (NADH dehydrogenase) and II (succinate dehydrogenase) accept electrons generated during the TCA cycle from the carriers NADH and FADH₂, respectively, and transfer them to the membrane localized ubiquinol (coenzyme Q10, Q). Q carries electrons to complex III (cytochrome c reductase) where they are transferred to cytochrome c, and then to complex IV (cytochrome c oxidase). Complex IV conducts the final electron transfer to molecular oxygen, resulting in the production of water. The transfer of electrons from complexes I, III and IV is coupled with the pumping of protons out of the mitochondrial matrix into the intermembrane space, creating an electrochemical gradient. Complex V (ATP synthase) allows these protons to pass back into the matrix and uses the energy released to synthesize ATP from ADP and phosphate [13, 17, 18].

Assembly of the ETC complexes requires coordinated transcription and translation of a large number of genes that are located in two different genomes [19], making this a particularly unique aspect of biology in general. The OXPHOS complexes all consist of multiple subunits and complexes I, III, IV and V contain subunits that are encoded in the mitochondrial genome as well as subunits that are encoded in the nuclear genome. In contrast, complex II subunits are encoded entirely in the nuclear

genome. Complex I is the largest, and contains approximately 45 individual subunits (7 are mtDNA encoded). Complex II is the smallest with only 4 subunits. Complex III is 11 subunits with 1 mtDNA encoded, complex IV is 13 with 3 mitochondrial, and complex V is 16 or 17 subunits, with 2 encoded in mtDNA [18]. Failure to assemble OXPHOS complexes in the proper stoichiometric balance can lead to activation of the mitochondrial unfolded protein response and induce the expression of chaperone proteins [20].

The ETC is also the major producer of endogenous reactive oxygen species (ROS), mainly from electrons that leak from complexes I and III to molecular oxygen creating superoxide [21]. Both complexes produce superoxide into the mitochondrial matrix, while complex III can also generate superoxide in the intermembrane space [22]. Mitochondrial ROS has been hypothesized to create a vicious cycle in which mitochondrial dysfunction leads to ROS production, which in turn creates mitochondrial dysfunction and further ROS production [23]. ROS can be toxic through their ability to damage DNA (reviewed in [24]), proteins [25] and lipids [26]. Mitochondrial ROS production increases with age, in conjunction with a decrease in mitochondrial function [27], and oxidative damage has been linked with many aging related pathologies. Cells possess a number of antioxidant defense systems that protect against and regulate these ROS [28, 29]. The mitochondria themselves contain multiple antioxidant enzymes, presumably to protect against ETC generated ROS. They include

the manganese superoxide dismutase (MnSOD), and glutathione peroxidase. SODs convert the highly reactive superoxide anion to the less reactive hydrogen peroxide [30], which can then be converted to water by catalase or detoxified through glutathione conjugation (reviewed in [28]).

The increase in ROS production with aging has led to the development of the Oxidative Stress Theory of Aging (also referred to as the Free Radical Theory of Aging), which was first introduced in 1956 [31]. It suggests that aging is driven by the generation and accumulation of oxidative damage arising from mitochondrial ROS [31]. This theory has undergone considerable revision, and is still a topic of debate today [29, 32, 33] as recent work has suggested that ROS are not the driving factor in aging. In some studies, *C. elegans* lacking the main mitochondrial superoxide dismutase (*sod-2*) actually live longer than their wild-type counterparts [34], though others have found no effect [35]. Furthermore, treatment with low levels of the ROS generating pesticide paraquat extends lifespan [36].

Mitochondrial ROS are also a potent retrograde signaling molecule, facilitating cross-talk between the mitochondria and the nucleus [37]. Contrary to the results from SOD knockouts in *C. elegans*, ROS are critical for normal development in mice, as overexpressing MnSOD results in increased developmental abnormalities and reduced fertility [38]. Cellular redox state has also been linked to the developmental processes of proliferation and differentiation [39].

1.3 Mitochondrial DNA

The mitochondrial genome in humans is approximately 16.5 kilobases in size, and codes for 13 proteins that are all critically involved in oxidative phosphorylation (OXPHOS), as well as 22 tRNAs and 2 ribosomal RNAs [2]. Mitochondrial genomes are normally present at between 1000 and 100,000 copies per cell [3], however mtDNA copy number is significantly reduced during certain developmental stages [3]. In primordial germ cells in mice, mtDNA copy number can reach as low as approximately 200 copies per cell [4, 40] representing a potential critical window for mitochondrial genotoxicant exposure. Mitochondrial DNA is inherited entirely maternally, as paternal mitochondria are actively degraded in newly fertilized oocytes [41, 42]. Mitochondrial genomes are organized into structures called nucleoids. Nucleoids are protein-DNA structures that contain as few as a single mtDNA [43] associated with the protein Transcription Factor A, Mitochondrial (TFAM), which acts both as a structural component, and also as a transcription factor for mtDNA [44-46]. TFAM is conserved in many mammals, as well as zebrafish. The *hmg-5* gene in *C. elegans* has recently been identified as a putative homologue of the mammalian *Tfam* gene [47].

1.4 Mitochondria and disease

Deficits in mitochondrial function are implicated in numerous common human diseases [48] including cancer [49], diabetes [50], heart disease [51], and neurodegenerative diseases [52]. Reduced oxidative metabolism in tumor cells is a

common phenotype, termed the Warburg effect[53], and other alterations to mitochondrial metabolism can promote tumor growth [54]. Many of these diseases have been linked to increases in mitochondrial ROS, and while direct causality due to mitochondrial dysfunction is suspected in some cases, definitive evidence of this is still lacking.

Mutations in mtDNA were first associated with human diseases in the late 1980's [55, 56], and since then over 270 mutations in human mtDNA, with widely varying clinical phenotypes, have been characterized [6, 57]. Some examples of mtDNA diseases resulting from mtDNA mutations are Leber's hereditary optic neuropathy (LHON), myoclonic epilepsy and ragged red fiber (MERRF), and mitochondrial encephalomyopathy, lactic acidosis and stroke-like episodes (MELAS) [2]. Additionally, reductions in mtDNA copy number and OXPHOS capacity are seen in insulin resistance and type 2 diabetes mellitus [58, 59], while specific point mutations in mtDNA cause maternally inherited diabetes and deafness (MIDD) [60] indicating a role for mitochondrial dysfunction in metabolic diseases.

Mutations in nuclear genes coding for mitochondrial proteins can result in mitochondrial diseases as well. Alper's syndrome and Leigh's syndrome are caused by mutations in the mitochondrial DNA polymerase γ [61], and mutations in mitochondrial dynamics genes OPA1 and Mitofusin2 cause neurodegenerative disorders, optic atrophy and Charcot-Marie-Tooth disease [62, 63]. These diseases often result from what is

referred to as Mitochondrial DNA Depletion Syndrome (MDS), which also includes Progressive External Ophthalmoplegia (PEO) and other recessive myopathies [61], and is characterized by a decrease in mtDNA content in specific tissues [64]. Cells often contain more than one population of mtDNA (for example 70% of mitochondrial genomes may be normal, while 30% contain a particular mutation), a condition termed heteroplasmy. Physiological effects are not seen unless a threshold of mutant DNA ratio is reached, and this threshold can vary by mutation [60]. Deletions in mtDNA are also a common factor in both aging and disease. Clonal expansion of mtDNA's harboring large deletions in neurons of the substantia nigra has been implicated in the loss of respiratory capacity in those neurons [65] and with Parkinson's Disease [66].

1.5 mtDNA is an important target of environmental toxicants

Many characteristics of mtDNA make it more susceptible to damage than nuclear DNA [67]. mtDNA lacks the protective histone packaging present in nuclear DNA, and does not undergo Nucleotide Excision Repair (NER)[7, 68, 69]. NER removes bulky, helix distorting adducts, such as those caused by some polycyclic aromatic hydrocarbons (PAHs) and UVC radiation induced dimers, in nuclear DNA [8]. Data from our lab and others indicates that UVC induced mtDNA damage persists in both *C. elegans* and human fibroblasts, while nuclear damage is efficiently repaired [7, 9, 10, 70]. Also, some toxicants, particularly those that are lipophilic or charged, are concentrated in the mitochondria due to their abundance of phospholipid bilayers and the slight

negative charge in the matrix [67]. For example, BaP, a lipophilic aromatic hydrocarbon, is reported to induce between 2 and 100 fold more mtDNA damage than nuclear [71, 72]. mtDNA is also located in close proximity to the ROS generating electron ETC. While oxidative damage to DNA can be detrimental, mtDNA undergoes relatively robust Base Excision Repair (BER), the process that repairs the majority of oxidative DNA lesions, and mitochondria possess many other antioxidant defenses [67].

The significance of chemically induced mitochondrial toxicity is well illustrated through the striking example of the antiretroviral Nucleoside Reverse Transcriptase Inhibitors (NRTIs) used in HIV-AIDS treatment. NRTIs inhibit DNA polymerase γ , resulting in reduced mtDNA replication, reduced oxidative phosphorylation capacity and mitochondrial dysfunction [73, 74]. NRTI toxicity often results in cardiac dysfunction, hepatic failure, mtDNA depletion, defective mtDNA replication, and increases in mtDNA mutations [75, 76]. However, this toxicity was not generally considered a concern, until two children born to mothers who were receiving NRTIs died within the first year of life due to severe mitochondrial dysfunction [77]. Recent work indicates that primates exposed to NRTIs *in utero* show mitochondrial DNA depletion in heart and brain cells that persists to at least 3 years of age, roughly the equivalent of 15 human years of age [78]. This illustrates not only the susceptibility of mitochondria and mtDNA to toxicant exposure, but also the potential for persistent effects resulting from developmental exposures affecting mtDNA.

There are a few well-known gene-environment interactions that involve mtDNA mutations. For example, aminoglycoside antibiotics can cause deafness in patients with specific point mutations in the mitochondrial 12s ribosomal RNA [79]. 2 individual mutations each result in the mt-rRNA more closely resembling the bacterial rRNA and an altered binding pocket for the aminoglycoside [80]. Also, the risk for developing vision loss resulting from LHON mutations is significantly increased by smoking [81].

The unique vulnerability of mtDNA to environmental genotoxicants, combined with the recently discovered health effects of mutations and pharmaceuticals that affect mtDNA, highlight the importance of elucidating the effect of persistent mtDNA damage caused by environmental exposures.

1.6 mtDNA Damage reduces whole organism ATP levels

Bulky DNA adducts and dimers can block the progression of DNA and RNA polymerases, therefore impeding both transcription and replication [12, 82], potentially leading to a stoichiometric imbalance of OXPHOS complex proteins or reduced mtDNA copy number, respectively. Furthermore, the mtDNA polymerase γ , while not efficient at translesion synthesis, is prone to misincorporation opposite BaP- and UVC-induced DNA adducts, representing a possible mechanism of mutagenesis [12, 83]. We thus hypothesized that persistent mtDNA damage could lead to inhibition of OXPHOS, reduced energy production, and/or mitochondrial dysfunction [2] resulting in an increase in potential adverse outcomes.

Preliminary experiments were conducted to test the effects of UVC-induced mtDNA damage on whole organism ATP levels in *C. elegans*. UVC, while not a pollutant, serves as an excellent tool to study the effects bulky DNA damage caused by important contaminants such as polycyclic aromatic hydrocarbons [84]. Briefly, a luciferase expressing strain of *C. elegans* (PE255 [85]) in the first larval stage of development was maintained without food, and exposed to 3 doses of UVC radiation, 24 hours apart. The 24 hour time period between doses allows for nuclear DNA damage to be repaired, whereas mtDNA damage accumulates [9]. After the 3rd dose, the nematodes were given food and allowed to develop. ATP levels were measured in live worms, through the addition of a Luciferin salt substrate and quantification of the resulting luminescence [85]. At this dose, which does not significantly impede development [9], UVC exposure dramatically reduces ATP levels at the whole-organism level between 24 and 48 hours post treatment, which encompasses the metabolically important transition from larval stage 3 (L3) to 4 (L4) described below [11].

1.7 Metabolic rate and lifespan in *C. elegans*

C. elegans are a widely used model for the study of aging, and lifespan extension. One of the four major pathways that can increase lifespan in *C. elegans* is RNA interference mediated knockdown of electron transport chain genes during larval development [86, 87]. Knockdown of ETC subunits in complexes I, III, IV and V during development, but not adulthood, was initially shown to increase lifespan and reduce

ATP levels, independent of the Insulin/IGF signaling pathway [86]. This has since been further refined to specifically during the L3/L4 stages of development [87]. This is an interesting developmental window in the worm, as the L3/L4 transition marks a switch from primarily glycolytic metabolism to oxidative metabolism, and in fact depends on functional mitochondria [88]. There is also a threshold effect in that above a certain degree of knockdown lifespan is no longer extended, and can actually be shortened [87]. Furthermore, lifespan extension functions cell non-autonomously, as ETC subunit knockdown specifically in neurons activates the UPR^{mt} in intestinal cells, and is sufficient to induce lifespan extension [89].

Recent work indicates that the lifespan extension induced by knockdown of ETC subunits results from an imbalance between mtDNA encoded and nucDNA encoded OXPHOS proteins, termed Mitonuclear protein imbalance [20]. Mitonuclear protein imbalance activates the mitochondrial unfolded protein response (UPR^{mt}) [20, 90, 91]. UPR^{mt} activation leads to an increase in transcription of many nuclear encoded mitochondrial chaperone proteins to relieve the stress of accumulated, unfolded proteins in the organelle [90]. Mitonuclear protein imbalance and UPR^{mt} activation have recently been identified as a conserved mechanism for lifespan extension in both *C. elegans* and mice [20].

Other evidence suggests a separate and distinct pathway that responds to mitochondrial dysfunction without mitonuclear protein imbalance, can alter metabolism

without extension of lifespan, and is dependent on the nuclear hormone receptor NHR-49 [92]. Suppression of complex II subunits, which are encoded entirely in nucDNA, results in a reduction in ATP levels and oxygen consumption yet does not alter lifespan [93]. Furthermore, point mutations and RNAi knockdown of the same ETC genes lead to drastically different patterns of gene expression, behavior, and stress responses, even though both result in lifespan extension [94]. This evidence suggests that at least 2 different mechanisms can regulate nematode metabolism in response to mitochondrial dysfunction, and the resulting metabolic changes may be significantly different.

1.8 The Developmental Origin of Health and Disease hypothesis (DOHaD)

The developmental origin of health and disease hypothesis, which has become an entire field of research, suggests that deleterious exposures during development can lead to adverse outcomes later in life [95]. Also referred to as “Barker’s Hypothesis”, it is supported by a growing body of literature. Much of the work in this field has focused on the link between fetal nutritional deficiencies and adult diseases, and the potential involvement of epigenetic regulatory mechanisms [96-98]]. The Dutch Famine Cohort studies provide significant epidemiological evidence for the theory, demonstrating increased likelihood of many diseases, including cardiovascular disease, obesity, diabetes, and schizophrenia, in adults who had been exposed to very low nutrient intake *in utero* [97]. Thus, as mitochondrial function is directly linked to metabolism, and metabolic regulation during development plays a significant role in adult disease

susceptibility, it seems plausible that mitochondrial dysfunction during development may influence adverse outcome potential later in life.

1.9 The *C. elegans* model

C. elegans is a free living nematode whose habitat consists of decaying organic matter, though it is not a soil nematode [99]. It was originally introduced as a model organism for laboratory study in the 1970's by Sydney Brenner [100]. Its genome is fully sequenced and shares above 80% homology with that of humans [101]. Furthermore, the developmental fate of every cell in the worm is known [102], allowing for the use of nuclear DNA copy number as a marker for development. The life cycle of the worm takes approximately 3 days at 20°C, each worm produces roughly 300 progeny over the span of 3 days, and the average lifespan of wild type worms is about 20 days [103].

C. elegans is an excellent model species for the study of mitochondrial biology and mtDNA. It's mitochondrial genome is highly evolutionarily conserved with that of humans [103], and it encodes at least 12 (likely 13) of the proteins found in the mammalian mtDNA [104] [105]. Numerous studies have used the *C. elegans* model to investigate mitochondrial dysfunction and, to an even greater extent, the connection between mitochondrial function and aging [103]. Transgenic strains are available that allow for the visualization of mitochondria via fluorescence microscopy [106], and measurement of *in vivo* steady state ATP levels [107]. Mutants in genes associated with mitochondrial dysfunction are also powerful tools. Furthermore, *C. elegans* represent an

in vivo model in which to study mitochondrial function and dysfunction, a significant difference from the *in vitro* use of cultured cells. It is generally accepted that cells in common culture techniques, particularly those derived from cancers, generate the majority of their ATP via glycolysis rather than OXPHOS, thereby relying less on mitochondrial function, a phenomenon known as the Warburg effect [108, 109]. This makes studying the effects of mitochondrial toxicants in cultured cells difficult.

Furthermore, recent evidence suggests that the mitochondrial quality control process of mitophagy may not occur in cultures of primary neurons, possibly due to their reliance on OXPHOS [110]. These results highlight the difficulty of accurately assessing mitochondrial function in cultured cells and the need for simple *in vivo* models of mitochondrial dysfunction. Lastly, with the significant changes in mtDNA copy number in development, a model that allows for the study of development is also important for mitochondrial biology. The *C. elegans* model provides us with both of these tools.

1.10 Dissertation objectives

The primary goal of this work is to determine if developmental mtDNA damage results in metabolic changes later in life, and to investigate whether these changes lead to adverse outcomes later in life, or stress resistance. I hypothesize that mtDNA damage incurred during development will be removed, but before removal is complete, this damage will induce mitochondrial dysfunction, which will in turn reprogram the metabolism of the developing nematode.

The majority of this work is presented in chapter 2 of this dissertation, as it will be submitted for publication as one large research article. I have used an exposure protocol developed in our lab to induce an accumulation of mtDNA damage in 1st larval stage *C. elegans* and then investigated a variety of molecular and biochemical mitochondrial health related endpoints throughout the life of the nematode.

Chapter 3 describes a second project designed to investigate the contribution of the environment to mutations in mtDNA. This work is currently in progress and this chapter includes a detailed explanation of the rationale and current state of the project, as well as the methods being used.

Chapter 4 is a summary of the results and implications of this work from a broader impacts perspective.

2. Developmental mitochondrial DNA damage results in lifelong deficits in energy production in *C. elegans*

2.1 Introduction:

The mammalian mitochondrial genome (mtDNA) encodes 13 proteins, 22 tRNA's and 2 rRNAs. The proteins are all subunits of the mitochondrial respiratory chain (MRC) complexes, and are essential for it's proper function, while the tRNA's and rRNA's are required for translation of those proteins. The MRC consists of 5 protein complexes, each made up of multiple subunits, and while the majority of these subunits are encoded in the nucDNA, their proper stoichiometric balance with those encoded in mtDNA is extremely important for maintaining MRC function [20]. The MRC generates the vast majority of cellular ATP through oxidative phosphorylation (OXPHOS), and it's proper function is critical to overall organismal health. MRC function is directly linked to the integrity of the mtDNA, and mutations in protein coding genes and tRNAs in the mtDNA lead to a broad spectrum of clinically variable human diseases. One reason for this variability is that, in contrast to the nuclear genome, which is present in only 2 copies per cell, there are normally between 1000 and 10,000 copies of mtDNA per cell. This variation in the number of mtDNA genomes per cell is a result of tissue and life stage specific differences, with certain developmental stages having drastically lower mtDNA content [3]. Due to this high and variable copy number, mutations must be present in a threshold proportion (heteroplasmy) of mtDNA before they become pathogenic [6]. The threshold and pathogenicity are dependent on the tissue affected

and the specific mutation. Furthermore, Mitochondrial DNA Depletion Syndrome (MDS), the reduction of mtDNA content in specific tissues, also leads to human disease [64]. Mitochondrial dysfunction in general has been implicated in many more common human diseases as well, including cancer, diabetes, metabolic syndrome and neurodegenerative conditions.

Mitochondria, and specifically the mtDNA, are becoming more appreciated as important targets of environmental toxicants [67]. There are many factors that contribute to their susceptibility, including high lipid content resulting in attraction of lipophilic pollutants such as polycyclic-aromatic hydrocarbons (PAHs). Also, while the DNA repair capacity of the mtDNA is much more robust than initially believed, and includes both long and short patch base excision repair (BER), homologous recombination and non-homologous end joining mechanisms, evidence of functional nucleotide excision repair (NER) is still nonexistent [7, 68, 70]. Without NER, DNA lesions such as cyclobutane pyrimidine dimers caused by ultraviolet light, and bulky benzo-a-pyrene and aflatoxin DNA adducts are irreparable in mtDNA. *In vitro*, these lesions can impair the progression of pol- γ [12], and in developing *C. elegans* ultraviolet C (UVC) induced mitochondrial DNA damage results in a reduction in the normal increase of mtDNA, changes in mtDNA transcript levels, and a reduction in steady state ATP levels [11]. In adult *C. elegans*, these lesions are slowly removed via a process involving autophagic

machinery [9, 10]. However, it is not known if the changes in mitochondrial biology during development will manifest as adverse outcomes later in life.

The model organism *Ceanorhabditis elegans* provides us with an excellent opportunity to study mitochondrial function *in vivo*, which has significant benefits over *in vitro* approaches. Mainly, mtDNA content and mitochondrial function rely heavily on developmental and organismal contexts that cannot be replicated *in vitro*. For example, cells cultured in standard high glucose media can be completely depleted of their mtDNA and still survive [111, 112]. Mitochondrial function and susceptibility to mitochondrial toxicants are significantly affected by culture conditions [113]. Furthermore, mitophagy, the targeted degradation of dysfunctional mitochondria, has been shown not to occur in primary cells grown under conditions that require mitochondrial function for energy production (without glucose) [110]. And lastly, as previously mentioned, mtDNA content changes dramatically during development, and mitochondrial function is significantly affected in the aging process [3, 104, 114].

A growing body of literature suggests that environmental exposures during development can lead to adverse outcomes later in life (reviewed in [97] and [98]), however exposures specific to mitochondrial toxicity have not been investigated in depth. Evidence does suggest that latent adverse effects may be associated with mitochondria. Supporting this hypothesis is the latent mitochondrial myocardial toxicity seen in patients receiving doxorubicin as chemotherapy [115]. Short term exposure to

dichloroacetate (DCA), a metabolic remodeling agent that drives oxidative metabolism, leads to latent liver carcinogenicity in mice at comparable rates to lifelong exposure [116]. Survivors of childhood cancers also develop symptoms similar to mitochondrial diseases later life at greater rates than control populations [117]. Yet, in *C. elegans*, mitochondrial stress during development resulting from mutations in, or knockdown of respiratory chain subunit genes leads to increased lifespan and stress resistance [20, 86, 118, 119]. Here, we ask if an environmental exposure (modeled with UVC) that leads to irreparable mtDNA damage during development will result in adverse later life outcomes related to mitochondrial function.

2.2 Results:

2.2.1 Mitochondrial DNA damage is removed

UVC induced damage in mtDNA is not repaired, as nucleotide excision repair does not take place within the mitochondria [7]. However, mtDNA damage is slowly removed [9]. Previously, removal was measured in adult worms through 120 hours post exposure, and complete removal was not seen. We hypothesize that the dynamics of mtDNA turnover are different in adult worms as opposed to larvae, as there is a major increase in mtDNA copy number during development [114] and a slow decline in adulthood [120]. Therefore, we expect removal kinetics of mtDNA damage to be faster and more complete in larvae. To investigate if complete removal occurs, we measured both mtDNA and nucDNA damage levels at 0 (immediately after), 2, 4, 6, and 8 days

after a larval exposure of 3 doses of 7.5J/m²UVC radiation 24 hours apart. This exposure protocol, developed in our laboratory, results in accumulation of mtDNA damage, while allowing for repair of the majority of nucDNA damage [9].

Our serial UVC exposure results in 2.7 lesions/10kb of mtDNA immediately after the 3rd and final dose (time 0 days). 2 days later this is reduced to 0.68 lesions per 10kb, and 0.14, 0.28 and 0.42 lesions/10kb at days 4,6, and 8, respectively. Damage is not detectable in control samples. The main effect of treatment was significant ($p < 0.0001$) as was time ($p < 0.0001$) and their interaction ($p < 0.0005$) (Figure 1). Interestingly, while mtDNA damage appears to be reduced to background levels at days 4 and 6, it is present above background again at day 8. One hypothesis is that the damage created directly via UVC exposure is completely removed, and new damaging events occur later in life only in the context of early life exposure.

This same exposure results in 0.95 lesions/10kb in nucDNA, and by 2 days post exposure no significant damage is detectable. This is expected, as nucleotide excision repair is robust in the nucleus. Damage was also not significant at 4, 6 and 8 days post exposure. Again, damage is not detectable in the control samples.

2.2.2 Mitochondrial DNA copy number is permanently reduced

We hypothesized that bulky lesions in mtDNA would block the mitochondrial DNA polymerase (pol- γ), as pol- γ has little capacity for thymine dimer lesion bypass *in vitro* [12], and result in reduced mtDNA content per cell. Indeed, this does occur through

the first 48 hours after exposure [11]. mtDNA content per worm increases through development, peaking at the 4th larval (L4) stage [114], and this increase is reduced in UVC exposed nematodes [11]. However, as damage appears to be largely removed (above and [9]), we expected mtDNA copy number in exposed nematodes to eventually reach that of their control counterparts.

Mitochondrial / nuclear DNA copy number ratio was significantly reduced in both the JK1107 *glp-1(q224)* and PE255 *glp-4(bn2)* strain of *C. elegans* after 3 developmental exposures to 7.5 J/m² UVC radiation. In the JK1107 *glp-1(q224)* strain, mtDNA copy number per worm and mtDNA/nucDNA ratio were reduced in the UVC exposed nematodes (main effects of treatment $p < 0.005$ and $p < 0.001$ by 2 factor ANOVA, respectively) (Figure 2). Furthermore, there was a significant treatment by time interaction for mtDNA/nucDNA copy number ($p < 0.05$). There was no effect on nucDNA copy number. In the PE255 *glp-4(bn2)* strain, there was no detectable effect on mtDNA or nucDNA copy number per worm, yet mtDNA/nucDNA ratio was significantly reduced by UVC exposure ($p < 0.05$) (Figure 3).

Interestingly, the reduction in copy number persists throughout the entire experiment, and thus for the majority of the life of the nematode (average lifespan of wild type *C. elegans* is approximately 12-18 days at 20°C). This result was unexpected, as I hypothesized that, due to removal of damaged genomes and replication of undamaged genomes, any reduction in copy number would be transient.

2.2.3 Developmental mtDNA damage does not induce mito-nuclear protein imbalance

Mito-nuclear protein imbalance is a conserved mechanism for lifespan extension and can be triggered by reduced transcription of mtDNA-encoded OXPHOS subunits [20]. Since bulky DNA lesions and dimers block the mtDNA polymerase, we hypothesized that they may also block the RNA polymerase, which could reduce transcript levels of mtDNA-encoded genes. However, the multiplicity of mtDNAs per cell may act to buffer against such transcriptional blocks. We have previously shown a slight decrease in mtDNA-encoded transcripts 12 hours after larval UVC exposure, followed by an increase at 24 and 48 hours [11]. Here, mtDNA encoded transcript levels in UVC treated nematodes are unchanged at 4 at 8 days post exposure. nucDNA encoded OXPHOS transcripts are also unchanged (Figure 4).

As complex 2 of the MRC is entirely nuclear encoded, we hypothesized that its expression may be upregulated in a compensatory manner to overcome potential electron transport deficits resulting from impaired function of other MRC complexes. We therefore measured the transcript levels of 4 subunits of complex 2, *sdhA-1*, *sdhB-1*, *sdhC-1* (*mev-1*) and *sdhD-1*, after developmental UVC exposure. Again, we found no significant changes in expression levels (Figure 5). Lastly, we found no change in the transcript levels of the mitochondrial structural protein / transcription factor *hmg-5* (Tfam in mammals) (Figure 5).

Transcript levels are not always representative of protein levels. This is of particular interest in this case, as the tRNAs and rRNAs required for translation of mtDNA transcripts are also encoded in mtDNA. The genes *hsp-6* and *hsp-60* code for mitochondrial chaperone proteins that are strongly induced in response to accumulating misfolded proteins in the mitochondria. Expression of these genes and the proteins they code for is commonly used as an indicator of protein stress in the mitochondria. Notably, while we did observe a small increase in *hsp-6* and *hsp-60* transcripts at 4 days post UVC exposure, there was no increase in protein levels as measured via GFP fusion reporter strains (Figure 6). This data suggest that there is not a mito-nuclear protein imbalance as a result of UVC exposure.

2.2.4 ATP levels are permanently reduced in response to developmental mtDNA damage

While mtDNA damage appears to be removed completely, the persistent reduction in mtDNA copy number suggests that other mitochondrial endpoints may also be persistently altered. Products of mtDNA encoded genes play essential roles in electron transport and ATP production [121], and mtDNA damage reduced ATP levels during *C. elegans* development [11]. Therefore, we investigated whether this reduction in mtDNA copy number would reduce ATP production in UVC exposed nematodes later in life.

Steady state ATP levels were reduced in both JK1107 and PE255 nematodes in response to UVC exposure. ATP levels were measured in the JK1107 strain at 4 and 8

days post final UVC exposure, and were significantly reduced by 32.5% and 40% respectively (main effect of treatment, $p < 0.002$) (Figure 7). Consistent with previous results [122], ATP content decreased by roughly 50% between days 4 and 8 in both control and UVC exposed animals.

In the PE255 nematodes, ATP levels were again significantly reduced by UVC exposure (main effects of time and treatment, $p < 0.001$ and $p < 0.03$, respectively) (Figure 8). Relative steady state ATP levels were measured at 2, 4, 6, 8, and 10 days post final UVC dose. More measurements were possible with this reporter strain as far fewer animals per measurement were required. The largest reduction (44%) was seen at day 8, however due to lack of a significant treatment by time interaction we were unable to statistically compare values at individual time points.

2.2.5 Oxygen consumption is increased

ATP levels are directly linked to oxygen consumption, therefore one explanation for reduced ATP levels would be reduced oxygen consumption. To investigate this hypothesis, basal, maximal and non-mitochondrial respiration rates were measured at days 4 and 8 post final UVC dose *in vivo*, in whole JK1107 nematodes using a Seahorse XF^e24 extra cellular flux analyzer.

Basal oxygen consumption rates were significantly increased in UVC exposed nematodes at 4 days post exposure ($p < 0.05$) (Figure 7). Non-exposed nematodes had a basal oxygen consumption rate of 8.08 pMoles O₂/minute/ug protein, which was nearly

doubled to 15.48 pMoles O₂/minute/ug protein with UVC exposure. Furthermore, the mitochondrial uncoupler FCCP increased oxygen consumption in non-exposed animals 2.2 fold to 17.64 pMoles O₂/minute/ug protein, while the UVC exposed nematodes increased only 1.1 fold over their basal rate to 17.22 pMoles O₂/minute/ug protein. This rate is statistically the same as the basal rate, thus there is little to no spare respiratory capacity (maximal respiration rate – basal respiration rate) in UVC exposed nematodes. Both exposed and non-exposed animals had similar sodium azide induced non-mitochondrial respiration rates at 3.47 and 4.55 pMoles O₂/minute/ug protein, respectively.

At 8 days post UVC exposure respiratory rates are reduced overall, and the large increase in basal respiratory rate in response to UVC exposure is alleviated. There are no statistical differences between control and treated nematodes at this time point. Basal rates are 4.22 and 5.84 pMoles O₂/minute/ug protein in control and UVC exposed samples, respectively. FCCP induced maximal rates are 11.46 and 11.44 pMoles O₂/minute/ug protein, and non-mitochondrial rates are 1.86 and 3.16 pMoles O₂/minute/ug protein.

The increased basal oxygen consumption and lack of spare respiratory capacity combined with reduced ATP levels in UVC exposed nematodes suggests persistent, inefficient mitochondrial function. Importantly, at 8 days post exposure when basal oxygen consumption rates are no longer elevated in UVC treated worms, ATP levels are

still significantly lower indicating that mitochondrial efficiency is also still reduced. This results in a reduction in ATP produced per unit oxygen consumed (Figure 7).

2.2.6 Expression of intermediary metabolic enzymes are unchanged

We hypothesized that, in response to mtDNA damage and inefficient MRC function, UVC exposed nematodes would shift metabolism away from OXPHOS and engage intermediary metabolic pathways. To explore this we measured the transcript levels of key intermediary metabolic enzymes (Table 1) that regulate TCA cycle metabolism (*pdp-1*, *pdhk-2*), glycolysis (*gpd-3*), the glyoxylate cycle (*gei-7*), fatty acid β -oxidation (*acs-2*), and gluconeogenesis (*PEPCK*). Expression levels of these enzymes were not significantly different in UVC treated nematodes at either 4 or 8 days post exposure (Figure 9). While this suggests that transcriptional regulation of intermediary metabolic pathways is unlikely to be occurring, it does not rule out significant metabolic alterations, as there are many mechanisms of enzyme activity regulation that do not rely on transcription of the enzymes themselves.

2.2.7 Targeted metabolomics reveals potential NADPH stress

To further probe potential shifts in metabolic pathways that may not be regulated via transcriptional control, we performed targeted metabolomics to measure levels of organic acids, amino acids and acyl carnitines.

Malate and fumarate were the only organic acids that were elevated in UVC exposed nematodes at both 4 and 8 days post exposure (Figure 10), and while not

statistically significant, these metabolites did trend together. This increase suggests cataplerosis from the TCA cycle, and may potentially drive the malate-aspartate shuttle. Amino acid levels generally declined with age ($p < 0.005$, main effect of time for all amino acids via 2 way ANOVA), which is consistent with reduced overall metabolism in aging nematodes, except for Asx (aspartate/asparagine), which was altered in response to UVC exposure (Figure 11). This result also supports the hypothesis of activation of the malate-aspartate shuttle. The malate-aspartate shuttle can be used to move NADH into or out of the mitochondria via cycling of malate across the inner membrane [123]. Malate in the cytoplasm can be converted to pyruvate via malic enzyme, yielding cytosolic NADPH. Inside the mitochondria NADH imported via Malate can be used to generate NADPH via the nicotinamide nucleoside transhydrogenase [54]. Lastly, a number of long chain acyl-carnitines (LCAC) were elevated in UVC samples (Figure 12), which is often indicative of defects or dysregulation of fatty acid beta-oxidation. When absolute LCAC are compared (Figure 13), treatment related increases are seen in both C18 and C18:1 LCAC species, which are both relatively abundant at both time points.

2.2.8 Screening for sensitive and protected mutants

Increased basal oxygen consumption in UVC exposed nematodes could be indicative of increased formation of reactive oxygen species. Complexes I and III of the MRC are considered major sources of intercellular ROS and mitochondrial dysfunction can result in a further increase in ROS production [21]. Furthermore, our metabolomic

data suggests the potential for an NADPH stress in UVC exposed worms. This also supports a mitochondrial oxidative stress phenotype, as NADPH is required to reduce oxidized glutathione in the mitochondria. To investigate the potential for increased mitochondrial ROS generation, we treated nematodes with loss of function mutations in key antioxidant genes (*sod-2, 3*), MRC genes (*gas-1, mev-1*), and ROS stress response associated genes (*daf-16, skn-1*) with our standard UVC exposure protocol, and measured their growth rate. In *C. elegans*, development past the 3rd larval stage (L3) requires functional mitochondria and mitochondrial dysfunction or inability to replicate mtDNA can lead to larval arrest [114, 124]. 7.5 J/m² UVC exposure leads to developmental delay in wild type worms, while higher doses can result in larval arrest. In order to increase throughput we use size as an indicator of development.

The superoxide dismutase (SOD) enzymes play critical roles in detoxifying ROS, by converting superoxide anions to hydrogen peroxide [30]. *C. elegans* have genes encoding 5 SOD enzymes, 2 are mitochondrial (*sod-2* and *3*) and are MnSODs [125-127], *sod-1* and *5* are cytosolic Cu/ZnSODs [128], and *sod-4* encodes an extracellular Cu/ZnSOD [129]. UVC induced larval delay was exacerbated in *sod-2* mutants, yet not in the *sod-3* mutant 72 hours post exposure (Figure 14). Interestingly, at 96 hours post exposure both mutants were more delayed (Figure 15) [130]. The double *sod-2;3* mutant was also significantly more growth delayed after UVC exposure, but the triple *sod1;4;5* mutant was not (Figure 16).

We also screened 2 mutants of the MRC, *gas-1* a subunit of complex I, and *mev-1* a subunit of complex 2. *gas-1* mutants have reduced complex 1 activity [131], and reduced lifespan [132]. *mev-1* is the large subunit of cytochrome b [133], and mutations cause increased sensitivity to oxidative stress [134]. We hypothesized that, if in fact our UVC exposure was resulting in mitochondrial dysfunction that delayed growth, this would be exacerbated in mutants with compromised mitochondrial function. Indeed, both *gas-1* and *mev-1* are significantly more growth delayed than wild type nematodes (Figure 17).

Skn-1, the nematode homologue of the mammalian Nrf-2 transcription factor, controls the expression of numerous genes related to phase 2 metabolic processes and oxidative stress defense [135]. Interestingly, *skn-1* mutant nematodes are completely protected from the UVC induced larval growth delay (Figure 18). This is intriguing, and suggests that developmental delay caused by UVC induced mtDNA damage is dependent on the *skn-1* mediated response to ROS.

Daf-16 is the nematode Forkhead box O (FOXO) transcription factor [136] that regulates the expression of numerous genes involved in stress resistance, longevity, metabolism, and reproduction [137]. It acts downstream of insulin like growth factor signals [138], and is required for lifespan extension via this pathway. *daf-16* mutants were slightly more sensitive to UVC induced growth delay than wild-type nematodes (Figure 18). This suggests that the transcriptional responses controlled by *daf-16* are

important for mitigating the stress induced by UVC exposure, yet they are not directly responsible for delaying growth.

2.2.9 Stress resistance is decreased and lifespan unchanged

The developmental origin of health and disease hypothesis suggests that environmental exposures during development result in increased risk of disease later in life [97]. Yet, in *C. elegans* RNAi mediated knockdown of mitochondrial respiratory chain components leads to increased stress resistance and lifespan extension. Often accompanying these traits are slow development, smaller adult size, and reduced ATP levels [86, 89, 118]. Developmental mtDNA damage resulted in many of these same phenotypes indicating the potential for a common mechanism. We therefore assayed stress resistance to the mitochondrial poisons rotenone and paraquat in adult worms, and measured adult size and lifespan in control and UVC exposed nematodes.

Adult size is significantly reduced in response to developmental mtDNA damage (main effects of treatment $p < 0.001$ and time $p < 0.001$, and their interaction $p < 0.04$, 2 way ANOVA) (Figure 19). Lifespan was measured in 7.5 J/m² UVC treated nematodes and was statistically unchanged from that of control nematodes (Figure 20). Median lifespans were both 15 days, and maximal lifespans were 20 and 22 days in control and UVC treated animals, respectively.

Finally, UVC treated nematodes are more sensitive to rotenone than their untreated counterparts, but not to paraquat (Figure 21). 4 days post UVC exposure, 24-

hour survival rates for both unexposed and UVC exposed nematodes were measured on plates that contained either rotenone or paraquat. Rotenone is an inhibitor of complex 1 of the MRC and reduced survival by 40% at exposures as low as 10 uM. Paraquat induces mitochondrial ROS production [139] and is commonly used to assay oxidative stress resistance in *C. elegans*. The data indicate the potential for increased sensitivity, though at this time the results are not statistically significant. The increased sensitivity to rotenone in UVC treated nematodes could be due to their lack of spare respiratory capacity, while the paraquat sensitivity would indicate reduced ability to detoxify further ROS.

2.3 Discussion

2.3.1 mtDNA damage and removal

We have shown that irreparable lesions in mtDNA (cyclobutane pyrimidine dimers) in developing *C. elegans* are removed, though more slowly than in nuclear DNA, yet lead to persistent metabolic changes and adverse outcomes later in life. Our data suggest two possibilities with regards to completeness of lesion removal: first, mtDNA lesions are completely removed, as evidenced by the reduction to the assay's limit of detection at days 4 and 6, and then new damaging events occur resulting in significant levels of mtDNA lesions reappearing at 8 days post exposure. Second, lesions are not completely removed, but are reduced to levels at or near the limit of detection, and variability in the data lead to statistical significance at 8, but not 4 or 6 days post

exposure. This is in contrast to previous work from our lab, which had shown just under 40% damage removal after 72 hours in adult nematodes [9]. A hypothesis for the differences in removal rates between developing and adult nematodes involves the natural changes in mtDNA copy number that occur during development. As *C. elegans* progress from larval stage 3 (L3) to 4 (L4) mtDNA copy number increases dramatically [114], however, in adult nematodes mtDNA copy number slowly declines, with a half-life of approximately 10 days [120]. This half-life roughly corresponds to the rate at which damage is removed, suggesting that mtDNA damage removal in adult nematodes is tied to turnover of mitochondrial genomes. Furthermore, mtDNA replication appears to stop in adulthood, as copy number declines at the same rate in nematodes treated with ethidium bromide as it does in untreated worms [120]. In contrast, mtDNA replication is essential during development, though we unfortunately are unable to measure genome half-life at this life stage due to technical limitations. We suspect that more mtDNA replication and potentially more frequent turnover leads to more complete damage removal during development.

Of these two hypotheses regarding completeness of lesion removal, the first is the more scientifically intriguing, and suggests that mtDNA damage may accumulate with aging in the context of early life exposure. A possible mechanism for this hypothesis begins with persistent mitochondrial dysfunction resulting from mtDNA damage that leads to increased ROS production, followed by a further increase in

oxidative damage in the mitochondria as a result of aging [140] leading to the re-occurrence of mtDNA damage. This hypothesis would result in different types of lesions at different time points, and thus potentially different mtDNA mutation spectrums. Sequencing mtDNA for rare mutations represents an approach to further investigate this hypothesis [141]. mtDNA mutations increase with age, and while this was often thought to result from increased ROS mediated DNA damage, the mutational spectrum in aged versus young human brain tissue are inconsistent with oxidative damage [142]. Therefore it would be particularly interesting to determine if environmental exposures that effect mitochondrial function could alter this mutational spectrum. Alternatively, antibodies to cyclobutane pyrimidine dimers and 8-oxo-guanine lesions could be used to determine which types of damage are more prevalent at different time points.

It is important to note that our method of DNA lesion quantification is relative to age matched control samples, so therefore represents damage levels above those that may naturally occur during aging. While this does not allow us to investigate mtDNA damage that is strictly a function of age, it does strengthen the case that this damage later in life is directly linked to exposure.

Alternatively, the reduction in lesion frequency in mtDNA could be due to dilution of the damage caused by the large increase in copy number during the L3/L4 transition. If undamaged mtDNAs are preferentially replicated during this time, a reduction in lesion frequency would be seen, even in the absence of damage removal.

Supporting this hypothesis, the increase in mtDNA copy number between days 0 and 2 (3.88 fold increase) is proportionally similar to the reduction in lesion frequency over the same time period (3.98 fold). This hypothesis, however, would suggest that dimers in mtDNA are not removed in any capacity during the first 2 days of *C. elegans* development.

2.3.2 mtDNA copy number

Persistent reductions are also seen in mtDNA/nucDNA copy number as a result of UVC induced mtDNA damage during development. As previously mentioned, mtDNA copy number increases dramatically between the L3 and L4 developmental stages [114], coinciding with a major increase in steady state ATP levels [11]. mtDNA copy number does increase in UVC exposed nematodes, though not to the same level as their age matched, unexposed counterparts. This is interesting, as our data also indicate that lesions in mtDNA are either completely or nearly completely removed. While these helix-distorting dimers can impede the progress of the mtDNA polymerase, pol- γ , complete removal would suggest that genome replication should be possible. Interestingly, expression of pol- γ appears to be increased after UVC exposure, though variability in these data result in a lack of statistical significance. We do note, however, that mtDNA replication appears to cease at some point between 3 and 6 days of age in untreated nematodes [120]. Therefore, it is possible that replication of some mtDNAs may be blocked by lesions until the point at which replication stops, resulting in fewer

mtDNA copies per cell. Also, the variability in our pol- γ expression data could relate to slight differences in developmental timing between experiments, resulting in some experiments being sampled before replication stops and some after.

This data also raises the interesting question of cell-type specific effects, as mitochondria themselves vary significantly between cell types [143]. One hypothesis is that mtDNA replication and removal rates are very different in different cell types. This theory is supported in the literature as mitochondrial turnover rates vary between tissue type in rats [144-146]. Another is that mtDNAs, and mitochondria themselves, are not recycled in certain tissues, as mitophagy has been shown not to occur in cultured primary neurons, and in galactose fed HeLa cells [110]. Thus, damaged genomes may persist in some cell types, resulting in impeded replication and reduced copy number in those cells. This is an intriguing hypothesis, as mitochondrial dysfunction specifically in neurons results in whole organism effects in *C. elegans* [89], and is implicated in many human diseases [52]. Additionally, many mitochondrial diseases have neurological components [6].

Lastly, a reduction in mtDNA copy number may be a signaling mediated, regulated response to environmental conditions. Supporting this theory, rotenone induced superoxide and H₂O₂ treatment of cultured mammalian cells induces strand breaks in mtDNA, leading to degradation of mitochondrial genomes [147].

2.3.3 ATP Levels and Oxygen Consumption

One of the most striking effects observed in response to early life mtDNA damage is the persistent reduction in steady state ATP levels. It is important to note that ATP levels are reduced even when mtDNA lesions are removed to below the limit of detection, and mtDNA encoded MRC transcript levels are at or above those in untreated nematodes. mtDNA copy number is reduced at this time, however this reduction, while statistically significant, is only approximately 20%. Data from our lab (not shown) indicate that a copy number reduction of this magnitude alone is not sufficient to reduce ATP levels. Though again, this does not take into account the possibility of cell type specific effects, and their potential to alter organismal biology.

Interestingly, oxygen consumption rates are not decreased as would be expected with decreased ATP levels, but are in fact increased. Combined with their complete lack of spare respiratory capacity, this suggests that the mitochondria in UVC exposed nematodes are functioning extremely inefficiently. Respiratory rates are at their maximum, yet ATP levels are still significantly lower than in unexposed nematodes. One explanation for this inefficiency is increased mitochondrial uncoupling. Uncoupling is the process of transporting H^+ back into the mitochondrial matrix by bypassing ATP synthase, and therefore reducing membrane potential without generating ATP [148]. Uncoupling is mediated by the uncoupling protein, UCP-1, in mammalian brown fat cells and is thought to function in thermogenesis [149]. Thermogenesis is not the only

function of uncoupling though, as is occurs in both endotherms and ectotherms [150]. There are 5 total UCP proteins (UCP-1, 2, 3, 4 and 5) in humans, and UCP-1, 2, and 3, are thought to play roles in mitochondrial uncoupling, while the functions of UCP-4 and 5 are still debated [151]. Importantly, uncoupling proteins are activated by both superoxide [152] and free fatty-acids [153] are generally considered a mechanism to mitigate mtROS production [150]. In *C. elegans*, reducing membrane potential is a common mechanism in lifespan extension and mild uncoupling actually induces lifespan extension [154]. This suggests that not only does uncoupling provide protection from mtROS generation, but that it may also induce pro-survival adaptations. *C. elegans* have only 1 ortholog to the human UCP proteins, encoded by the *Ucp-4* gene, though evidence suggests that it does not function to uncouple *C. elegans* mitochondria [151]. Instead, it is thought that uncoupling is mediated through the adenine nucleotide translocase (ANT-1), as it is a major contributor to basal mitochondrial proton conductance in mammalian muscle tissue [155].

2.3.4 A role for reactive oxygen species

Collectively our data suggest that ROS likely play a role in the persistent phenotypes of reduced ATP levels, increased oxygen consumption and sensitivity to mitochondrial poisons that result from developmental mtDNA damage in *C. elegans* (Figure 22). Increased oxygen consumption with reduced ATP production suggests significant mitochondrial inefficiency and / or uncoupling, both of which support the

theory or increased mtROS formation. Targeted metabolomics revealed increases in the organic acids malate and fumarate, and the amino acids aspartate and asparagine, suggesting UVC induced mtDNA damage results in the activation of the malate-aspartate shuttle. The malate-aspartate shuttle can be utilized to move malate into or out of the mitochondria. In the cytosol, malic enzyme can convert malate to pyruvate generating NADPH from NADP⁺ in the process. Furthermore, the malate-aspartate shuttle can be used to move NADH into the mitochondria, where reducing equivalents can be transferred from NADH to NADP⁺ via the nicotinamide nucleoside transhydrogenase (NNT) using energy from membrane potential, to generate NADPH inside the mitochondria [54, 156]. This is significant for an oxidative stress theory, as NADPH is required to reduce oxidized glutathione, a major component of the cellular defense mechanism against ROS. It should be noted that mitochondrial glutathione is essentially a separate from cytoplasmic glutathione [157], so its reduction largely takes place within the mitochondria. If there is significant oxidative stress resulting from UVC induced mtDNA damage, much of the reducing equivalent pool in the mitochondria could be used for reducing oxidized glutathione, making much less available for OXPHOS and ATP production, while at the same time depleting the mitochondrial membrane potential. However, for this to persist, enough ROS must be continually generated (likely via inefficient OXPHOS) to require reduced glutathione.

Alternatively, aberrant ROS generation during development could lead to signaling mediated metabolic alterations that program the developing nematode. ROS are both potentially toxic damaging agents as well as potent signaling molecules. Short term exposure to H₂O₂ in young nematodes induces oxidative stress and results in many similar outcomes to those seen here, including reduced movement and ATP levels, though these effects are transient [158].

While mtDNA is in close proximity to the MRC and could therefore be an important target for this ROS, it also undergoes relatively robust base excision repair. Notably, mtDNA mutations associated with aging have long been thought to originate from accumulation of oxidative damage, yet recent work investigating the patterns of rare mutations in mtDNA indicates this is not the case [142]. ROS also plays an important signaling role during development, and disruption of this signaling has been shown to alter differentiation and proliferation [39]. This represents another potential mechanism for perturbation via mtDNA damage.

2.3.5 DOHaD or lifespan extension and stress resistance

Based on these results, developmental mtDNA damage clearly supports the developmental origins of health and disease theory as opposed to lifespan extension by mitochondrial stress theory. This is not an altogether surprising result, as it is difficult to conceptualize how DNA damage could be beneficial. Likewise, the persistent reduction in ATP levels, along with the inefficiency of the MRC, resulting from developmental

mtDNA damage could certainly lead to adverse outcomes later in life. With inefficient or uncoupled mitochondria unable to maintain ATP levels without stress, any further insult that requires energy expenditure could be detrimental to the organism. This is evidenced by the sensitivity to oxidative stress seen in mitochondrial MRC mutants *mev-1* [133, 134], both of which are also short lived.

Much of the research pertaining to the DOHaD hypothesis has revolved around epigenetic mechanisms persistently altering metabolic function as a result of developmental nutritional deficiencies (reviewed in [98] and [159]). Until very recently it was believed that *C. elegans* did not methylate DNA, as studies had been unable to provide evidence of methylated cytosine residues in nematode DNA [160]. *C. elegans* do, however, methylate DNA though unlike methylation in other species it occurs on adenine as opposed to cytosine [161]. This raises the possibility of epigenetic alterations at the level of DNA methylation in *C. elegans* as a mechanism to alter gene expression, and should lead to expansion of the organisms use in this area. As additional evidence for the importance of epigenetic functions for responding to environmental stimuli, *daf-16* dependent lifespan extension relies on the chromatin remodeling complex SWI/SNF to alter gene expression and increase stress resistance [162].

C. elegans has been widely utilized in the study of aging and lifespan extension, and a major lifespan extending pathway involves the proteins of the MRC. An imbalance between nuclear and mitochondrial encoded subunits of the MRC leads to

activation of the mitochondrial unfolded protein response which triggers compensatory mechanisms that extend lifespan [20]. This is commonly achieved by knocking down genes for MRC subunits with RNA interference [20, 86, 89, 118], though some pharmacological treatments that alter NAD⁺ levels and Sirtuin protein activation have also been successful [119]. We note that the majority of these treatments, particularly the RNAi, result in major losses of protein. This is very different than what is seen in most human mitochondrial diseases that result from mutations in mitochondrial genes (whether mtDNA or nucDNA encoded). In fact, many *C. elegans* strains that harbor mutations in genes that when knocked down with RNAi result in lifespan extension, actually have reduced lifespans [118]. Interestingly though, some mutations in MRC subunit genes do lead to lifespan extension. Recent work demonstrates that a *nduf-7* (complex 1) mutation increases ROS, activates the UPR^{mt} and extends lifespan [163]. This suggests that different mutations can have differentially affect lifespan. Furthermore, lifespan extension in *C. elegans* is not always directly relevant to humans, as mutations in *elegans* mitochondrial genes that extend lifespan lead to shortened lifespan in humans [118]. Additionally, there are tradeoffs associated with extending lifespan. Reduced fertility, smaller adult size, and reduced movement are often seen in conjunction with lifespan extension. While RNAi mediated lifespan extension is scientifically intriguing, it seems as though it is less relevant to environmental exposures and toxicology.

2.3.6 Future directions

Our data indicate a role for NADPH and ROS in the persistent phenotypes seen as a result of mtDNA damage. If either NADPH or ROS stress are causative, rescue should be achievable by supplementing with antioxidants or reducing NADPH consumption. Treatment with Mito-Q, an antioxidant targeted to the mitochondria, during development may alleviate mtROS and should be explored. Furthermore, as NNT is required to reduce oxidized glutathione in the mitochondria, if mitochondrial ROS is significantly contributing the observed phenotypes then NNT mutants should be significantly more sensitive to UVC induced growth arrest. There are 3 NNT mutant strains of *C. elegans* commercially available that should be screened for growth arrest.

AMPK activation reduces NADPH consumption by blocking fatty acid synthesis, a major consumer of NADPH. The compound 5-Aminoimidazole-4-carboxamide 1- β -D-ribofuranoside (AICAR) activates AMPK, though experiments that treated *C. elegans* during development with AICAR lead to significant growth delay. Treatment after development may still rescue ATP levels and should be tested. Lastly, rapamycin induces autophagy, and autophagy is required for the removal of bulky lesions and dimers in mtDNA [9], therefore rapamycin treatment during development may increase mtDNA turnover resulting in increased rates of removal of damaged genomes.

Mitochondrial membrane potential measurements may further support the ROS hypothesis suggested above. If the model suggested is true, reduced membrane

potential would be expected, as ATP synthase, uncoupling proteins (ANT-1) and NNT would all be contributing to the movement of protons back into the matrix. Membrane potential has been measured in nematodes, though the accuracy of the methods used to do so are questionable. Likewise, ROS production measurements would be helpful, though they are also difficult to measure in whole nematodes.

In lieu of direct measurement of ROS production, measurement of ROS damage in the form of protein carbonyl or lipid peroxides would be beneficial. Oxiblots of mitochondrial proteins would be expected to show increased levels of oxidized proteins with time after UVC exposure. Lipid peroxidation can be measured via malondialdehyde production using many commercially available assays.

Lastly, as our metabolomics data indicate an increase in LCAC levels in UVC exposed samples, and NRTI's result in increased lipid storage, lipid accumulation should be measured in UVC exposed worms. Oil red O staining has been validated as a method to investigate fat storage in nematodes [164].

2.4 Methods

2.4.1 *C. elegans* Strains and Culture Conditions

Populations of *C. elegans* were maintained on K-agar plates seeded with *E. coli* OP50 bacteria, unless otherwise noted. N2 (wild-type), JK1107 *glp-1(q224)*, *sod-2(gk257 I)*, *sod-3 (gk235)*, *gas-1(fc21)*, *mev-1(Kn1)*, *glp-1(e2141)*, *daf-16(mu86)*, *skn-1(zu670)*, SJ4100 *zclS13[hsp-6::GFP]*, and SJ4058 *zclS9[hsp-60::GFP]* were obtained from the *Ceanorhabditis*

Genetics Center (CGC), University of Minnesota. PE255 *glp-4(bn2)* were provided by Christina Lagido, University of Aberdeen (Aberdeen, UK). The *sod-2/3* [*sod-2(gk257)* I; *sod-3* (tm760) X] double mutant strain and *sod-1/4/5* triple mutant strain [*sod-1*(tm776) ;*sod-5*(tm1146) II; *sod-4*(gk101) III] were a kind gift from Bart Braeckman (Ghent University, Ghent, Belgium).

2.4.2 UVC Exposure

UVC exposures are conducted in a custom-built exposure cabinet. UVC output is measured with a UVX radiometer (UVP, Upland, CA) and used to calculate length of exposure required to achieve the desired dose. Synchronized L1 nematodes are maintained on plates that contain no bacterial food, and therefore do not develop, and are exposed to for the calculated time. This exposure is repeated 24 hours later, and again 24 hours after that. Nematodes are then transferred to plates that contain OP50 *E. coli* as a food source and begin development. This serial exposure protocol, with sufficient time between doses, allows for the repair of nucDNA lesions, while lesions in mtDNA go unrepaired and thus accumulate [9].

2.4.3 DNA Damage Assay

Mitochondrial and nuclear DNA damage levels were measured essentially as previously described [165-167] with some exceptions. The assay is based on the quantitative amplification of large PCR products (10 kb or larger) from both the mtDNA

and nucDNA. DNA damage impedes the progress of the polymerase, therefore resulting in quantitatively less product with increasing amounts of DNA damage.

6-9 nematodes are picked into PCR tubes containing 90 uL of lysis buffer (25mM Tricine, 80mM KoAc, 10% wt/vol glycerol, 2.25% vol/vol DMSO, 1 ug/mL Proteinase K (Qiagen)) and quickly frozen at -80°C for at least 10 minutes. Samples are then heated in a thermal-cycler to 65°C for 1 hour, followed by 95°C for 15 minutes. This crude worm lysate is used as template for the long-amplicon quantitative PCR assay.

Lysate (5 uL) is added to PCR reactions containing the following: 25 uL LongAmp Hot Start Master Mix (New England Biolabs, Ipswich, MA), 2 uL each Forward and Reverse primer (10 uM stock, 0.4 uM final. Primers are genome specific, sequences in (Table 2)), and 16 uL sterile, molecular biology grade water. "50% control" reactions must always be run to assure that the reaction is stopped during the exponential phase and is thus truly quantitative. 50% control reactions consist of undamaged worm lysate diluted 1:1 with water. No template controls are also run. Reactions are cycled in a Biometra T1 Thermocycler (Biometra GmbH, Göttingen, Germany) as follows: 94°C for 3 mins, followed by the optimized number of cycles (26-28) of 94°C for 15sec, annealing temperature (68°C) for 12 min, followed by a final extension for 10 min at 72°C. and then held at 4°C. The exact number of cycles required will vary somewhat between experiments due to life stage and strain differences and

must therefore be optimized. The number of cycles is acceptable when the 50% control reactions result in 40-60% of the product of undamaged controls.

PCR products are quantified using Quant-it Pico Green (Invitrogen, Carlsbad, CA). Pico green values are normalized to genome copy number (see below for protocol), and relative amplification is used to calculate DNA lesion frequency as previously described [167].

2.4.4 Genome Copy number

mtDNA and nucDNA copy numbers were measured at 2, 4, 6, 8, and 10 days post final UVC exposure as previously described [168]. Briefly, 6 worms were transferred to 90 μ L proteinase K-containing lysis buffer using a platinum worm pick, and lysed and digested by freezing at -80°C followed by thawing, and incubation at 65°C for one hour. Crude worm lysate was used as template DNA for real-time PCR based determination of mtDNA and nucDNA copy numbers. A plasmid-based standard curve for mtDNA is employed, allowing for the determination of absolute mtDNA copy number [168]. 3 samples per treatment per time point were measured in triplicate PCR reactions and averaged. 3 individual experiments were performed. Primer sequences can be found in (Table 2).

2.4.5 ATP Levels

ATP levels were measured in 2 different strains, by 2 different methods.

First, using the JK1107 *glp-1(q224)* strain, ATP levels were determined as described in [169] at 4 and 8 days post final UVC dose. Briefly, approximately 500 worms were washed and resuspended in 100 μ L of K-medium, snap frozen in liquid nitrogen, and stored at -80°C . Samples were removed from the freezer and 200 μ L 10% trichloroacetic acid (TCA) was added while samples were still frozen, and allowed to thaw on ice. 0.5mm diameter zirconia beads were added to each sample (approx. 250 μ L), and two 30 second pulses at maximum speed in a Bullet Blender (Next Advance, Averill Park, NY) were performed to lyse the worms. Lysates were neutralized by the addition of 100 μ L of 1.33 mM KHCO_3 and 100 μ L Sigma water (St. Louis, MO, USA). 50 μ L-150 μ L aliquots were removed at this time for total protein determination. Samples were vacuum centrifuged for 10 minutes to remove bubbles, and then centrifuged at 14,000 rpm for 8 minutes at 4°C to pellet protein. The ATP containing supernatants were removed and transferred to sterile tubes. ATP was measured from 1:50 and 1:100 dilutions of these samples using the Molecular Probes ATP determination Kit (Invitrogen/Life Technologies, Carlsbad, CA, USA). Luminescence was measured every 2 minutes for 30 minutes after the addition of the luciferin/luciferase reagent using a FLUOstar Optima plate reader (BMG Labtech, Offenburg, Germany) equipped with a luminescence optic. ATP concentrations were determined by comparing luminescence values to an ATP standard curve measured at the same time points. The calculated ATP concentrations were then averaged over the 15 time points, and normalized to total

protein concentrations as measured with the BCA method (Thermo Fisher Scientific, Rockford, IL.). One or two technical replicates (averaged) were performed in 3 separate experiments, resulting in a statistical n of 3.

Second, the firefly luciferase expressing PE255 *glp-4(bn2)* strain was used to investigate relative, steady state ATP levels *in vivo*, in live nematodes at 2, 4, 6, 8, 10 and 12 days post final UVC dose, as previously described [9, 85, 170]. Worms were washed with K-medium, and approximately 100 worms in 100 μ L K-medium were aliquoted into wells of a white 96 well plate. 4 to 5 technical replicates (wells) were averaged per treatment per time point. All measurements were made using a FLUOstar Optima microplate reader. First, GFP fluorescence was measured with an excitation wavelength of 485 nm and an emission wavelength of 520 nm. Then, luminescence was measured 3 minutes after the automated addition of luminescence buffer consisting of citrate-phosphate buffer (pH 6.5), 0.1 mM D-luciferin, 1% DMSO, and 0.05% Triton-X. Luminescence values were normalized to GFP fluorescence at each time point, as the transgene expressed in the PE255 *glp-1(bn2)* strain is a luciferase-GFP fusion, and consequently GFP fluorescence can be used to control for the amount of luciferase enzyme in each well. Four individual experiments were conducted.

2.4.6 Oxygen Consumption

Oxygen consumption was measured using a Seahorse Biosciences XF^e24 extracellular flux analyzer. Nematodes were rinsed off of K-agar plates and washed

twice in K-media, then were incubated in k-media at 25°C for approximately 30 minutes to allow for gut clearance. They were then washed again with 25°C bicarbonate free EPA-H₂O, counted and diluted to approximately 1 worm / μ L in the same solution. The dilutions were counted again to achieve a more accurate count, and worms were aliquoted into seahorse V7e plates. Worm density used was between 25 and 35 worms per well, in an initial volume of 525 μ L. 7 wells were measured for each treatment at each time point. The nematodes were then incubated at 25°C for 30 minutes prior to starting the Seahorse run.

Basal respiration was measured 10 times for 3 minutes over a period of approximately 70 minutes. In between each measurement the samples were mixed to re-oxygenate the media, and the nematodes were allowed to settle to the bottom of the wells. The first 2 measurements were not used to calculate the basal respiration rate, as they were observed to be highly variable. The following 8 measurements were averaged to obtain a basal respiratory rate for each sample.

Following the final basal respiratory measurement, FCCP (in 2%DMSO) is injected into each well at a final concentration of 15 μ M, and 8 respiratory rate measurements are made as described above. Again, the first 2 measurements were not used to calculate the average FCCP induced respiratory rate.

Finally, 10mM sodium azide (final) is injected into each well and 4 respiratory rate measurements are recorded and averaged.

2.4.7 Gene Expression Assays

RNA was isolated from between 1000 and 2000 nematodes. Briefly, worms are washed off of agar plates with K-media and rocked at room temperature for 20 minutes to clear gut contents. Worms are then washed 3 times in fresh K-media, pelleted, resuspended in 500uL Qiagen buffer RLT with 1% 2-mercaptoethanol added, and flash frozen in liquid nitrogen. Samples are thawed and zirconia beads are added at an approximate 1:1 volume. Samples are homogenized in the Bullet Blender (NextAdvance, Averill Park, NY) for 1 minute, and this is repeated 3-5 times. Samples are placed on ice for 1 minute between homogenizations, and drops of worm suspension are monitored under a dissecting microscope for lysis. When worms are sufficiently lysed, the lysate is removed from the beads, transferred to a fresh tube, and incubated at room temperature for 10 minutes. Samples are centrifuged at 12,000 x G for 15 minutes at 4°C, and the aqueous phase is transferred to a fresh tube. 1 volume of 70% ethanol is added, and the samples are then processed according to the Qiagen RNeasy Min Kit protocol.

cDNA was created from 100 ng of the isolated RNA using the High Capacity Reverse Transcription kit (Life Technologies) as per the manufacturer's instructions. Gene expression was measured via real-time PCR using the Power SYBR Green PCR Master Mix (Life Technologies). Changes in expression levels are calculated based on the standard delta-delta-cT method, compared to housekeeping genes *cdc-42* and *pmp-3*. Primer sequences and PCR conditions can be found in Table 3.

2.4.8 Targeted Metabolomics

At 4 and 8 days post exposure control and UVC exposed nematodes (approximately 7500 for each sample) were washed off of OP50 plates, allowed to settle, and were washed twice more with K media. They were then incubated in K-media at 20°C for 30 minutes to allow for gut clearance, spun down at 2200 x G for 2 minutes, and washed twice in ice cold PBS. The supernatant was removed, the pellet resuspended in 0.6% formic acid, and samples were stored at -80°C. Samples were thawed on ice and lysed by sonication and aliquots were removed for total protein determination. 270 uL acetonitrile was added to each sample, they were vortexed for 1 minute and centrifuged at 15,000 x G for 10 minutes to pellet proteins. Samples were then delivered to the Duke metabolomics core facility where organic acids, amino acids and acyl-carnitines were measured via LC-MS using standard methods. Metabolite levels were normalized to total protein as determined by BCA (Thermo Scientific, Rockford, IL) and fold changes compared to day 4 control samples were calculated.

2.4.9 Growth and Size Assays

Growth assays are conducted using 2 different methods. The first uses a COPAS Biosorter (Union Biometrica, Holliston, MA), which, much like a flow cytometer, measures extinction and time of flight of individual *C. elegans*. These parameters can be used as estimates of nematode size. After UVC exposure, nematodes are measured in the Biosorter at various time points, and the effect of treatment is assessed by comparing

size to that of untreated controls non-parametrically. The second method, which is also used to measure adult nematode size, involves freezing small aliquots of nematodes at the time points of interest, and then thawing and imaging at 10x magnification on a Zeiss Axioskop. Images were analyzed and nematode length measured using NIS elements BR software (Nikon Inc. Melville, NY, USA). Results are compared in the same manner as Biosorter generated results.

While nematode size is linked to growth and development, it should be noted that the relationship is not linear and therefore care must be taken when comparing growth delay between strains that do not develop at the same rate. Furthermore, it is not a direct reflection of larval development, as progression through developmental stages is not entirely dependent on an increase in overall size. It is, however, an excellent indicator of, and provides a fast and powerful screening mechanism for development.

2.4.10 Survival

Survival assays were conducted 4 days after the 3rd and final UVC dose. 10-15 nematodes were transferred to plates containing either rotenone or paraquat that were seeded with UVC killed *uvrA* deficient OP50 *E. coli* to prevent the bacteria from metabolizing the chemicals. Nematodes were scored for survival 24 hours later, and were counted as dead if they did not respond (move) to gentle prodding with a worm pick.

2.4.11 Rescue Assays

Rescue assays were conducted with the mTOR activator rapamycin and the AMPK activator AICAR. Exposures were carried out in the same manner as for other experiments, and after the 3rd UVC dose nematodes were transferred to seeded plates that either contained 100 uM rapamycin or 1 mM 5-Aminoimidazole-4-carboxamide 1- β -D-ribofuranoside (AICAR) or nothing. The rapamycin plates were seeded with live OP50 bacteria [171], while the AICAR plates were seeded with UVC killed *uvr-A* deficient OP50 bacteria to prevent metabolism of the compound by the bacteria. Size measurements were then taken at 4 days post exposure.

The AICAR treatment resulted in significant growth arrest (data not shown) and was therefore not continued. Instead, control and UVC treated PE255 *glp-1(bn2)* nematodes were exposed to AICAR 3 days post UVC exposure, and ATP levels were measured 24 hours later as described above.

Table 1: Targets for Transcriptional Regulation of Intermediary Metabolism

Gene	Name / Function	Pathway
<i>pdhk-2</i>	Pyruvate Dehydrogenase Kinase - phosphorylates Pyruvate Dehydrogenase Complex (PDC) to inactivate	TCA Cycle
<i>pdp-1</i>	Pyruvate Dehydrogenase Phosphatase - dephosphorylates PDC to activate	TCA Cycle
<i>acs-2</i>	acyl-CoA synthetase	Fatty Acid Oxidation
<i>gei-7</i>	isocitrate lyase / malate synthase	Glyoxylate cycle
<i>gpd-3</i>	Glyceraldehyde 3- Phosphate Dehydrogenase	Glycolysis

PEPCK	Phosphoenolpyruvate carboxykinase	Gluconeogenesis
-------	-----------------------------------	-----------------

Table 2: Primers for DNA Damage and Copy Number Assays in *C. elegans*

Target	Direction	Sequence (5'-3')	Annealing Temp. (°C)	Ref.
mtDNA, long (10.9 kb)	F	CCATCAATTGCCCAAAGGGGAGT	64	[165]
	R	TGTCCTCAAGGCTACCACCTTCTTCA		
nucDNA, long (9.3 kb)	F	TGGCTGGAACGAACCGAACCAT	64	[165]
	R	GGC GGT TGT GGA GTG TGG GAA G		
mtDNA, short (75 bps)	F	AGCGTCATTTATTGGGAAGAAGAC	60	[172]
	R	AAGCTTGTGCTAATCCCATAAATGT		
nucDNA, short (164 bps)	F	GCCGACTGGAAGAACTTGTC	60	[173]
	R	GCG GAG ATC ACC TTCCAG TA		

Table 3: Real Time PCR Primers for Gene Expression

<u>Gene</u>	<u>Direction</u>	<u>5'-3' Seq</u>	<u>Amplicon Size</u>
acs-2	F	GGCACACCGACCATGTTTAT	194
	R	ATGGTGA CTAGAGGGGATGTC	
C34B2.8	F	CTTTTCCGAAGCTTGTCTGG	197
	R	CTTGCCAACAATTTGAGC	
ctb-1	F	TTCCAATTTGAGGGCCA ACT	116
	R	AACTAGAATAGCTCACGGCAATAAAAA	
D2030.4	F	GCGAGATGAAGGCTACTTGG	115
	R	GGTGCATTTTGGGTTTGG	
K09A9.5 (gas-1)	F	AGTCATCATCAAGGCCATCC	185
	R	TTGTTGGGATGTCAATACCG	
gei-7 (icl-1)	F	TGCTCATCCAGGATTGGTGC	198
	R	CTGAGCCAAGAGTCGAGGTATCCA	
gpd-3	F	CCAGTACGATTCCACTCACGGA	104
	R	CTGGGTCTCTTGAGTTGTAGACCTT	
hmg-5 (TFAM)	F	TGTCTGGAGCTGGAATGGAA	108
	R	GCTTCTTCGCTTCGTCTGTG	
hsp-16.2	F	CGCCAAAGAAAGAAGCGGTT	60
	R	CTTCGACGATTGCCTGTTGA	
hsp-16.41	F	TGGACGA ACTCACTGGATCTG	133
	R	TGAGAGACATCGAGTTGAACCG	
hsp-4	F	CGTTC AAGATCGTCGACAAGT	138
	R	GACCAAGGTAGGATTCGGCA	
hsp-6	F	TCGTGTCATCAACGAGCCAA	76
	R	AGCGATGATCTTATCTCCAGCG	
hsp-60a	F	AGGCTCTTACCACTCTTGTCT	123
	R	CTCCCGTCGCAATTCCCATA	
hsp-60b	F	CCAAGAAGGTCACCATCACC	64
	R	TCTGTTTGATCTCCACGCC	
mev-1 (sdhC-1)	F	GTTGGACAGATCTACAAATCGGG	100
	R	TCTTGTTGCTCTTGTTCTGGC	
nd-5	F	TTAGCAAGTTTGGTCGAAGAAGATT	88
	R	GGCCCAAAGTAACTATTGAAAAACC	
pck-1	F	GGGACTTCCACGTCCAGTTAAGCAA	117
	R	TAGCCCGAGCCGAATGACCA	
pdhk-2	F	CGAAACAATGGCTGAAGGAT	208

	R	CACATCACAGGCAGGATCAA	
pdp-1	F	CTCACGATGGAATGCTGATG	109
	R	TGGATTATTTGCGGCTAGTTG	
polg-1	F	CTGCCTAATACCGTTGCCTTCTT	
	R	AATCCGGACGGCTCCAA	
sdhA-1	F	TCGCAGCTCAAGGAGGAATC	115
	R	ATGGCATCCTGATCTCCGAG	
sdhB-1	F	ATGCAAGCCTACAGATGGGT	148
	R	CCTTAGCTGGGTTCAAGTGTTTT	
sdhD-1	F	CCAGAAGCGCTCCAAGAATC	112
	R	GCCCAAAGACGTTCAAGCTTA	
cdc-42	F	GAGAAAAATGGGTGCCTGAA	111
	R	CTCGAGCATTCTGGATCAT	
pmp-3	F	GTTCCCGTGTTTCATCACTCAT	115
	R	TCTACAGCTTCTCGACGGTGT	

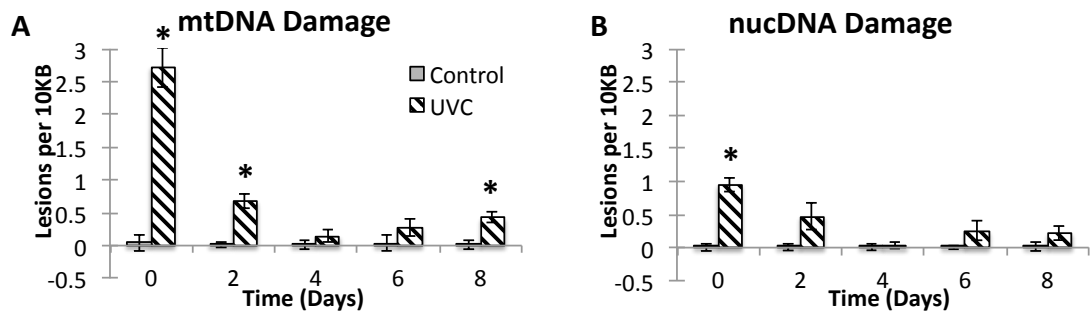


Figure 1: UVC induced mtDNA damage is removed, yet re-occurs later in life.

A. UVC induces mtDNA damage that is not repaired but is removed slowly and is undetectable by 4 days post exposure. However, damage is present again later in life at 8 days post exposure. **B.** nucDNA damage is quickly repaired. A 3 factor ANOVA indicates a significant interaction term for treatment x time x genome. Asterisks denote significant differences at each time point by post hoc T-tests, $p < 0.05$. Error bars +/- SEM.

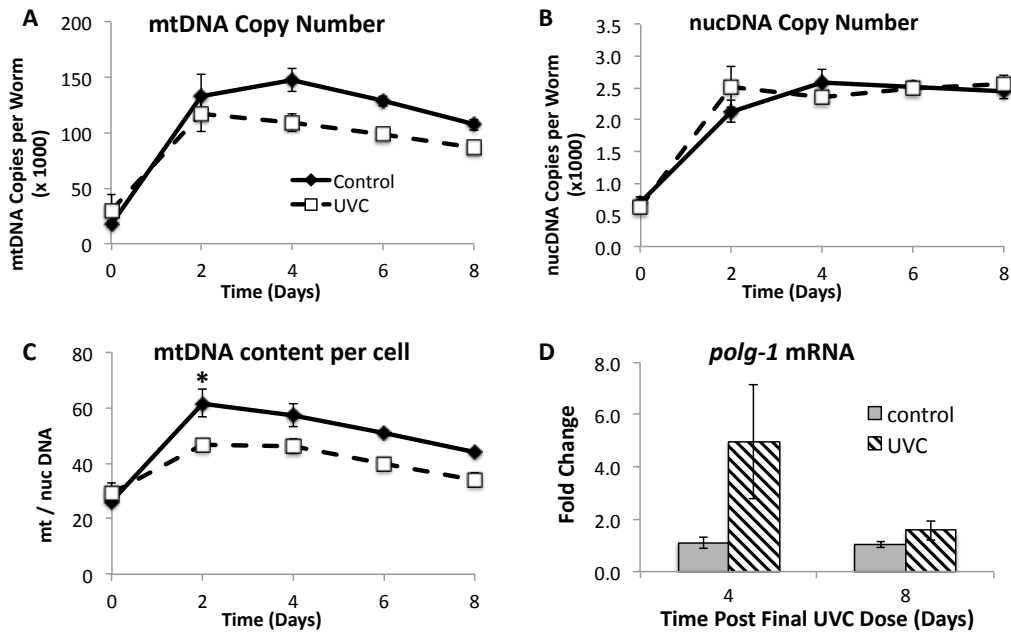


Figure 2: mtDNA damage during development permanently reduces mtDNA/nucDNA copy number ratio in JK1107 *glp-1(q224)* nematodes.

A. mtDNA copy number is reduced (main effect of treatment $p < 0.005$ by 2 way ANOVA) **B.** nucDNA copy number is not changed **C.** mtDNA / nucDNA copy number ratio is reduced (main effect of treatment $p < 0.001$, time $p < 0.001$, and interaction $p < 0.04$). This persists for the length of the experiment, and **D.** occurs despite a large (but variable) transcriptional induction of the mitochondrial DNA polymerase gamma (*polg-1*). Asterisks denote significant differences at each time point by post hoc T-test, $p < 0.05$. Error bars +/- SEM.

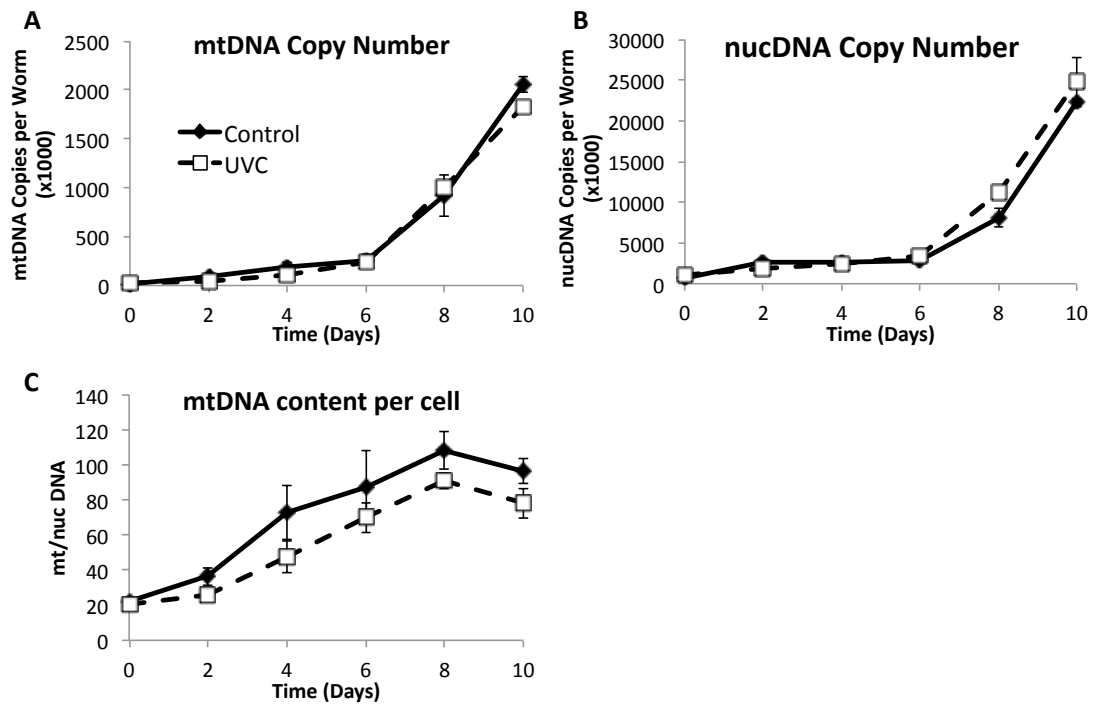


Figure 3: mtDNA damage during development permanently reduces mtDNA/nucDNA copy number ratio in PE255 *glp-4* nematodes.

A. mtDNA copy number and **B.** nucDNA copy number are not changed in response to UVC exposure in PE255 *glp-4(bn2)* nematodes. **C.** However, mtDNA / nucDNA ratio is significantly reduced (main effect of treatment $p < 0.05$ by 2 way ANOVA). Error bars +/- SEM.

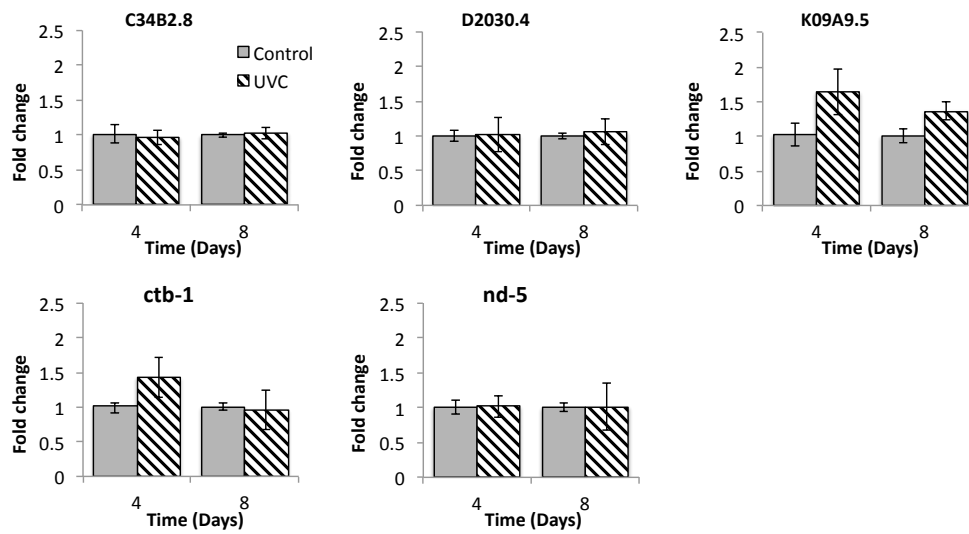


Figure 4: UVC induced mtDNA damage does not change mitochondrial respiratory chain transcript levels

Transcript levels of mitochondrial respiratory chain genes encoded in nucDNA (C34B2.8, D2030.4, K09A9.5) and mtDNA (*ctb-1*, *nd-5*) are not changed in response to UVC exposure. Error bars +/- SEM.

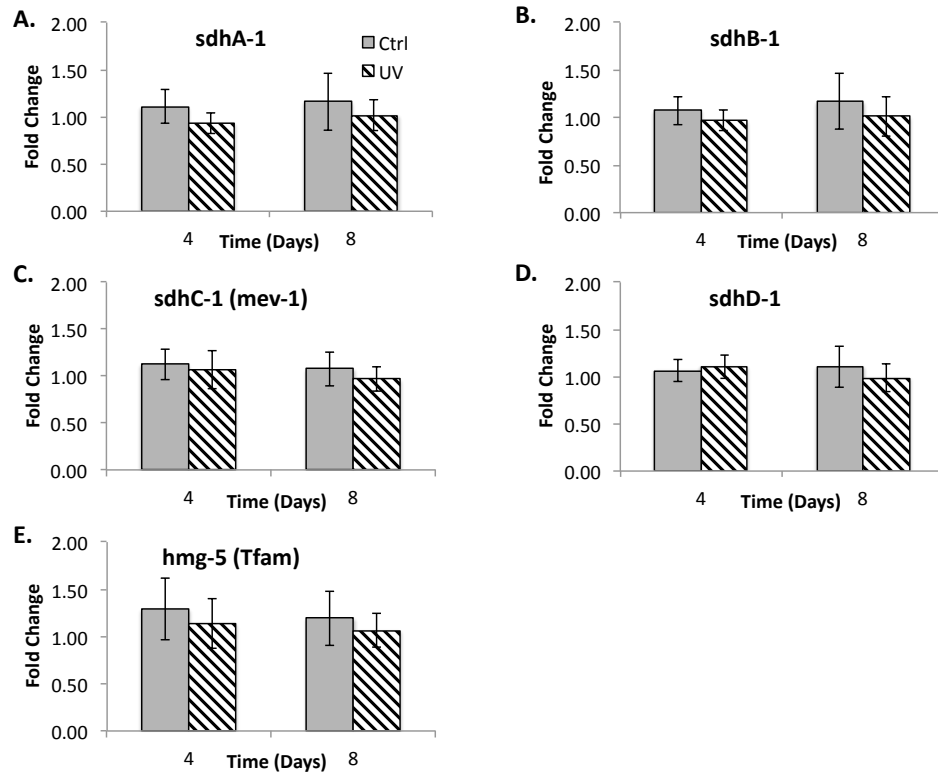


Figure 5: Complex II and Tfam Transcript Levels

A, B, C, D. Transcript levels of subunits of complex 2 of the mitochondrial respiratory chain are not changed in response to UVC exposure. **E.** Transcript levels of *hmg-5*, the nematode homologue of Tfam (a structural component of the nucleoid and the transcription factor for mtDNA) is also unchanged. Error bars +/- SEM.

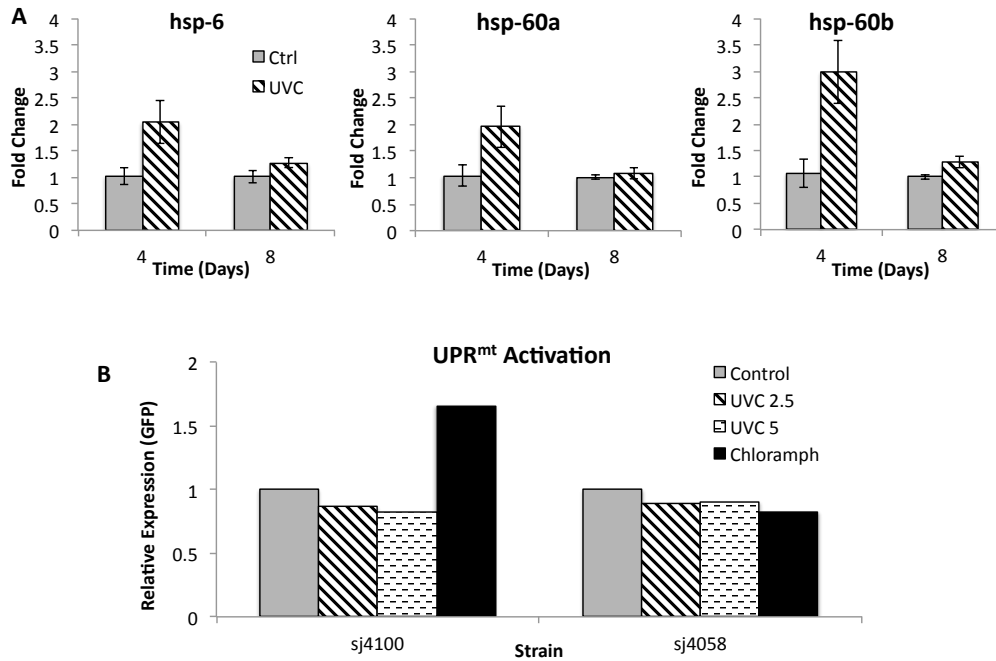


Figure 6: Mitochondrial Unfolded Protein Response

A. Transcript levels of mitochondrial chaperone proteins Hsp-6, Hsp-60a, and Hsp-60b appear to be increased however these results are not statistically significant. **B.** UPR^{mt} activation was measured with Hsp-6 (SJ4100) and Hsp-60 (SJ4058) GFP fusion reporters. UVC exposures of 2.5 and 5 J/m² did not increase GFP expression in either strain, while chloramphenicol (positive control) did in SJ4100. UVC exposure of 7.5 J/m² induced significant larval arrest in SJ4100 nematodes. Error bars +/- SEM.

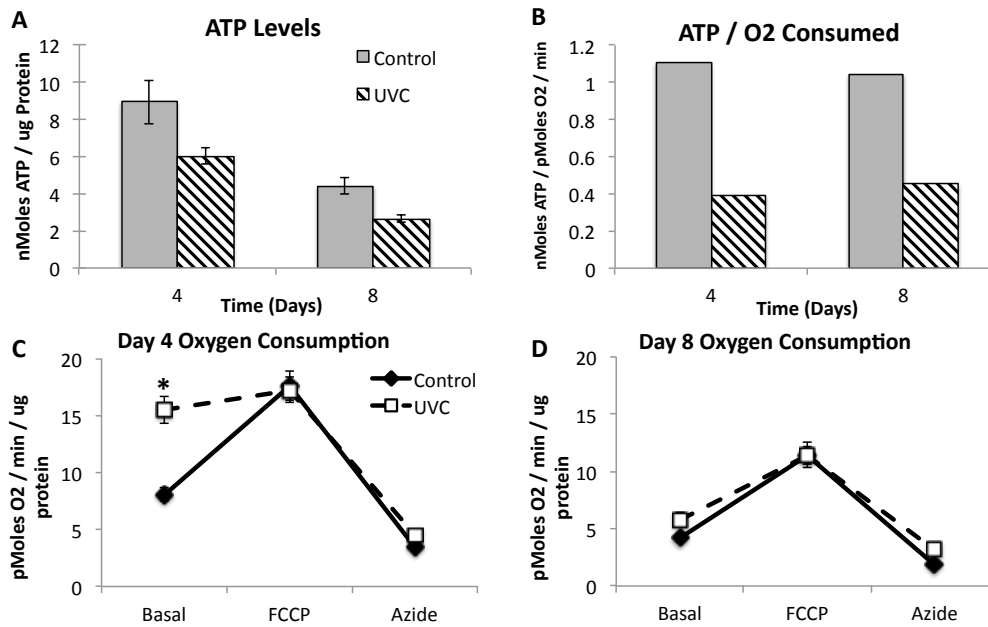


Figure 7: ATP Levels are reduced, however oxygen consumption is increased.

A. UVC exposure significantly lowers ATP levels in JK1107 (main effect of treatment $p < .002$ by 2 way ANOVA) **C.** However, basal respiratory rates were significantly increased in UVC exposed nematodes at 4 days post treatment ($p < .05$), **D.** but not at 8 days. Furthermore, maximal respiratory rates were significantly higher than basal in control nematodes ($p < .05$), but not in UVC exposed, indicating a lack of spare capacity. **B.** Illustrates the relationship between ATP produced and oxygen consumed. Importantly, on day 8 post exposure this ratio is still reduced in UVC exposed nematodes even though respiratory rates have declined to that of controls. Asterisks denote significant differences at each time point by post hoc T-test, $p < 0.05$. Error bars \pm SEM.

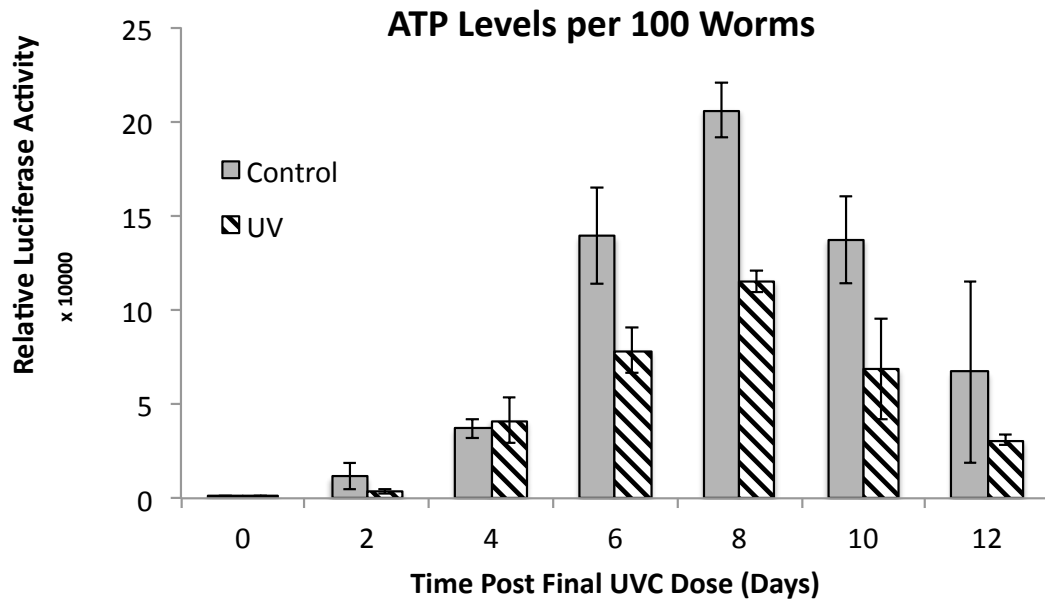


Figure 8: ATP levels are permanently reduced in PE255 *glp-4* nematodes.

UVC exposure significantly lowers ATP levels in PE255 *glp4(bn2)* nematodes (main effect of treatment $p < .03$ by 2 way ANOVA). Again, this reduction persists for as long as the experiments were conducted, in this case 12 days. Error bars +/- SEM.

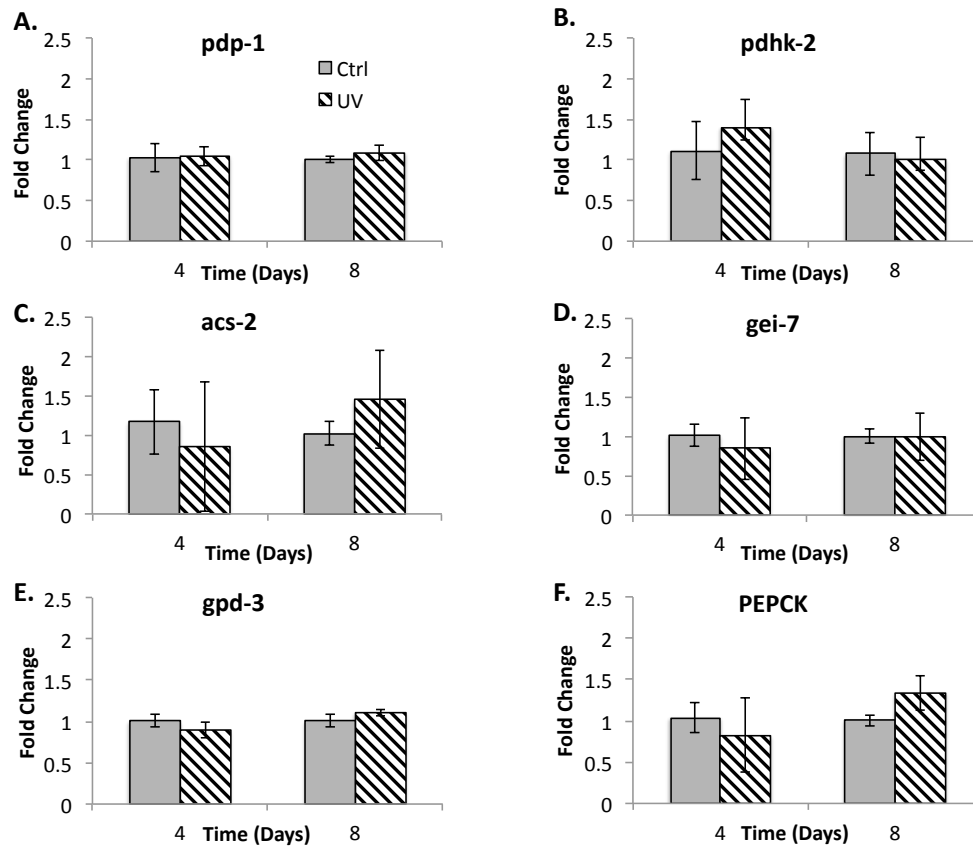


Figure 9: No evidence of transcriptional regulation of intermediary metabolism genes.

Transcript levels are unchanged after UVC exposure for: **A.** *pdp-1*; pyruvate dehydrogenase phosphatase, dephosphorylates pyruvate dehydrogenase complex (PDC) to activate, drives TCA cycle. **B.** *pdhk-2*; pyruvate dehydrogenase kinase, phosphorylates PDC to inactivate, reduces TCA cycle. **C.** *acs-2*; Acyl-CoA synthetase, measure of beta-oxidation of fatty acids. **D.** *gei-7*; isocitrate lyase / malate synthase, dual function enzyme of the glyoxylate cycle. **E.** *gpd-3*; glyceraldehyde 3-phosphate dehydrogenase, marker of glycolysis. **F.** *PEPCK*; phosphoenolpyruvate carboxykinase, required for gluconeogenesis. Error bars +/- SEM.

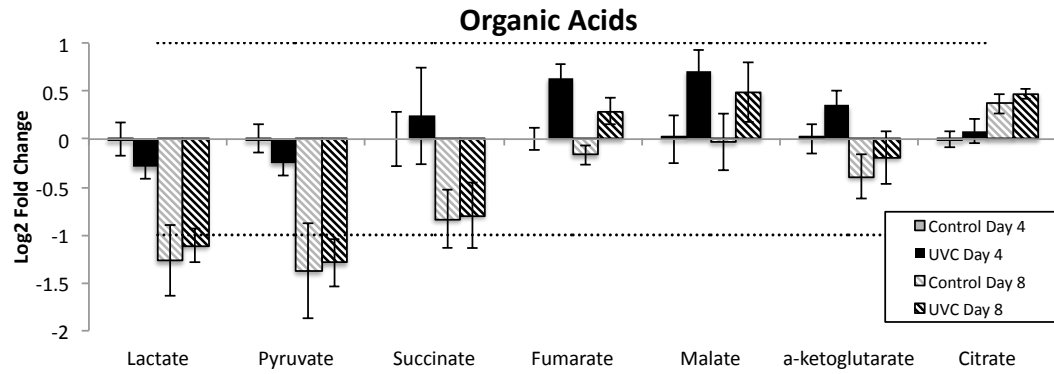


Figure 10: Organic Acid Levels.

Malate and fumarate are increased in response to UVC at both 4 and 8 days post exposure. Lactate, pyruvate, and succinate declined with age but there was no effect of UVC treatment.

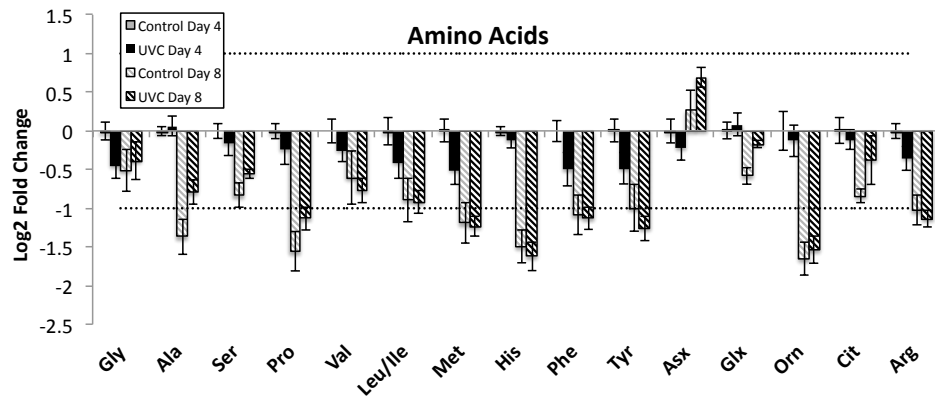


Figure 11: Amino Acid Levels.

Generally, amino acid levels appear to decline with age, however Asx increases in both control and UVC exposed nematodes at day 8. Though not statistically significant, Asx levels in UVC treated samples appear elevated compared to controls at day 8. Asx includes both asparagine and aspartic acid (aspartate).

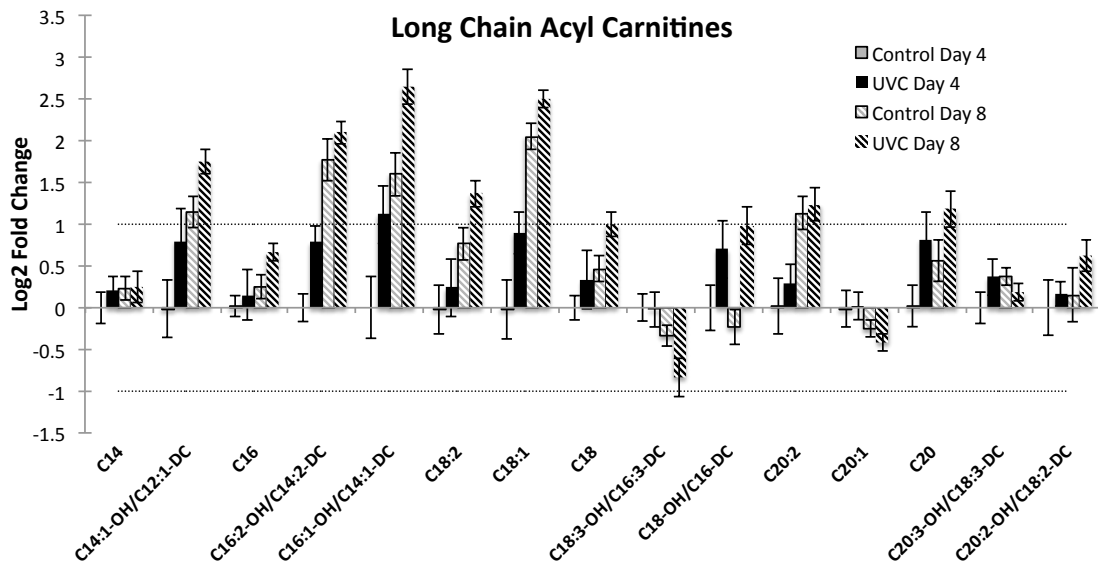


Figure 12: Long Chain acyl-Carnitine Levels

Increases are seen in a number of long chain acyl-carnitines after UVC at both 4 and 8 days post exposure.

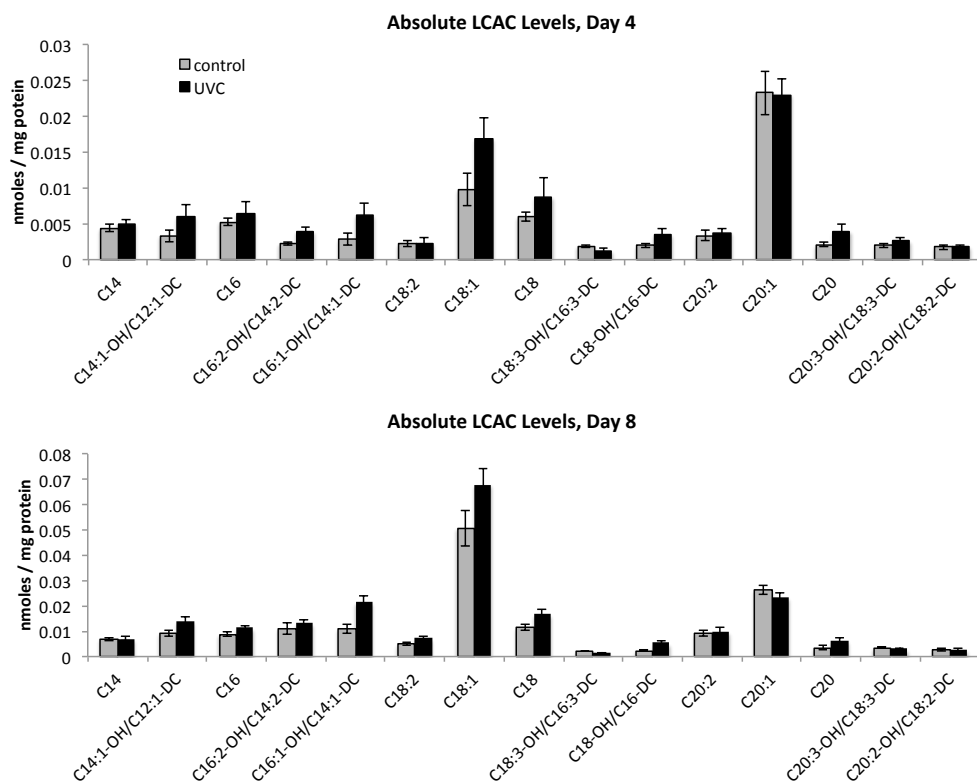


Figure 13: Absolute LCAC Levels

Increases in abundant LCAC species C18 and C18:1 are revealed when absolute LCAC levels are compared.

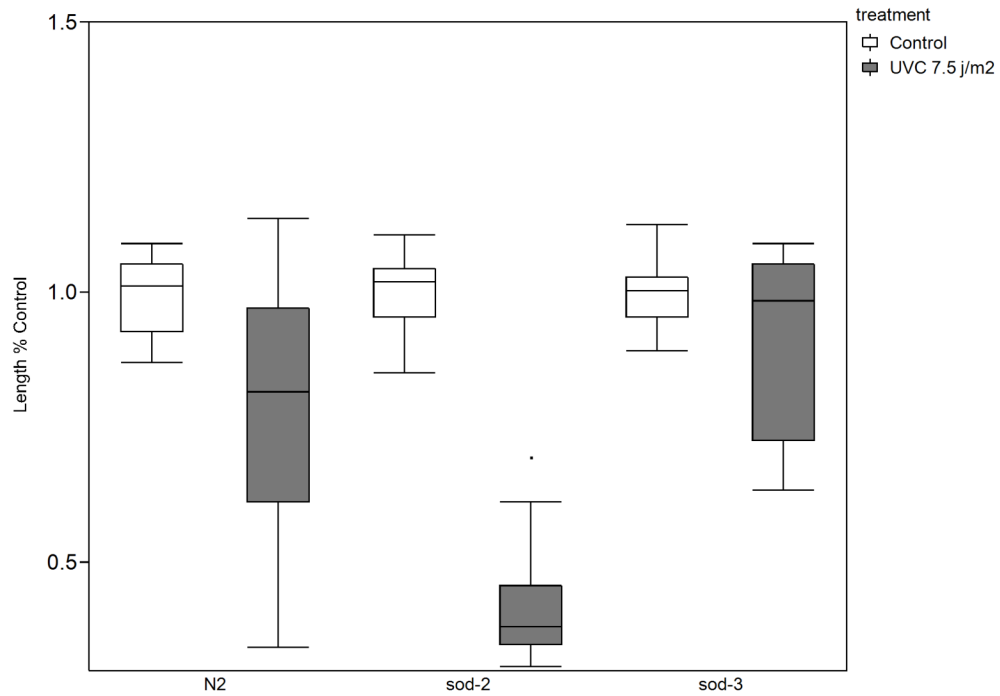


Figure 14: *sod-2* mutants are more sensitive to UVC exposure

Sod-2 mutants are significantly more sensitive to UVC exposure, though *sod-3* mutants are not, as measured by developmental delay ($p < 0.001$ Mann Whitney U test with bonferroni correction). Nematodes were flash frozen and then placed on a microscope slide and measured at 10x magnification, differences in percent control growth reduction were compared.

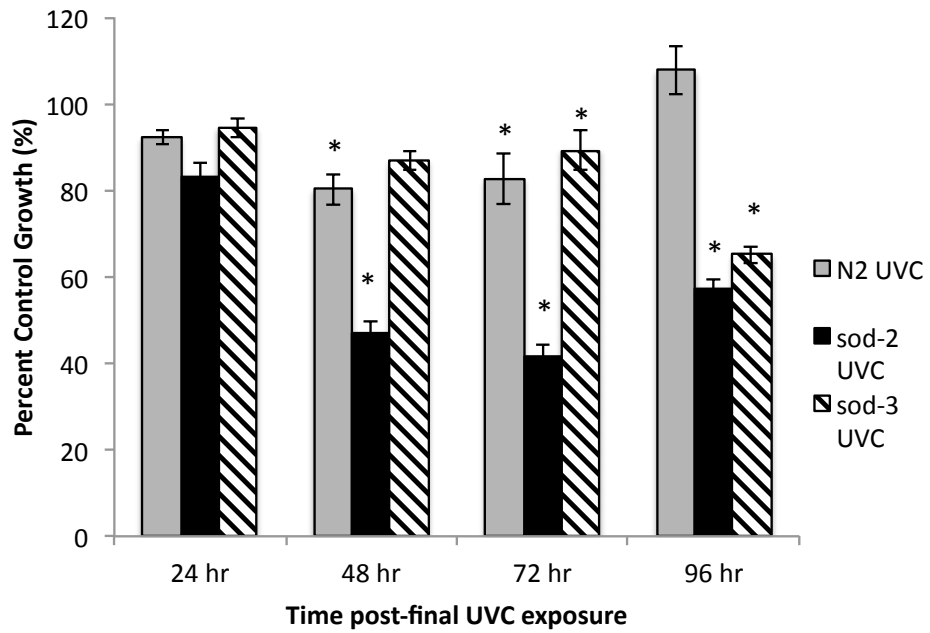


Figure 15: *sod-2* and *sod-3* mutants are more sensitive to UVC induced growth delay 96 hours post exposure

Percent control growth of N2, *sod-2*, and *sod-3* after 3 exposures to 7.5 J/m² UVC (n=15). *Indicates statistically significant difference between control and UVC at $\alpha = 0.05$. Adapted from Donoghue, 2014 [130].

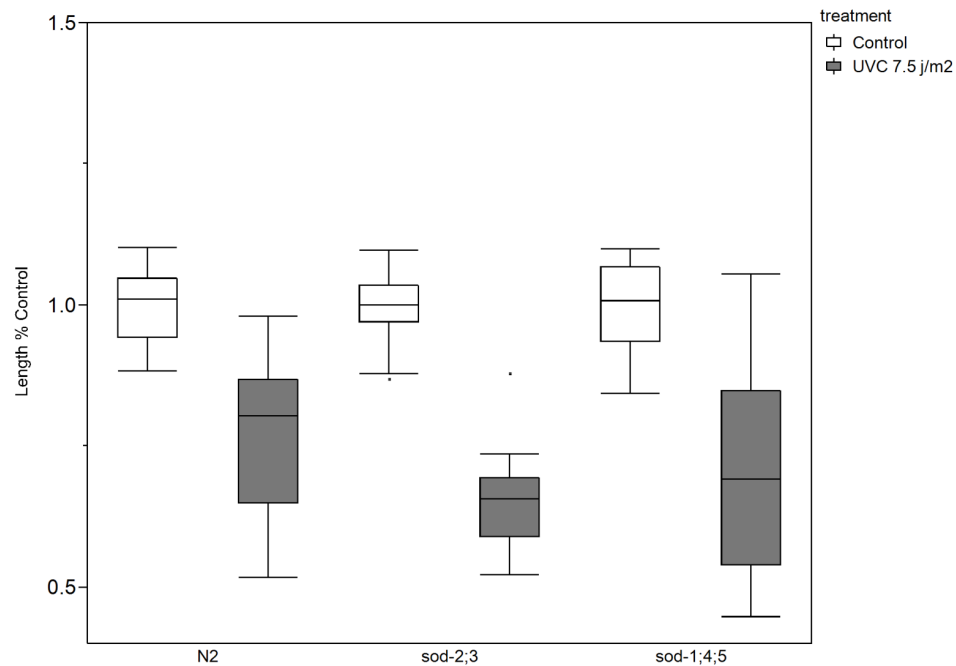


Figure 16: Mitochondrial SOD mutants are more sensitive to UVC

The mitochondrial SOD double mutant, *sod-2;3*, is more sensitive to UVC induced growth delay than wild type N2 ($p < 0.001$ Mann Whitney U test with bonferroni correction), though the cytosolic and intracellular combination knockout (*sod 1;4;5*) is not ($p < 0.15$). Nematodes were flash frozen and then placed on a microscope slide and measured at 10x magnification, differences in percent control growth reduction were compared.

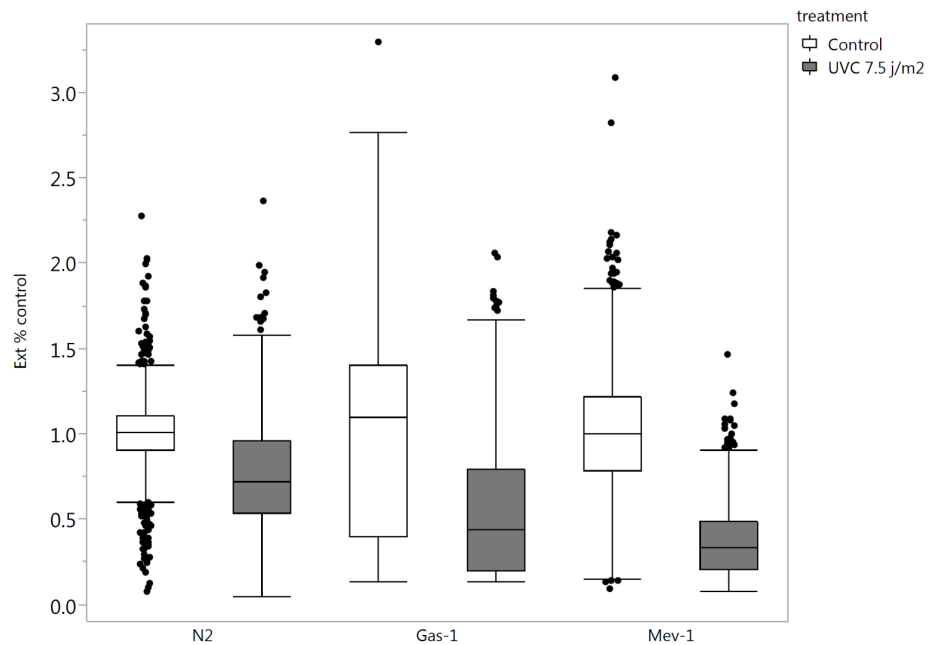


Figure 17: MRC mutants are more sensitive to UVC

Both *gas-1* and *mev-1* are statistically more sensitive to UVC induced growth delay than N2 ($p < 0.0001$, $p < 0.0001$, respectively, Mann Whitney U test with bonferroni correction). Nematodes were measured using the COPAS Biosort, and percent control extinction was compared between treatments.

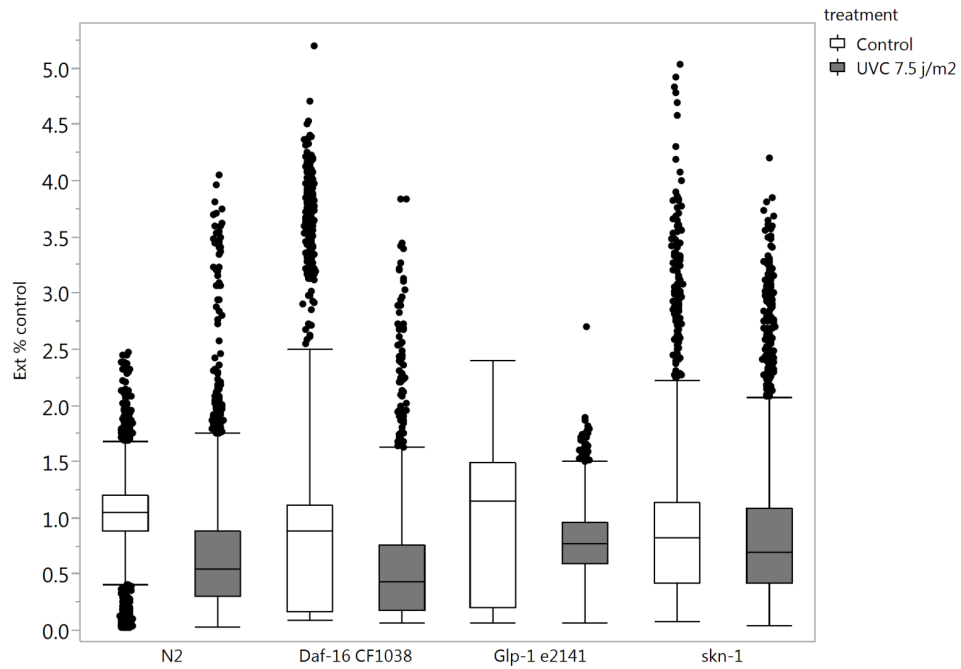


Figure 18: Skn-1 mutants are protected from UVC induced growth delay

Daf-16 mutants are mildly, but statistically ($p < 0.0001$), more sensitive to UVC induced larval growth delay, while *skn-1* mutants are protected from growth delay ($p < 0.0043$, Mann Whitney U test with bonferroni correction). *Glp-1* nematodes are also statistically more sensitive to UVC induced growth delay, though the biological significance of this result is questionable. Nematodes were measured using the COPAS Biosort, and percent control extinction was compared between treatments.

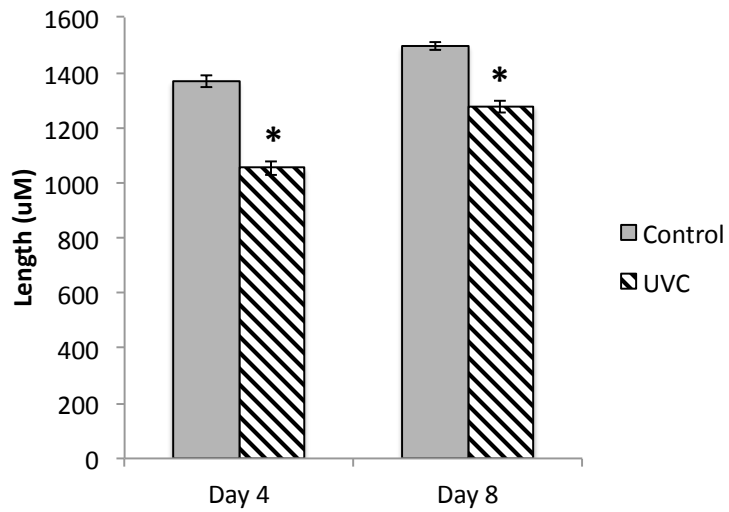


Figure 19: Adult size is reduced in response to UVC induced developmental mtDNA damage.

Adult size is significantly reduced (main effects of treatment $p < 0.001$ and time $p < 0.001$, and their interaction $p < 0.04$, 2 way ANOVA) in response to UVC exposure. $n = 60-70$ individuals in 2 experimental replicates.

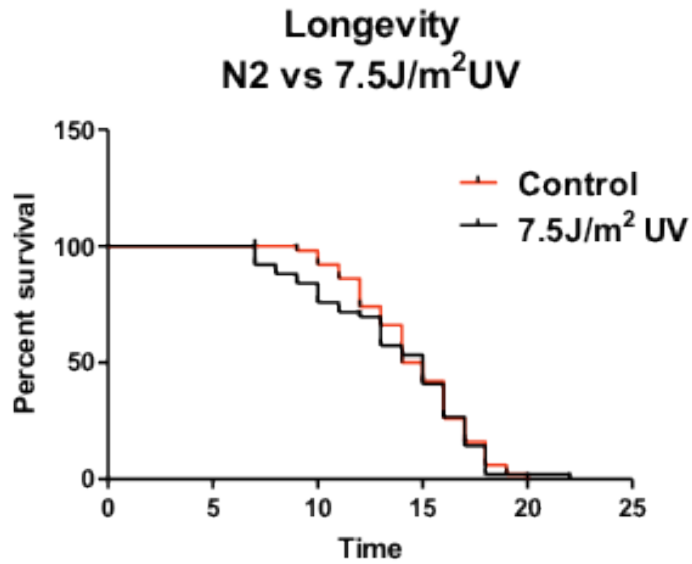


Figure 20: Lifespan is unchanged.

Lifespan is unchanged in nematodes exposed to 7.5 J/m² UVC radiation 3 times over 48 hours. Median lifespan was 15 days for both controls and UVC exposed, while maximal lifespans were 20 days in the controls and 22 days in UVC exposed.

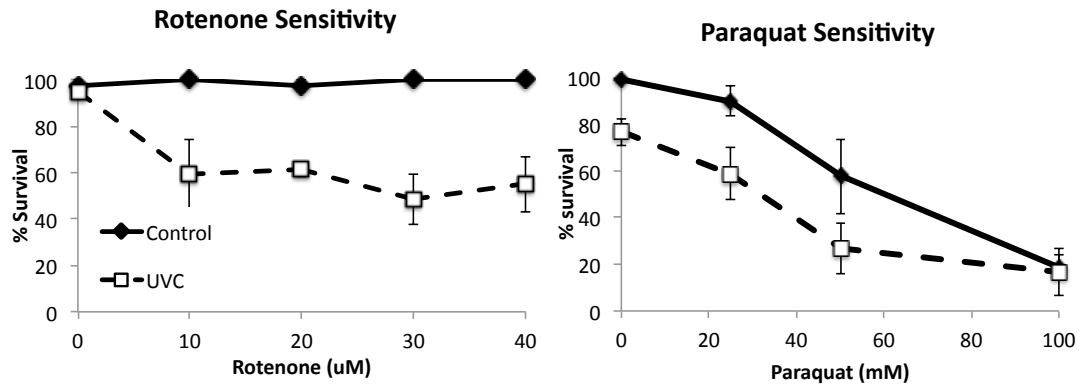


Figure 21: Sensitivity to rotenone, but not paraquat, is increased in UVC exposed nematodes.

UVC exposed nematodes are more sensitive to the complex 1 inhibitor rotenone (main effects of treatment $p < 0.0001$, time $p < 0.0001$, and their interaction $p < 0.02$ by 2 way ANOVA), however not to the ROS generating paraquat later in life (main effects of UVC and paraquat $p < 0.005$ and $p < 0.0001$, respectively, but no significant interaction term. 2 way ANOVA). Asterisks denote significant differences at each time point by post hoc T-test, $p < 0.05$. Error bars +/- SEM.

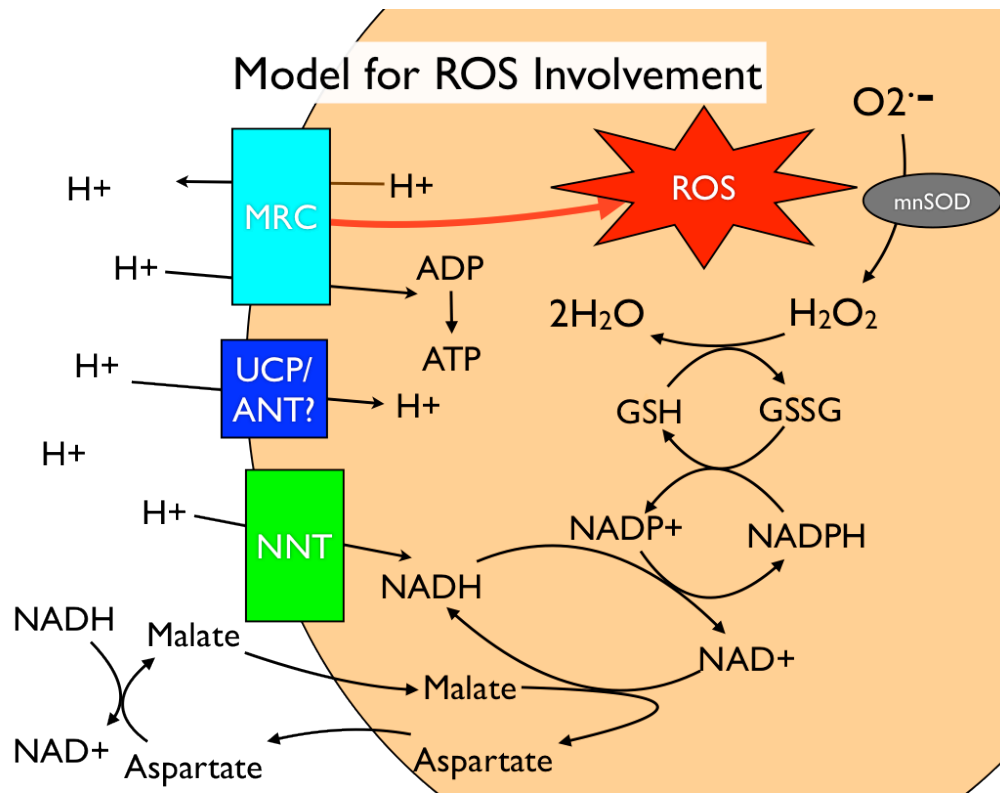


Figure 22: Model for ROS Involvement

ROS generated from the MRC as superoxide requires MnSOD to be converted to H_2O_2 , which is detoxified by oxidizing reduced glutathione. Superoxide also activates uncoupling proteins (UCP/ANT) in some systems, though this remains to be tested in nematodes. NADPH is required to reduce oxidized glutathione in the mitochondria, and could be generated via NADH imported by the malate-aspartate shuttle and H^+ from the proton gradient, mediated by NNT. This would result in ATP synthase, UCP/ANT and NNT all working to dissipate membrane potential, potentially leading to increased oxygen consumption as a compensatory mechanism.

3. Gene x Environment interactions in the origin of mitochondrial DNA mutations

3.1 Introduction

Mutations in mtDNA lead to a wide range of diseases with clinically variable phenotypes [174]. Over 270 disease-causing point mutations in mtDNA have been described and collectively, mtDNA related diseases affect 1 in approximately 5000 people [6]. The drivers of mtDNA mutagenesis, however, are largely unknown. Defects in the only mtDNA polymerase, pol- γ , induce mtDNA mutations and mutations in the *POLG* gene are causative in a multitude of mitochondrial diseases [61, 175, 176]. As evidence of environmental impacts on mtDNA mutagenesis, the alkylating agent MMS further increases the mutation rate of some disease associated *POLG* variants [177]. Yet, little evidence exists for an environmental component to mtDNA mutagenesis in the context of wild-type pol- γ .

The mutagenic potential of irreparable lesions in mtDNA, such as thymine dimers resulting from UVC exposure, has not been investigated. While oxidative damage to mtDNA from mitochondrial generated reactive oxygen species (mtROS) was long thought to play a significant role in mutagenesis, recent evidence suggests otherwise [142]. Base excision repair (BER), the DNA repair mechanism that repairs oxidative damage to DNA, is robust in the mitochondria, likely due to the close proximity of mtDNA to the ROS generating mitochondrial respiratory chain [7, 69]. Nucleotide excision repair (NER), however, is not present in the mitochondria [7, 70].

NER repairs bulky lesions and dimers in nuclear DNA, such as those resulting from UVC exposure, some polycyclic-aromatic hydrocarbons and aflatoxins [67]. Importantly, pol- γ has the potential for mutagenic bypass of these lesions *in vitro* [12]. Additionally, increases in mtDNA mutations in humans have been attributed to treatment with the nucleoside reverse transcriptase inhibitors (NRTIs) used in HIV/AIDS treatment [76], which are known to impede pol- γ .

Mitochondrial dynamics and maintenance are critical to mitochondrial health, and mutations in genes involved in these processes lead to disease. Mitochondria are dynamic, networked organelles that fuse and divide through the processes of fusion and fission (reviewed in [178]). The mitofusins *Mfn-1* and *Mfn-2* are GTP-ases that regulate inner membrane fusion that, when mutated, lead to the peripheral neuropathy Charcot-Marie-Tooth disease, type 2A [62]. *Opa-1* facilitates outer membrane fusion, and mutations in this gene result in optic nerve atrophy and other neurological disorders [179]. *Drp-1*, a dynamin related protein that is required for mitochondrial fission, has a single confirmed case of mutation in humans and lead to severe encephalopathy and was fatal early in life [180].

Mitophagy is the targeted removal of depolarized or dysfunctional mitochondria [181]. Mutations in the human genes *Pnk-1* and *Parkin* lead to juvenile onset Parkinson's disease [182, 183], both are critical components of mitophagy. *Pnk-1* is a serine/threonine kinase that accumulates on the membranes of depolarized mitochondria and recruits

Parkin, an E3-ubiquitin ligase that targets the dysfunctional mitochondria for degradation [184, 185]. Mitochondria are also degraded non-selectively through the general autophagy pathway [186], which can be induced via starvation or nutrient deprivation [187]. Defects in autophagic processes have also been linked to neurodegenerative conditions [188]. Furthermore, autophagy and mitochondrial dynamics in general are required for the removal of UVC induced mtDNA lesions [9, 10].

As bulky lesions and dimers in mtDNA are irreparable, and the mtDNA polymerase, pol- γ , has the potential for mutagenic bypass of these lesions, we hypothesize that they will increase mtDNA mutagenesis. In addition, deficiencies in mitochondrial fission and mitophagy may further increase mutagenesis when combined with mtDNA damage.

3.2 Experimental Design

The model organism *C. elegans* will be used to investigate the potential for UVC induced dimers to increase mtDNA mutagenesis. *C. elegans* is an excellent model for this study for a number of reasons. First, its mtDNA genome is highly conserved with humans [103]. Perhaps more importantly, as an *in vivo* model, it provides an organismal and developmental context to mitochondrial and mtDNA biology that may not be achievable *in vitro*. For instance, mtDNA copy number increases dramatically during development, and deficiencies in mtDNA replication can result in larval arrest [104,

114]. However, *in vitro* many cell types can be depleted of their mtDNA and still survive [111, 112]. Additionally, many mutant strains are available with deficiencies in the mitochondrial maintenance pathways of fission, fusion, autophagy and mitophagy.

We chose 4 different strains of *C. elegans* to investigate different aspects of mtDNA mutagenesis. First, JK1107 *glp-1(q224)* nematodes were used to probe somatic mtDNA mutagenesis. This strain lacks a germ line when raised at 25°C due to a temperature sensitive mutation that results in terminal differentiation of germ cells [189]. Germ cell proliferation in *C. elegans* includes a large increase in mtDNA copy number [114], which could potentially dilute and mutational signal from somatic cell mitochondria. Second, wild-type N2 nematodes will be used to investigate the potential for the increase in mtDNA copy number during germ cell proliferation to increase mutation frequency. And finally, 2 mutant strains (*drp-1* and *pink-1*) deficient in mitochondrial fission and mitophagy respectively, will be used to investigate the potential for these processes to increase mtDNA mutation rates both in the context of irreparable damage and without it.

3.3 Methods

First larval stage (L1) *C. elegans* were exposed to 3 doses of 7.5 J/m² UVC radiation, with 24 hours in between doses. This exposure results in the accumulation of mtDNA damage while allowing for nucDNA to be repaired [9, 11]. Nematodes were

then allowed to develop to the young adult (JK1107) or gravid adult (N2, *drp-1*, and *pink-1*) stage, at which point they were harvested for mtDNA isolation.

JK1107 *glp-1* nematodes were cultured for 4 days after dosing at 25°C. At this temperature, germ cells in *glp-1* nematodes terminally differentiate resulting in sterile animals. All other strains were cultured at 20°C until gravid adulthood. Approximately 10,000 nematodes were harvested per mtDNA isolation. Nematodes were washed off of plates with K-media, washed 3 times in 10 mL K-media, and then allowed to clear their guts by incubating in K-media on a shaker at 20°C for 30 minutes. After gut clearance, nematodes were pelleted and mitochondria were extracted essentially as previously described [190]. Briefly, nematodes were washed twice in ice cold MSM-E buffer, and then transferred to glass/Teflon homogenizers in approximately 500uL of MSM-E buffer. Samples were homogenized until most nematodes were ruptured, as monitored by placing a drop of sample on a slide and examining under a dissecting microscope. 1 volume of MSM-EB was added to each sample, and samples were then centrifuged at 300 x G for 10 minutes at 4°C to pellet cellular debris. The supernatant was removed and saved (contains the mitochondria) and the pellet was re-extracted in 500 uL MSM-EB as above. This extract was also centrifuged at 300 x G for 10 minutes at 4°C, and the supernatants were combined. Supernatants were centrifuged at 7000 x G for 10 minutes at 4°C to pellet mitochondria, and mitochondria were then washed once each with MSM-E buffer and MSM buffer. Mitochondria were frozen as pellets after the final wash.

Frozen mitochondrial pellets were processed with a Qiaprep Spin Miniprep plasmid isolation kit (Qiagen, Germantown, MD) to isolate mtDNA. After mtDNA isolation, any contaminating linear DNA was digested with ExoV exonuclease (New England Biolabs, Ipswich, MA) as per manufacturers instructions. Digests were then cleaned up with Ampure XP paramagnetic beads (Beckman-Coulter, Indianapolis, IN) as per manufacturers instructions with one exception: 0.4 volumes of beads were used per sample.

Real-time PCR was performed to measure the enrichment of mtDNA vs nucDNA achieved using this protocol. mtDNA and nucDNA copy numbers were measured as previously described [173] and the following calculation was used to estimate purity of mtDNA:

$$\begin{aligned} & (C. elegans \text{ nuc Genome size}) / (2^{(C_t^{\text{Nuc}} - C_t^{\text{mtDNA}})} * C. elegans \text{ mt genome size}) \\ & = 100,258,171 / (2^{15.8}) * 13,794 \\ & = 0.127 \end{aligned}$$

This ratio indicates nearly 90% of our sample by mass is mtDNA, well above the suggested 50% [141, 142].

Library construction and sequencing will be carried out in Dr. Simon Gregory's lab using the Duplex Sequencing method, essentially as described [141, 142, 191]. Minor modifications to the protocol will be made as needed. Duplex sequencing allows for the barcoding of individual DNA fragments prior to any PCR amplification or sequencing,

resulting in significantly lower limits of detection by virtually eliminating PCR or sequencing errors [141, 142]. This is extremely important in mtDNA sequencing, as the high copy number of small genomes would render rare mutations impossible to detect with other methods.

3.4 Progress to Date

All samples have been generated and mtDNA has been isolated. Optimization of library preparation is currently underway, after this hurdle data should be generated quickly.

4. Conclusions

4.1 Summary

The major goal of this work was to investigate the potential for irreparable mtDNA damage incurred during development to result in adverse outcomes later in life. Much of the research done on mtDNA damage has focused on oxidative damage, as the mtDNA is in close proximity to the ROS generating MRC, though this type of damage is efficiently repaired in mtDNA. Many environmental pollutants, however, cause bulky DNA lesions that are repaired via the nucleotide excision repair pathway, which is absent in the mitochondria. Pollutants that induce these types of lesions include polycyclic aromatic hydrocarbons (PAHs) such as Benzo-a-pyrene, ultraviolet radiation, and aflatoxins.

Using UVC as a model toxicant exposure, I have shown that mtDNA during the first larval stage of *C. elegans* development leads to persistent changes in mitochondrial function later in the life of the organism. mtDNA damage is removed over time, but re-occurs later in life. mtDNA copy number is persistently reduced, as are steady state ATP levels, though oxygen consumption is increased. These results suggest a role for environmental exposures in mitochondrial dysfunction. Metabolomics and mutant sensitivity screens suggest that ROS may be involved in this response, and that an NADPH stress may also play a role. Experiments are underway to investigate both of these possibilities.

In a separate project, we are investigating the potential for irreparable lesions in mtDNA to drive mutagenesis. The source of mtDNA mutations is relatively poorly understood, and *in vitro* evidence suggests that these lesions have the potential to be mutagenic [12]. We are also investigating gene x environment interactions between irreparable mtDNA damage and mitochondrial maintenance genes, as they are required for lesion removal [9, 10]. These experiments are utilizing a relatively new sequencing technique, termed duplex sequencing, due to its ability to detect mutations at far lower levels than conventional next generation sequencing techniques. Currently, the library preparation phase of this protocol is being optimized. mtDNA samples have been generated and are ready for sequencing once this has been done.

4.2 Broader Impacts

This work is important to the fields of environmental toxicology as well as mitochondrial biology and human mitochondrial disease, and also relates to the developmental origins of health and disease field.

Mitochondrial diseases as a group affect roughly 1 in 4000 people [5, 6] and are therefore a significant public health burden. While some causes of mitochondrial diseases are known on the genetic level, there are still many unknowns related to these diseases. Furthermore, mitochondrial dysfunction is implicated in even more common human diseases including cancer [54], neurodegenerative conditions such as Parkinson's disease and Alzheimer's disease [52, 192], diabetes and metabolic syndrome [58] and

heart disease [51]. Little is known with regards to mitochondrial dysfunction being causative in these diseases, though. This work suggests that the environment, and particularly environmental pollutants that can damage mtDNA, have the potential to result in persistent mitochondrial defects that could lead to adverse outcomes later in life. This is supported in the pharmaceutical sphere, as nucleotide reverse transcriptase inhibitors used to treat HIV/AIDS, which impede the progression of the mtDNA polymerase much like bulky DNA adducts and dimers, have resulted in mitochondrial toxicity in humans [77] and persistent mitochondrial dysfunction in primates [78] exposed *in utero*.

Appendix A - Effects of 5'-Fluoro-2-deoxyuridine on Mitochondrial Biology in *Caenorhabditis elegans*.

This chapter appears in *Experimental Gerontology*, issue 56 (2014), pages 69-76

The authors are: Rooney JP, Luz AL, González-Hunt CP, Bodhicharla R, Ryde IT, Anbalagan C, Meyer JN.

Duke University, Nicholas School of the Environment, Integrated Toxicology and Environmental Health Program. LSRC, PO Box 90328, Durham, NC 27708, USA

A.1 Abstract

5-Fluoro-2'-deoxyuridine (FUdR) is a DNA synthesis inhibitor commonly used to sterilize *Caenorhabditis elegans* in order to maintain a synchronized aging population of nematodes, without contamination by their progeny, in lifespan experiments. All somatic cells in the adult nematode are post-mitotic and therefore do not require nuclear DNA synthesis. However, mitochondrial DNA (mtDNA) replicates independently of the cell cycle and thus represents a potential target for FUdR toxicity. Inhibition of mtDNA synthesis can lead to mtDNA depletion, which is linked to a number of diseases in humans. Furthermore, alterations in mitochondrial biology can affect lifespan in *C. elegans*. We characterized the effects of FUdR exposure on mtDNA and nuclear DNA (nucDNA) copy numbers, DNA damage, steady state ATP levels, nematode size, mitochondrial morphology, and lifespan in the germ line deficient JK1107 *glp-1(q224)* and PE255 *glp-4(bn2)* strains. Lifespan was increased very slightly by 25 μ M FUdR, but was reduced by 400 μ M. Both concentrations reduced mtDNA and nucDNA copy numbers, but did not change their ratio. There was no effect of FUdR on mitochondrial morphology. Although both concentrations of FUdR resulted in smaller sized animals, changes to steady-state ATP levels were either not detected or restricted to the higher dose and/or later timepoints, depending on the method employed and strain tested. Finally, we determined the half-life of mtDNA in somatic cells of adult *C. elegans* to be between 8 and 13 days; this long half-life very likely explains the small or undetectable

impact of FUdR on mitochondrial endpoints in our experiments. We discuss the relative pitfalls associated with using FUdR and germline deficient mutant strains as tools for the experimental elimination of progeny.

Keywords: mitochondrial DNA; mitochondrial DNA half-life; mitochondrial toxicity; FUdR; copy number; lifespan; aging; *Caenorhabditis elegans*.

Abbreviations: mtDNA, mitochondrial DNA; nucDNA, nuclear DNA; FUdR, 5-fluoro-2'-deoxyuridine; MRC, mitochondrial respiratory chain.

A.2 Introduction

Caenorhabditis elegans is a free-living nematode found largely in decaying organic matter such as leaf litter [193]. It is widely used as a model organism in studies of aging, due mainly to this organism's short lifespan of approximately 2-3 weeks, as well as its completely sequenced and annotated genome [194], the availability of mutant strains, and the ease of gene knockdown via RNA interference [195]. *C. elegans* has played a role in the discovery of a number of cellular pathways that influence aging, including IGF/insulin signaling [196], dietary restriction [197], and inhibition of mitochondrial respiration [86, 118].

Hermaphroditic nematodes normally lay 200-300 eggs, which upon hatching are difficult to separate from an age-synchronized adult population. To overcome this, it is common practice to add 5-fluoro-2'-deoxyuridine (FUdR) to the nematode growth media [198]. FUdR is a DNA synthesis inhibitor that acts by inhibiting the enzyme thymidylate synthase. FUdR and its metabolites can also be incorporated into RNA, replacing uracil and affecting RNA synthesis [199]. There is evidence that FUdR causes chromosomal breaks specifically during S-phase of the cell cycle [200]. *C. elegans* undergo a finite number of cell divisions during larval development; therefore, after reaching maturity, DNA synthesis is not required for survival, though its inhibition effectively sterilizes nematodes [198]. Early studies demonstrated that exposure to FUdR from the L4 larval stage (the final larval stage) or later results in a small decrease in

nematode length, and an increase in lifespan of 39% in axenic medium and 7% in monoxenic medium [198]. Since that early report, there have been conflicting results reporting that FUdR exposure either has no effect on lifespan [201, 202] or that it can extend lifespan, particularly in specific mutant backgrounds [203, 204]. FUdR also significantly alters the metabolomic profile of *C. elegans*, and may do so differently in different mutant backgrounds [205].

While the effects of FUdR on nuclear DNA (nucDNA) have been relatively well studied, its effects on mitochondrial DNA (mtDNA) have not. Mitochondria are responsible for producing the majority of cellular ATP and their proper function is critical to cellular and organismal health [1]. Mitochondria contain multiple copies of their own genomes which encode approximately 13 (depending on the species) proteins that are all essential for the process of oxidative phosphorylation [2]. The importance of mtDNA integrity has recently been more fully appreciated, as mutations, deletions, and depletion of mtDNA have all been linked to human disease [55, 56, 64]. Importantly, mtDNA replication occurs independently of the cell cycle [206], raising the concern that FUdR inhibition of DNA synthesis may interfere with normal mtDNA replication even after nematodes have completed their final somatic cell divisions. Interestingly, the original report on the use of FUdR in *C. elegans* [198] included observations of decreased pharyngeal pumping and slow movement, which could both result from decreased energy availability. Other studies in *C. elegans* have identified abnormalities in FUdR-

treated nematodes [202, 207], and research in other organisms has also suggested that FUdR has mitochondrial toxicity [208-210]. While it has been argued that the effects of FUdR on nucDNA replication are greater than the effects on mtDNA replication [211], it is unclear whether this would be true in postmitotic tissues. Potential FUdR-mediated mitochondrial toxicity is of concern for lifespan studies because inhibition of mitochondrial respiration during larval development extends nematode lifespan [86, 118].

These experiments were designed to test the hypothesis that FUdR exposure inhibits mtDNA replication and mitochondrial function. We investigated impacts of FUdR on mitochondrial function, including mtDNA and nucDNA copy numbers, DNA damage levels, steady state ATP levels, and mitochondrial morphology in response to FUdR exposure. To place our experiments in the context of other reports on the effects of FUdR on lifespan, we also measured lifespan. FUdR is typically applied to worm cultures at the L4 larvae or young adult stages of development. In order to err on the side of detecting any potential phenotypes, we exposed nematodes to the highest and lowest commonly used FUdR concentrations (25 μ M and 400 μ M) slightly earlier in development, starting at the L3/L4 transition.

A.3 Methods

A.3.1 Strains and culture conditions

Populations of *C. elegans* were maintained on K agar plates seeded with OP50 *E. coli*. The wild-type (N2), JK1107 *glp-1(q224)*, and SJ4103 strains were obtained from the Caenorhabditis Genetics Center (CGC, University of Minnesota). The PE255 *glp-4(bn2)* strain was generously provided by Cristina Lagido, University of Aberdeen (Aberdeen, UK). All strains were maintained at 15°C prior to experiments. Synchronized L1 populations were obtained by bleach-sodium hydroxide isolation of eggs followed by overnight hatch in liquid K-medium at 20°C with shaking [212]. Synchronized L1 larvae were transferred to K agar plates seeded with OP50 and incubated at 25°C for approximately 24 hours prior to being transferred to K agar plates containing 0µM, 25µM or 400µM FUdR. Worms were washed and transferred to fresh plates daily to reduce the potential for bacterial contamination. Nematode samples were removed at 4, 8 and 12 days post FUdR exposure for experimental analysis.

A.3.2 Genome Copy Number Analysis

mtDNA and nucDNA copy numbers were measured before (day 0) and 4, 8 and 12 days post FUdR exposure, in both JK1107 *glp-1(q224)* and PE255 *glp-4(bn2)* strains as previously described [168]. Briefly, 6 worms were transferred to 90µL proteinase K-containing lysis buffer using a platinum worm pick, and lysed and digested by freezing at -80°C followed by thawing, and incubation at 65°C for one hour. Crude worm lysate

was used as template DNA for real-time PCR based determination of mtDNA and nucDNA copy numbers. A plasmid-based standard curve for mtDNA is employed, allowing for the determination of absolute mtDNA copy number [168]. 3 samples per treatment per time point were measured in triplicate PCR reactions and averaged. 3 individual experiments were performed.

A.3.3 DNA Damage Analysis

mtDNA and nucDNA damage levels were measured in wild type N2 nematodes at both 15°C and 20°C by the quantitative PCR (QPCR) method, essentially as previously described [165, 167]. Nematodes were synchronized and grown to L4, and were then transferred to K-agar plates containing 0µM, 25µM or 400µM FUdR. 3 samples of 6 worms each were picked at days 4 and 8 of treatment for analysis. 2 individual experiments were performed.

A.3.4 Steady State ATP Level Analysis

Steady state ATP levels were determined in two strains, by two different methods.

First, using both the JK1107 *glp-1(q224)* and PE255 *glp-4(bn2)* strains of nematodes, ATP levels were determined as described in [169]. Briefly, approximately 500 worms were washed and frozen at -80 °C in 100 µL of K-medium. Samples were removed from the freezer and 200 µL 10% trichloroacetic acid (TCA) was added while samples were still frozen, and allowed to thaw on ice. 0.5mm diameter zirconia beads

were added to each sample (approx. 250 μ L), and two 30 second pulses at maximum speed in a Bullet Blender (Next Advance, Averill Park, NY) were performed to lyse the worms. Lysates were neutralized by the addition of 100 μ L of 1.33 mM KHCO₃ and 100 μ L Sigma water (St. Louis, MO, USA). 50 μ L-150 μ L aliquots were removed at this time for total protein determination. Samples were vacuum centrifuged for 10 minutes to remove bubbles, and then centrifuged at 14,000 rpm for 8 minutes at 4 °C to pellet protein. The ATP containing supernatants were removed and transferred to sterile tubes. ATP was measured from 1:50 and 1:100 dilutions of these samples using the Molecular Probes ATP determination Kit (Invitrogen/Life Technologies, Carlsbad, CA, USA). Luminescence was measured every 2 minutes for 30 minutes after the addition of the luciferin/luciferase reagent using a FLUOstar Optima plate reader (BMG Labtech, Offenburg, Germany) equipped with a luminescence optic. ATP concentrations were determined by comparing luminescence values to an ATP standard curve measured at the same time points. The calculated ATP concentrations were then averaged over the 15 time points, and normalized to total protein concentrations as measured with the BCA method (Thermo Fisher Scientific, Rockford, IL.). One or two technical replicates (averaged) were performed in 3 separate experiments, resulting in a statistical n of 3.

Second, the firefly luciferase expressing PE255 *glp-4(bn2)* strain (only) was used to investigate relative, steady state ATP levels *in vivo*, in live nematodes, as previously described [9, 85, 170]. Worms were washed with K-medium, and approximately 100

worms in 100 μ L K-medium were aliquoted into wells of a white 96 well plate. 4 to 5 technical replicates (wells) were averaged per treatment per time point. All measurements were made using a FLUOstar Optima microplate reader. First, GFP fluorescence was measured with an excitation wavelength of 485 nm and an emission wavelength of 520 nm. Then, luminescence was measured 3 minutes after the automated addition of luminescence buffer consisting of citrate-phosphate buffer (pH 6.5), 0.1 mM D-luciferin, 1% DMSO, and 0.05% Triton-X. Luminescence values were normalized to GFP fluorescence at each time point, as the transgene expressed in the PE255 *glp-1(bn2)* strain is a luciferase-GFP fusion, and consequently GFP fluorescence can be used to control for the amount of luciferase enzyme in each well. Three individual experiments were conducted.

A.3.5 Size Analysis

Nematode size was determined by light microscopy in both JK1107 *glp-1(q224)* and PE255 *glp-4(bn2)* strains. Small samples of worms were frozen in K-medium, thawed, and imaged at 10x magnification on a Zeiss Axioskop. Images were analyzed using NIS elements BR software (Nikon Inc. Melville, NY, USA). Length and total area of approximately 10 individual worms per treatment was determined. This was conducted twice for a total of approximately 20 individual worms per treatment.

A.3.6 Mitochondrial Morphology

Mitochondrial morphology was visualized at 6 days post FUdR exposure in the SJ4103 strain, which expresses a GFP transgene in body wall muscle cells that contains a mitochondrial matrix localization sequence. Worms were paralyzed in 10mM levamisole and mounted on 10% agar pads. GFP tagged mitochondria were imaged using a Zeiss LSM 510 upright confocal microscope.

A.3.7 Lifespan Assay

All assays were performed at 25 °C. Strain JK1107 *glp-1(q224)* nematodes were cultured as described above. Synchronized L1 larvae were placed on K agar plates seeded with OP50 bacteria and incubated at 25°C for 24 hours. 25 individuals were then transferred to K agar plates seeded with OP50 bacteria that contained 0µM, 25 µM or 400 µM FUdR. Nematodes were monitored daily and scored as dead when they failed to move in response to repeated probing. The lifespan of each individual was calculated from L1 to death. The data presented are for 50 individuals assayed in 2 individual experiments separated in time.

A.3.8 mtDNA Half-life Analysis

Strain JK1107 *glp-1(q224)* nematodes were synchronized as described above, grown for 48 hours at 25°C (approximately young adult stage), and were then transferred to K agar plates containing either 0 µg/mL or 5 µg/mL ethidium bromide (EtBr). mtDNA and nucDNA copy numbers were determined in 3 to 4 samples of 6

worms each at days 3, 6, 9 and 12 of treatment, as described above. 4 individual experiments were performed.

A.4 Results

A.4.1 Genome Copy Number and Damage Analysis

We hypothesized that inhibition of DNA synthesis by FUdR exposure would reduce mtDNA copy number in post mitotic *C. elegans* over time, as a result of FUdR-mediated inhibition of adult mtDNA replication. Of note, we carried out the majority of these experiments in germ cell-deficient nematodes, because the very number of mtDNAs produced associated with germ cell production [114] would likely obscure any ability to detect an effect of FUdR on mtDNA metabolism.

The nematode mitochondrial respiratory chain (MRC) consists of over 75 protein subunits, most of which are encoded in nuclear DNA and are then translocated to the mitochondria [121]. However, 12 [121] or 13 [213] of these subunits are encoded in the mtDNA, and proper stoichiometric balance between nuclear- and mitochondrial-encoded proteins is important for normal MRC function [20]. Furthermore, mtDNA depletion leads to disease [61, 64]. Thus, proper maintenance of mtDNA copy number is critical to organismal health. FUdR and other DNA synthesis inhibitors have been shown to block replication of mtDNA and lead to reductions in mtDNA copy number. Ethidium bromide, a DNA intercalating agent that blocks mtDNA replication, leads to a reduction in mtDNA copy number over time in exposed nematodes [114], and FUdR

reduces mtDNA content and cytochrome C oxidase expression in cultured lymphoblasts [208].

mtDNA copy number per worm (Figure 23) was significantly reduced in the JK1107 *glp-1(q224)* worms by FUdR treatment as analyzed by two way ANOVA (significant main effects of time ($p < 0.0001$) and treatment ($p < 0.0005$) but not their interaction ($p = 0.057$)). However, nucDNA copy number per worm was also altered by FUdR exposure (main effects of time ($p < 0.0001$), treatment ($p < 0.0001$) and their interaction ($p < 0.005$) are all significant). The resulting mtDNA / nucDNA copy number ratio was not affected by FUdR treatment, although there was a significant decrease in mtDNA / nucDNA ratio over time ($p < 0.0001$). Thus, the observed reduction in mtDNA copy number per worm can be attributed to the reduction in nucDNA copy number, as this ratio is unchanged. An age-related decline in nucDNA copy number in a germline deficient strain (*glp-4*) of *C. elegans* has previously been reported [214].

The approximate expected number of nucDNA copies in germ cell-deficient adult *C. elegans* is 3134 (959 2n somatic cells, 34 32n intestinal cells, and 98 4n hypodermis cells) [214, 215]. Our FUdR treated worms, however, only achieve slightly over 2000 nucDNA copies. As observed previously by other researcher using a germline deficient (*glp-4*) strain [214], our control (0 μ M FUdR) worms never reach the expected number of nucDNA copies (or potentially do so before day 4 which would not be detected given our experimental design). It is not possible from our data to determine

the mechanism of the FUdR-induced decrease nucDNA copy number; we speculate that it may be a result of fewer somatic cells in the FUdR treated groups, a reduction in the endoreduplication that occurs in the intestinal and hypodermal cells, or a combination of the two.

The lack of a difference in mtDNA:nDNA ratio after FUdR could be explained in two ways. It is possible that the same number of mtDNAs are present per cell, and there are simply less cells in the FUdR treated groups. Or, if some of the difference in nucDNA copy number is attributable to a lack of endoreduplication, mtDNA copy number per cell may in fact be reduced by FUdR treatment.

Copy number determination experiments were also performed using the PE255 *glp-4(bn2)* strain and again FUdR decreased both mtDNA and nucDNA copy numbers, but did not alter their ratio. However, in this strain, the dynamics of mtDNA copy number with age were different (irrespective of FUdR treatment). mtDNA copy number per worm (Figure 24) increased throughout the length of the experiment in control and 25 μ M FUdR treated worms, and only decreased slightly at day 12 in the 400 μ M treatment group. The main effects of time ($p < 0.0001$) and treatment ($p < 0.0001$) as well as their interaction ($p < 0.001$) were all significant. nucDNA copy number showed a similar trend with controls increasing throughout, 25 μ M treated decreased slightly from days 4 to 8 but increased again at day 12, and the 400 μ M group plateaued at roughly 1500 copies at day 4 and remained unchanged thereafter. Main effects of time ($p < 0.0001$) and

treatment ($p < 0.0001$), and their interaction ($p < 0.0001$) were all significant. This resulted in an mtDNA / nucDNA ratio that increased slightly over the 12 day exposure for all treatments ($p < 0.0001$), but was unaltered by FUdR treatment. Thus, the trends in copy numbers were different than what was seen in the JK1107 *glp-1(q224)* strain, and while we do not have an explanation for the differences seen between the strains, we have seen similar trends in copy number in the PE255 *glp-4(bn2)* strain in other experiments (unpublished). We have also seen differences in gene expression between wild-type N2 worms and the PE255 N2 (wild type background) strain in response to UVC treatment that inhibits mtDNA replication during development [11].

Finally, we tested for DNA damage in both genomes of wild type (N2 Bristol strain) nematodes, grown at both 15°C and 20°C, at 4 and 8 days of exposure to 0, 25, or 400 μ M FUdR. We did not detect any damage (Table 4). The limit of detection of this assay is approximately 1 lesion/ 10^5 nucleotides [165].

A.4.2 Steady State ATP Levels

Next, we investigated whether FUdR exposure would alter ATP levels in post-mitotic, adult *C. elegans*. If mtDNA copy number were in fact reduced by FUdR treatment, or if FUdR affected RNA or protein synthesis in the mitochondria [208], it is possible that MRC function could be altered, leading to reductions in steady state ATP levels.

ATP levels were measured in JK1107 *glp-1(q224)* mutants at 4 and 8 days post FUdR treatment. Unfortunately, too few worms survived until day 12 to obtain reliable measurements of ATP levels. ATP levels per unit protein (Figure 25) were unaffected by all FUdR concentrations at both days 4 and 8 post treatment. Interestingly, we observed a very slight decrease in ATP levels per unit protein from day 4 to 8, whereas previous reports in N2 nematodes have shown decreases closer to 50% over that time [86].

ATP levels were also measured in the PE255 *glp-4(bn2)* *C. elegans* strain, and using this method, the results were different. The PE255 transgenic strain expresses a luciferase-GFP fusion protein, and relative ATP levels are measured as light output from live worm. Importantly, ATP levels are normalized to GFP levels as opposed to protein concentrations. ATP levels were slightly higher in 25 μ M FUdR treated worms, and slightly lower in 400 μ M treated worms at day 4. However, at days 8 and 12 ATP levels were significantly higher in the control worms than in either of the treatment groups (Figure 26).

Lastly, we measured ATP levels in the PE255 *glp-4(bn2)* strain using the same method that was used with the JK1107 *glp-1(q224)* strain, to determine if the differences in ATP level responses to FUdR were attributable to different biological responses between the strains or differences in the measurement techniques used. ATP levels (Figure 27) appear to decrease with FUdR treatment, and in fact, there is a significant main effect of treatment ($p < 0.005$). However, this effect is driven solely by the 400 μ M

FUdR exposed nematodes. These nematodes were much smaller compared to other treatments, and it was difficult to extract significant quantities of ATP and of total protein, making this data questionable. Without the 400 μ M FUdR exposed nematodes, the significant main effect is lost ($p=0.126$), though the trend towards lower ATP still appears.

A.4.3 Nematode Size

FUdR can cause a reduction in overall nematode length depending on when it is administered. For example, a dose of 400 μ M reduced length by approximately 20% when nearly mature nematodes were exposed [198]. We measured the length and area of both JK1107 *glp-1(q224)* and PE255 *glp-4(bn2)* worms exposed to FUdR beginning at the L3/L4 transition (as described above) on days 4, 8 and 12 of treatment.

In the JK1107 *glp-1(q224)* average nematode area was significantly reduced by FUdR (main effects of treatment ($p<0.0001$) and time ($p<0.0001$)), as was length (treatment ($p<0.0001$), time ($p<0.005$) and their interaction ($p<0.005$) were all significant) as shown in (Figure 28). The maximum reduction in area for the 25 μ M dose was 33% and occurred on day 4, and for 400 μ M was 68% occurring on day 12. Maximum reduction in length at 25 μ M FUdR was 15% on days 4 and 8, and at 400 μ M was 45% at day 12.

The PE255 *glp-4(bn2)* nematodes were also significantly smaller when exposed to FUdR (Figure 29). Area was significantly reduced (main effects of treatment ($p<0.0001$),

time ($p < 0.05$) and their interaction ($p < 0.0001$), as was length (main effect of treatment ($p < 0.0001$) and treatment by time interaction ($p < 0.005$)). The maximum reduction in area at the 25 μM concentration was 65% on days 4 and 8, and at 400 μM was 77% on day 12. Length was maximally reduced at 25 μM FUdR by 33% on day 8, and at 400 μM by 49% on day 12.

A.4.4 Mitochondrial Morphology

Mitochondria are dynamic structures; their morphology responds to many types of damage through the processes of fusion and fission, and they can be selectively degraded through mitophagy [181, 186, 216]. We examined the mitochondrial morphology of the SJ4103 strain of *C. elegans*, which expresses a GFP protein with mitochondrial matrix localization sequence under the control of a body wall muscle cell promoter, after 8 days of exposure to 25 μM and 400 μM FUdR. There were no obvious differences in mitochondrial morphology in any worms examined (representative images can be found in Figure 30).

A.4.5 Lifespan

Since the somewhat conflicting reports of the effects of FUdR on lifespan found in the literature suggest that experimental conditions may alter those effects, we tested the effects of FUdR on lifespan in our experimental conditions. We measured the lifespan of the germ-line proliferation defective JK1107 *glp-1(q224)* mutant strain of *C.*

elegans in response to lifelong treatment with 0 μM (control), 25 μM and 400 μM FUdR beginning from the L3/L4 transition.

Compared to controls (0 μM FUdR), 400 μM FUdR resulted in a significant ($p < 0.0001$) reduction in mean lifespan by 6 days. Conversely, 25 μM FUdR significantly ($p < 0.0427$) increased mean lifespan by approximately 1 day. Lifespan data were statistically analyzed using the Mantel-Cox test (Figure 31).

A.4.6 mtDNA Half-life Analysis

The lack of mtDNA depletion seen in response to FUdR treatment prompted us to measure the half-life of mtDNA, as a long half-life is one potential explanation for these results. To measure half-life, we transferred young adult JK1107 *glp-1(q224)* nematodes to K-agar plates containing ethidium bromide (EtBr). EtBr is a DNA intercalating agent that blocks mtDNA replication by impeding the mtDNA polymerase, including in nematodes [114]. By measuring the decrease in mtDNA copy numbers in the presence of EtBr we can approximate the half-life of mitochondrial genomes in adult worms.

Based on the decrease in mtDNA copy number from days 3 to 12 in the presence of EtBr, we determined the mtDNA half-life to be 8.2 – 13.2 days (Figure 32). Interestingly, we saw nearly the same rate of decline (half-life of 6.5 to 11.7 days) in untreated nematodes, however mtDNA copy number did not begin to decrease until day 6. Half-life was determined by linearizing the portion of the graph that showed a

consistent decrease (day 3-12 for EtBr treated, and day 6-12 for control) by plotting the natural log (LN) of the mtDNA / nucDNA ratio vs. time (Figure 33). The slopes of these lines were used to calculate half-life (half-life = LN(2)/slope). The range of the estimates of half-life were made by plotting the steepest and least steep possible lines based on the SEM at the first and last points used in the plot.

Statistical analysis by ANCOVA did not reveal an interaction between treatment and day ($p=0.62$) indicating that there was not a statistically significant difference in the slopes of the control and EtBr treated lines, and therefore no significant difference in the half-life of mtDNA between treatments.

A.5 Discussion

We have investigated the impact of FUdR exposure, a DNA synthesis inhibitor commonly used to sterilize nematodes in aging and lifespan studies, on mitochondrial biology in *C. elegans*. We have also determined the half-life of mtDNA in adult germ cell-deficient nematodes.

A.5.1 Use of Germ Line Deficient Strains

Mutations in the *glp-1* gene cause germ cells to enter meiosis as opposed to mitosis, and terminally differentiate, resulting in sterility [189]. The exact function of the *glp-4* gene is less well characterized, however mutations also result in a temperature sensitive sterility phenotype. Nematodes with *glp-1(q224)* or *glp-4(bn2)* mutations are reproductively competent when maintained at 15°C, but are sterile at the restrictive

temperature of 25°C [189, 217, 218]. We chose to perform the majority of the experiments in these strains to specifically remove the influence of germ cells on the results, as we are interested in the effects of FUdR on mitochondrial function in somatic cells. Nematodes that lack germ line stem cells live longer than those that contain them [219, 220], and while this would not be altered by FUdR exposure, there is evidence that lack of fertility can influence stress resistance [221, 222] and that FUdR alters metabolism [205]. Furthermore, mtDNA copy number in wild type nematodes increases dramatically during egg laying [114], and would therefore obscure any comparisons between untreated and FUdR treated wild type animals.

A.5.2 Copy number

There are two potential explanations for the observed lack of FUdR-mediated reduction in mtDNA/nucDNA copy numbers. The first is that mitochondrial dTTP pools are not depleted by FUdR treatment, and mtDNA replication continues as normal. mtDNA replication rates in cultured mouse L-cells are less sensitive to inhibition by FUdR than are nucDNA replication rates [223]. Also, mtDNA precursor pools in cultured HeLa cells expand when treated with FUdR, while nuclear dNTP pools are depleted [224]. The second possibility is that the half-life of mitochondrial DNA in adult *C. elegans* is long enough that inhibition of mtDNA replication has little effect on copy number. This is supported by the relative lack of a decline in mtDNA copy number in adult nematodes in the presence of ethidium bromide [114]. A sharp decline was seen

after nematodes exposed from the L3 stage laid their broods, but copy number then remained relatively constant during adulthood [114]. If mtDNA were turning over at an appreciable rate it would be expected that copy number would continue to decline. Supporting that observation, our own unpublished results also indicate that exposure to ethidium bromide in adult *glp-1* nematodes resulted in a maximal decrease of only 25% in mtDNA copy number throughout adulthood.

Nonetheless, an effect on mtDNA copy number in specific tissues or after exposure to mtDNA genotoxicants remains an important concern. While the half-life of mtDNA is not well-studied, it has been investigated in rats and reported to be 6.7 days in heart, 9.4 days in liver, 10.4 days in kidney, and 31 days in brain [225]. Organellar half-life has been measured in rat livers as 3.8 days using radioactive labeling of proteins [145]. More recently, a proteomics approach has demonstrated that median half lives of mouse liver and cardiac mitochondrial proteins are 4.26 and 17.2 days, respectively, and that individual proteins turn over at different rates [226]. While these are not all direct measures of mtDNA turnover, they do suggest that turnover rates may differ by tissue type. It is also possible that mtDNA half-life is much shorter during development, or that turnover may be influenced by environmental factors that, for example, increase autophagy rates. mtDNA damaged by ultraviolet C radiation both induces autophagy and is removed slowly by mechanism that is dependent on it [9] and the mitochondrial DNA polymerase, pol γ , is upregulated 3.4 fold by UVC exposure in young adult *glp-1*

nematodes [227]. Thus, FUdR exposure may have significant effects on mitochondrial biology in the context of mitochondrial or mtDNA damage.

A.5.3 ATP Levels

In the context of a lack of depletion of mtDNA copy number per cell, it is not surprising that ATP levels per unit protein in adult nematodes were not significantly affected by FUdR treatment. While mtDNA depletion is certainly not the only mechanism by which mitochondrial dysfunction can be induced, it appears to be the most likely way that FUdR would do so. There is some evidence that suggests FUdR can inhibit RNA synthesis [199]. If this were to occur in the mitochondria it would be possible that ATP production could be altered without mtDNA depletion. However, this seems less likely as potential mechanism, especially when considering the multiplicity of mitochondrial genomes per cell and the ability of individual mitochondria to transfer contents and functionally complement others [228]. Furthermore, our results do not support this possibility, since we do not observe altered steady state ATP levels in response to FUdR.

A.5.4 mtDNA Half-life

To investigate the possibility that a long mtDNA half-life is the explanation for a lack of FUdR induced mtDNA depletion, we measured the rate at which mtDNA decreased in the presence of EtBr. To our knowledge, this is the first reported measurement of mtDNA half-life in *C. elegans*, and at 8.2 - 13.2 days it is surprisingly

similar to that measured in rats. This suggests that in adult nematodes, there is very little turnover of mtDNA. Furthermore, the rate of decline of mtDNA in untreated animals was the same as that in EtBr treated, although the decrease started slightly later in the life of the worm. This suggests that, after a certain point in the animal's life, mtDNA is degraded and is not replaced (i.e., mitochondrial biogenesis is halted). Interestingly, this data also implies that EtBr does not induce the degradation of mtDNA, even though it blocks replication. Importantly, these are whole animal measurements, and it is likely that degradation and turnover rates differ by cell or tissue type.

The potential ability of mtDNA damage to induce mtDNA degradation or turnover is an important question, as mtDNA depletion is linked to many human diseases [64]. Previously published work from our lab indicates that a 50 J/m² dose of Ultraviolet-C radiation (UVC) results in approximately 0.6 lesions per 10 Kb of mtDNA, that is reduced to approximately 0.4 lesions per 10 Kb over 72 hours [9]. Cyclobutane pyrimidine dimers, such as those caused by UVC, are not repaired in mtDNA, as the nucleotide excision repair pathway is not present in mitochondria [68, 69], they are however, slowly removed [9]. Based on these removal kinetics, the estimated half-life of UVC damaged mtDNA is approximately 5.1 days. While this is somewhat shorter than without damage, the difference is not striking, and suggests that dimers in mtDNA may not dramatically induce mtDNA degradation.

A.5.5 Strain differences

Throughout our experiments we made note of a number of FUdR-dependent and -independent differences between the two experimental strains used, JK1107 *glp-1(q224)* and PE255 *glp-4(bn2)*. The most striking of differences were copy number and ATP levels. While we lack an explanation for the copy number differences, it is worth noting that we have seen the same steady increase in both genome copy numbers over time in other work with the PE255 *glp-4(bn2)* strain (unpublished). Golden *et al.* have also observed large increases in nucDNA copy number with age in wild type nematodes due to the accumulation of masses of nucleic acids, though they reported substantially higher copy numbers than we report here [214]. Furthermore, the PE255 *glp-4(bn2)* nematodes have more mtDNA copies per nucDNA at day 0 than the JK1107 *glp-1(q224)* nematodes do at their peak on day 4, and this ratio does not decrease with age regardless of treatment.

The difference in steady state ATP levels may be explained somewhat by the different normalizations used between the strains. ATP in the JK1107 *glp-1(q224)* nematodes is normalized to total protein concentration in a sub-sample removed during the ATP preparation, and therefore accounts for animal size differences between samples quite well. ATP levels are reported per unit protein, not per animal. The PE255 *glp-4(bn2)* strain contains a luciferase-GFP fusion protein, and GFP fluorescence is used to normalize expression of the enzyme between samples. Measured ATP levels are

relative as no standard curve can be used, and are reported per animal. GFP normalization does account for some size difference, but in the case of large size differences may do so less well than total protein normalization. Furthermore, we have observed that GFP fluorescence levels decline with age at a greater rate than does size. When we extracted ATP from the PE255 *glp-4(bn2)* nematodes and used the same measurement and normalization methods as with JK1107 *glp-1(q224)*, the FUdR effect on ATP levels became much less drastic. Our data do, however, still indicate a main effect of FUdR on steady state ATP levels in the PE255 *glp-4(bn2)* strain. It is possible that this effect was amplified by the GFP normalization process, which may not be easily applicable in aging worms. We believe that both methods have merit, but care should be taken when interpreting results and especially when comparing results across methods.

A.5.6 Lifespan

We found small but significant effects of FUdR treatment on the lifespan of JK1107 *glp-1(q224)* nematodes. Interestingly, the lower FUdR concentration used extended lifespan, whereas the high concentration reduced it. However, previous research has shown that FUdR can have dramatic effects on lifespan in the contexts of genetic mutations. The normally short lived *gas-1* mutant lives twice as long on 100 μ M FUdR [204], and the lifespan of the *tub-1* mutant is also extended on FUdR [203]. Taken together, the research published to date suggests that FUdR has small effects on lifespan at most commonly used doses in a wildtype genetic background, but the large

confounding effects in non-wildtype genetic backgrounds. Such “gene-environment interactions” are common in toxicology, and this observation raises concerns for employing FUdR in lifespan studies of mutant strains. Another concern is that FUdR may interact in unexpected ways with other chemicals (eg., antioxidants and lifespan-extending agents) and stressors, particularly those affecting mitochondria and mitochondrial DNA [67]. The fact that our lifespan results are generally in line with those previously published, however, suggests that our mitochondria-related results may also be generally applicable.

A.6 Conclusions

Overall, our data suggest that FUdR exposure has little effect on mtDNA:nucDNA copy number ratio or steady state ATP levels. This may be a result of the long half-life of mtDNA in adult nematodes, which we report here to be between 8.2 and 13.2 days. This is encouraging with respect to the use of FUdR in lifespan and other studies. The utilization of germline-deficient strains, an alternate approach for studies in which proliferating cells are a confounder including DNA repair studies [227, 229] involves difficulties as well since the presence of germ cells clearly affects lifespan, immunity, mitochondrial biology, and fat metabolism [220, 230-233] (and our own results discussed above). Nonetheless, caution is still warranted when utilizing FUdR, because strain background, dose of FUdR, timing of exposure, and co-exposure to other chemicals or stressors are critical and may influence results. Finally, our work also

highlights the fact that different strains of *C. elegans* have substantially different mtDNA biology for reasons we do not yet understand.

Acknowledgements: We thank Samantha Hall, Lauren Donoghue and Alex Ji for their assistance with our literature search, and Kelsey Behrens for preliminary data for these experiments. This work was supported by NIEHS (R01-ES017540-01A2 and T32ES021432).

Table 4: FUdR Induced DNA Damage

Day	Temperature (°C)	FUdR (μM)	mtDNA		nucDNA	
			Lesions per 10kb	SEM	Lesions per 10kb	SEM
4	15	0	0.0364	0.1326	0.0050	0.0475
4	15	25	-0.2596	0.0818	0.0169	0.0694
4	15	400	-0.1983	0.0971	-0.1779	0.0431
8	15	0	0.0379	0.1319	0.0031	0.0339
8	15	25	-0.0627	0.1499	-0.1071	0.0367
8	15	400	-0.2467	0.1857	-0.2360	0.0772
4	20	0	0.0055	0.0495	0.0017	0.0248
4	20	25	-0.2248	0.1704	-0.0648	0.0380
4	20	400	-0.0644	0.0695	-0.1101	0.0453
8	20	0	0.0099	0.0658	0.0022	0.0285
8	20	25	-0.4868	0.1152	-0.2637	0.0687
8	20	400	-0.4116	0.0861	-0.3206	0.0948

FUdR does not cause DNA damage in wild type N2, nematodes. Damage was measured in 3 samples containing 6 worms each, and the experiment was repeated twice, resulting in an n of 6. The limit of detection of the assay is approximately 0.2 lesions per 10 kilobases at this n .

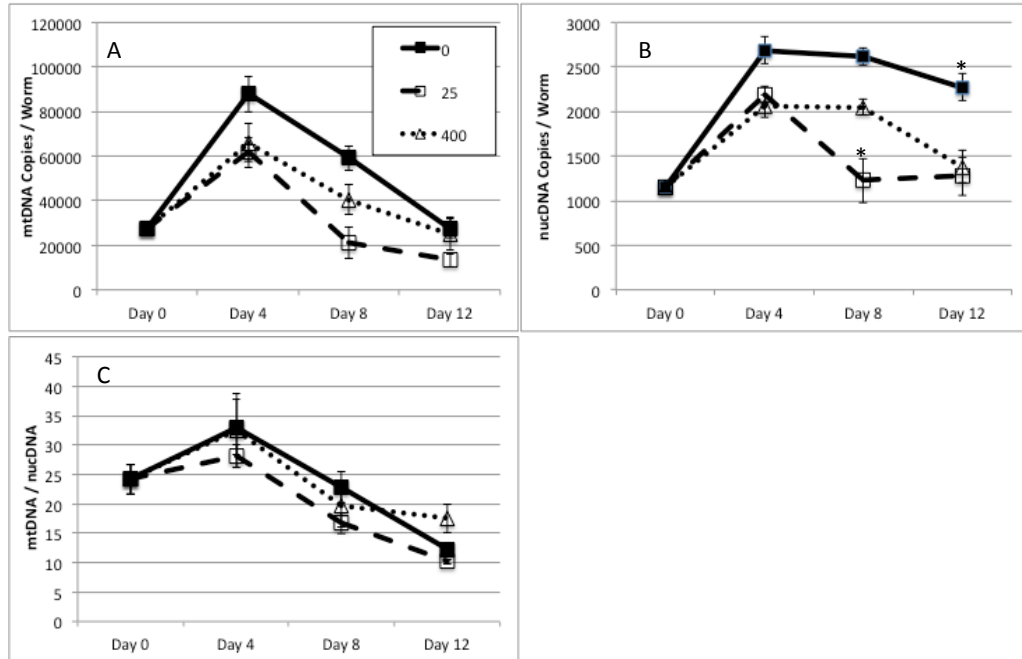


Figure 23: Effects of FUdR on mt and nuc DNA Copy Numbers in JK1107 *glp-1(q224)*

FUdR reduces both mitochondrial and nuclear copy number per worm in JK1107 *glp-1(q224)* mutants, but does not alter mt/nuc DNA ratio. **(A)** mtDNA copy number and **(B)** nucDNA copy number per worm at 0, 4, 8 and 12 days after beginning FUdR exposure. **(C)** mtDNA / nucDNA ratio at 0,4,8 and 12 days of FUdR exposure. All data are means +/- SEM from 3 separate experiments. Points with asterisks are significantly ($p < 0.05$) different from others by post-hoc Tukey's HSD test.

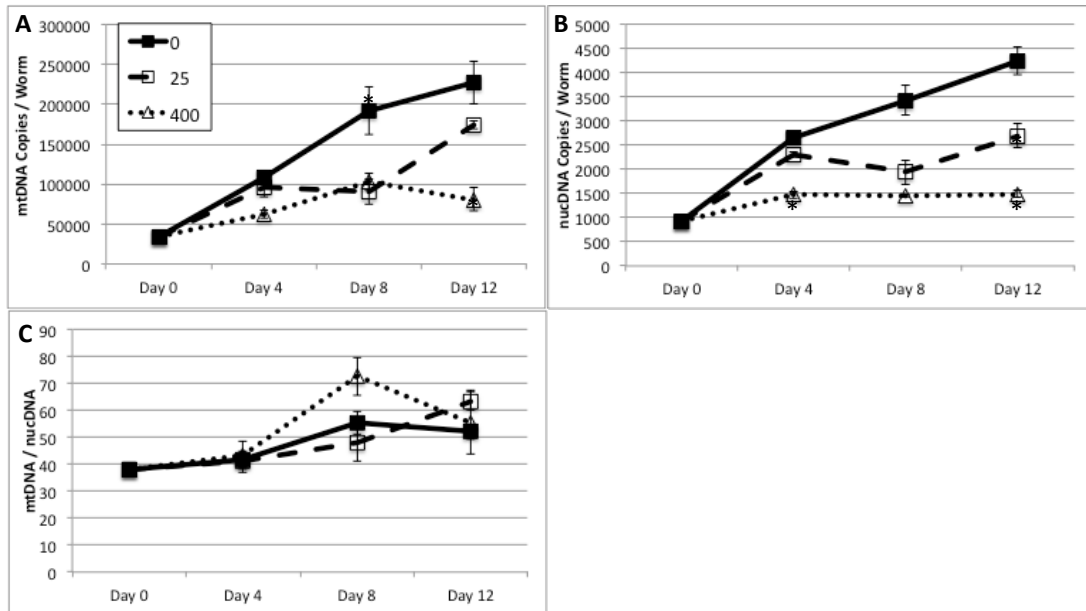


Figure 24: Effects of FUdR on mt and nuc DNA Copy Numbers in PE255 *glp-4(bn2)*

FUdR reduces both mitochondrial and nuclear copy number per worm in the PE255 *glp-4(bn2)* strain, but does not alter mt/nuc DNA ratio. (A) mtDNA copy number and (B) nucDNA copy number per worm at 0, 4, 8 and 12 days after beginning FUdR exposure. (C) mtDNA / nucDNA ratio at 0, 4, 8 and 12 days of FUdR exposure. All data are means +/- SEM from 3 separate experiments. Points with asterisks are significantly ($p < 0.05$) different from others by post-hoc Tukey's HSD test.

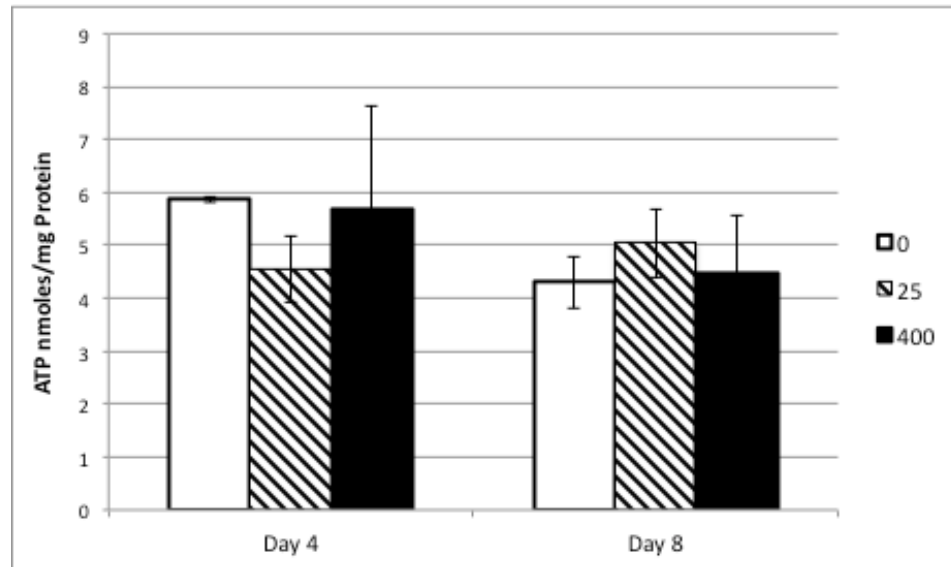


Figure 25: Steady State ATP Levels in JK1107 *glp-1(q224)*

ATP levels are unchanged as a result of exposure to either 25μM or 400μM FUDR. ATP was measured with a luciferase based assay and normalized to total protein from a matched sample. Data are means +/- SEM from 3 separate experiments.

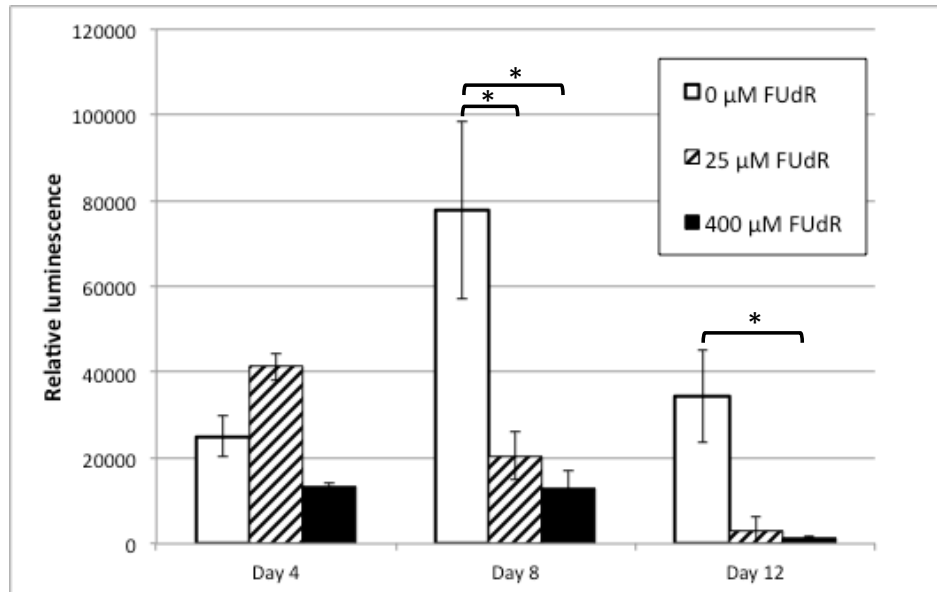


Figure 26: *In vivo* Steady State ATP Levels in PE255 *glp-4(bn2)*

FUdR significantly reduces ATP levels at both 8 and 12 days of treatment. ATP is measured as whole worm luminescence and normalized to GFP expression (see methods for more detail). Data shown are means +/- SEM from 3 separate experiments.

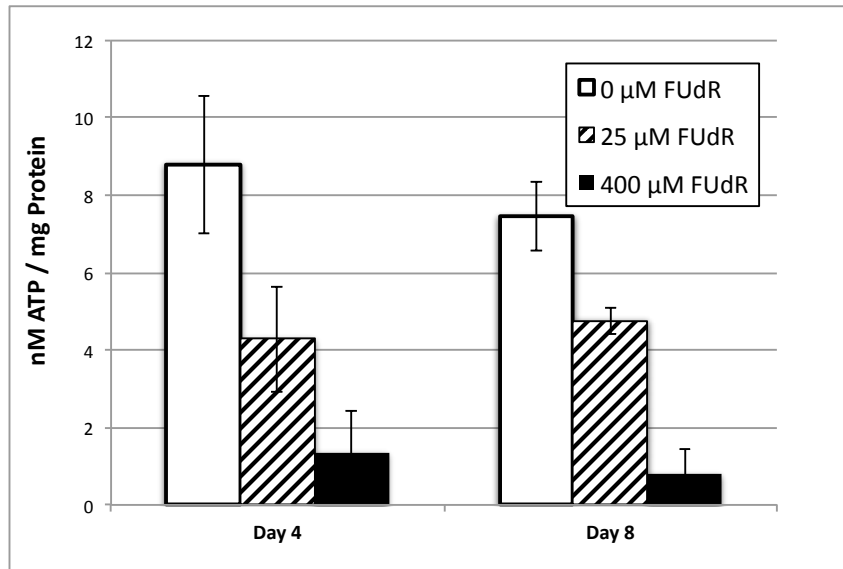


Figure 27: Steady State ATP Levels in PE255 *glp-4(bn2)*

ATP levels are reduced as a result of exposure to FUDR (main effect of treatment $p < 0.0002$). ATP was measured with a luciferase based assay and normalized to total protein from a matched sample. Data are means \pm SEM from 3 separate experiments.

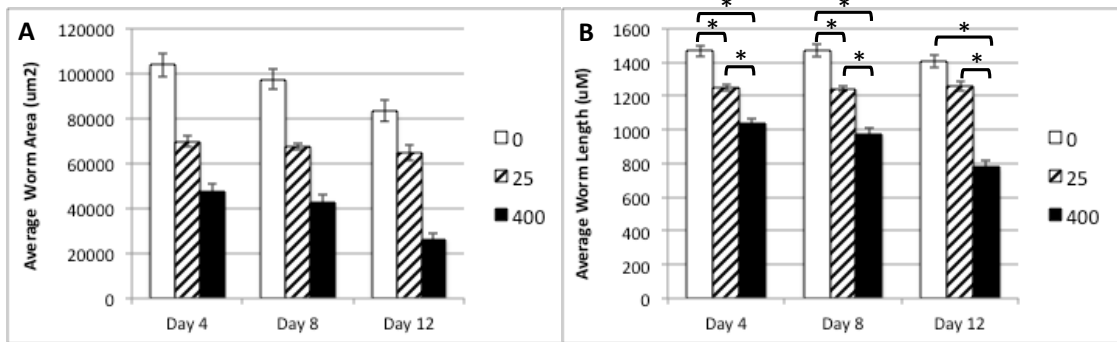


Figure 28: Effects of FUdR on Area and Length in JK1107 *glp-1(q224)*

FUdR treatment reduces both area (**A**) and length (**B**) of JK1107 *glp-1(q224)* worms. Bars connected by asterisks are significantly different ($p < 0.05$) by post-hoc Tukey's HSD test. Comparisons at each time point were not permitted for area as there was not a significant interaction between time and treatment ($p = 0.26$).

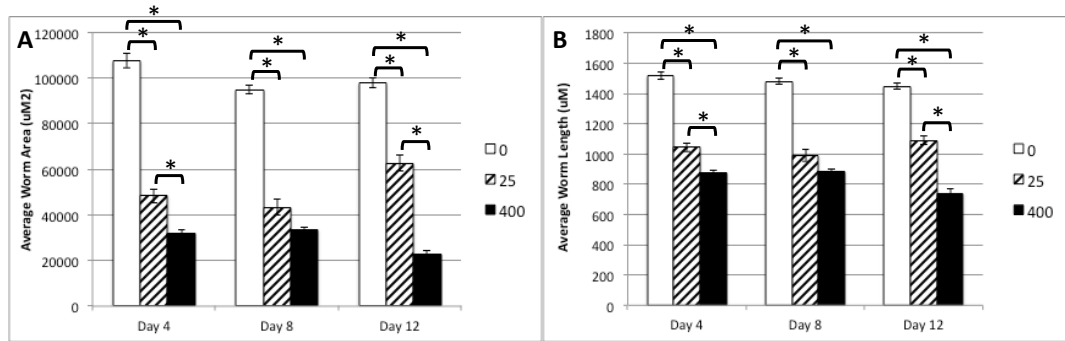


Figure 29: Effects of FUdR on Area and Length in PE255 *glp-4(bn2)*

FUdR treatment reduces both area (A) and length (B) of PE255 *glp-4(bn2)* worms. Bars connected by asterisks are significantly different ($p < 0.05$) by post-hoc Tukey's HSD test.

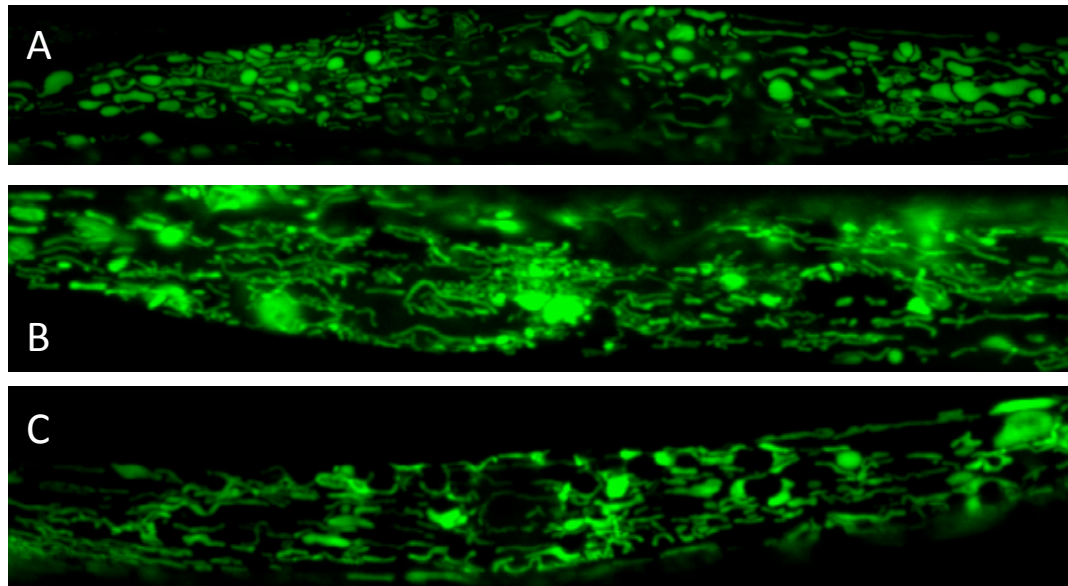


Figure 30: Mitochondrial morphology

Representative images of mitochondrial morphology at 6 days of treatment. **(A)** Control 0 μ M FUdR. **(B)** 25 μ M FUdR. **(C)** 400 μ M FUdR.

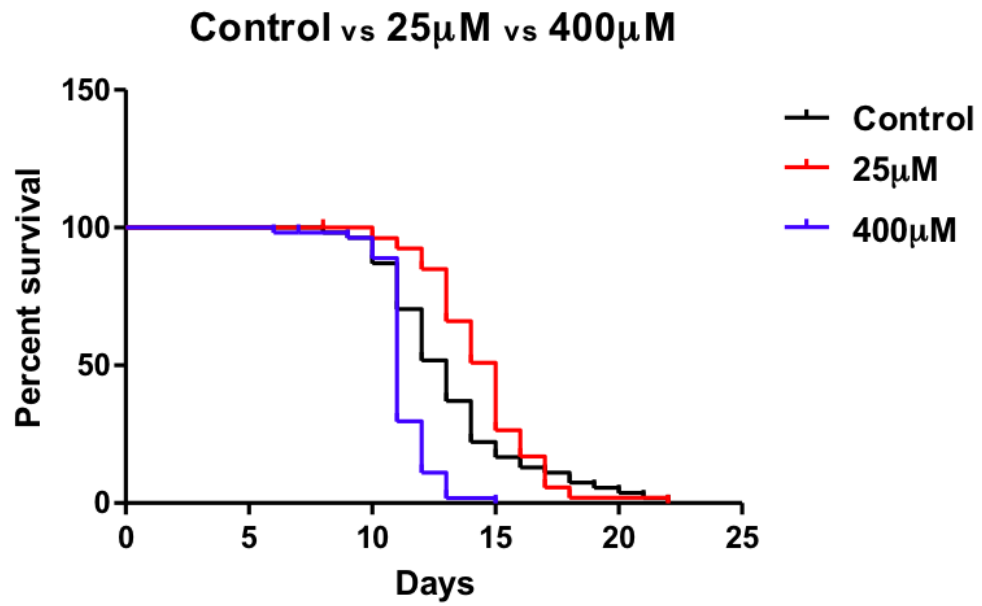


Figure 31: Lifespan

Lifespan of JK1107 *glp-1* (q224) worms exposed to 0 μ M, 25 μ M, or 400 μ M FUDR from the L3/L4 transition. n=50 in two separate experiments.

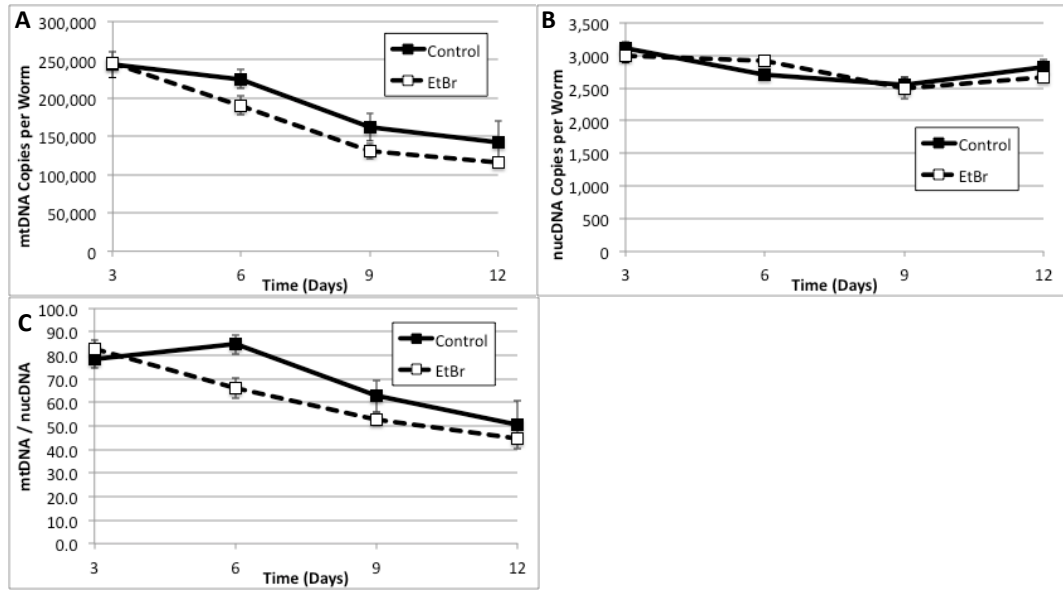


Figure 32: Determination of mtDNA Half-life in JK1107 *glp-1(q224)*

mtDNA half-life was determined by measuring the rate of decrease of mtDNA in adult nematodes in the presence of ethidium bromide. **(A)** mtDNA copy number per worm, **(B)** nucDNA copy number per worm, and **(C)** mtDNA / nucDNA ratio. Based on the rate of decline of mtDNA / nucDNA, the mtDNA half-life was calculated to be between 8.2 and 13.2 days.

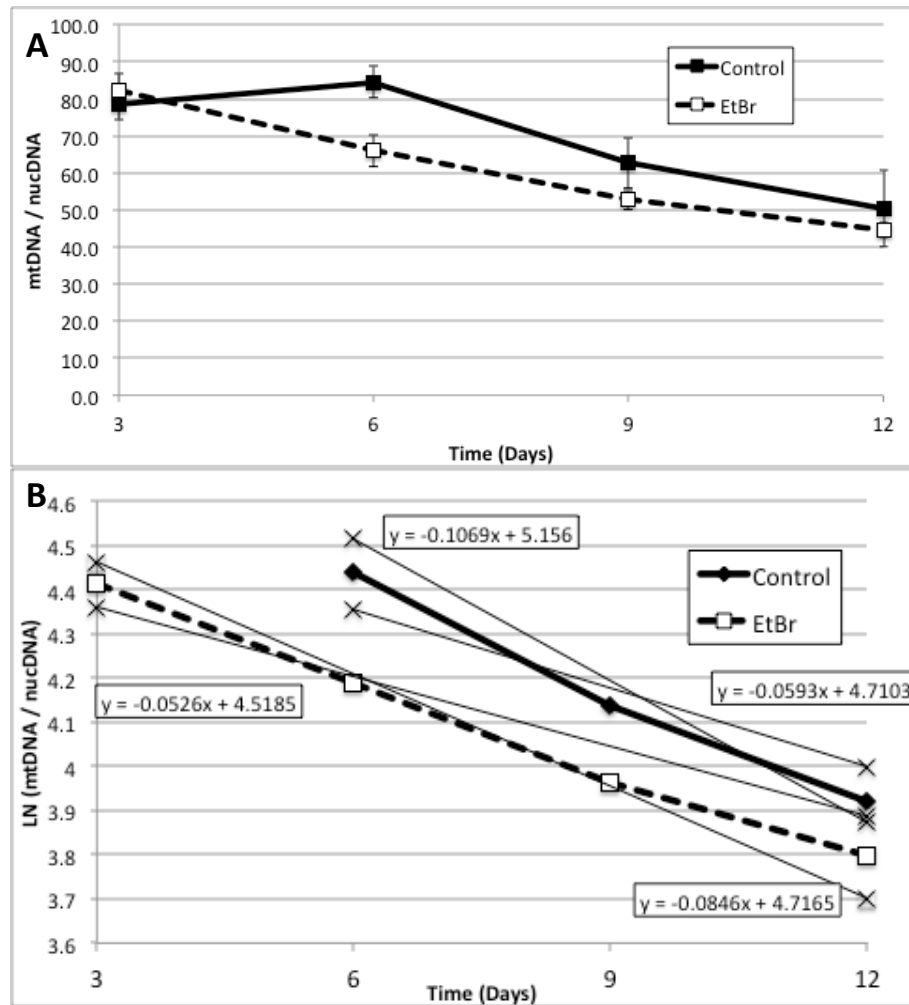


Figure 33: Determination of mtDNA Half-life in JK1107 *glp-1(q224)*

mtDNA half-life was determined by measuring the rate of decrease of mtDNA in adult nematodes in the presence of ethidium bromide. **(A)** mtDNA / nucDNA ratio. **(B)** LN (mtDNA / nucDNA) vs. time was plotted to linearize the data. Half life was calculated for each condition based on the slope of trend lines plotted +/- SEM, to achieve the largest possible difference in slopes and therefore be the most conservative estimate.

References

1. Nunnari, J. and A. Suomalainen, *Mitochondria: in sickness and in health*. Cell, 2012. **148**(6): p. 1145-59.
2. Wallace, D.C., *Mitochondrial DNA mutations in disease and aging*. Environ Mol Mutagen, 2010. **51**(5): p. 440-50.
3. Shoubridge, E.A. and T. Wai, *Mitochondrial DNA and the mammalian oocyte*. Current topics in developmental biology, 2007. **77**: p. 87-111.
4. Wai, T., D. Teoli, and E.A. Shoubridge, *The mitochondrial DNA genetic bottleneck results from replication of a subpopulation of genomes*. Nature genetics, 2008. **40**(12): p. 1484-8.
5. DiMauro, S. and E.A. Schon, *Mitochondrial respiratory-chain diseases*. The New England journal of medicine, 2003. **348**(26): p. 2656-68.
6. Schon, E.A., S. DiMauro, and M. Hirano, *Human mitochondrial DNA: roles of inherited and somatic mutations*. Nat Rev Genet, 2012. **13**(12): p. 878-90.
7. LeDoux, S.P., et al., *Repair of mitochondrial DNA after various types of DNA damage in Chinese hamster ovary cells*. Carcinogenesis, 1992. **13**(11): p. 1967-73.
8. Sancar, A., et al., *Molecular mechanisms of mammalian DNA repair and the DNA damage checkpoints*. Annu Rev Biochem, 2004. **73**: p. 39-85.
9. Bess, A.S., et al., *Mitochondrial dynamics and autophagy aid in removal of persistent mitochondrial DNA damage in Caenorhabditis elegans*. Nucleic acids research, 2012. **40**(16): p. 7916-31.
10. Bess, A.S., et al., *UVC-Induced Mitochondrial Degradation via Autophagy Correlates with mtDNA Damage Removal in Primary Human Fibroblasts*. Journal of biochemical and molecular toxicology, 2012.
11. Leung, M.C., et al., *Effects of early life exposure to ultraviolet C radiation on mitochondrial DNA content, transcription, ATP production, and oxygen consumption in developing Caenorhabditis elegans*. BMC pharmacology & toxicology, 2013. **14**: p. 9.

12. Kasiviswanathan, R., et al., *Human mitochondrial DNA polymerase gamma exhibits potential for bypass and mutagenesis at UV-induced cyclobutane thymine dimers*. The Journal of biological chemistry, 2012. **287**(12): p. 9222-9.
13. Storey, K.B., *Functional metabolism : regulation and adaptation*. 2004, Hoboken, N.J.: John Wiley & Sons. xvii, 594 p.
14. Calvo, S.E. and V.K. Mootha, *The mitochondrial proteome and human disease*. Annual review of genomics and human genetics, 2010. **11**: p. 25-44.
15. Lehninger, A.L., D.L. Nelson, and M.M. Cox, *Lehninger principles of biochemistry*. 4th ed. 2005, New York: W.H. Freeman.
16. Tait, S.W. and D.R. Green, *Mitochondria and cell death: outer membrane permeabilization and beyond*. Nat Rev Mol Cell Biol, 2010. **11**(9): p. 621-32.
17. Stryer, L., *Biochemistry*. 4th ed. 1995, New York: W.H. Freeman. xxxiv, 1064 p.
18. Papa, S., et al., *The oxidative phosphorylation system in mammalian mitochondria*. Advances in experimental medicine and biology, 2012. **942**: p. 3-37.
19. Garesse, R. and C.G. Vallejo, *Animal mitochondrial biogenesis and function: a regulatory cross-talk between two genomes*. Gene, 2001. **263**(1-2): p. 1-16.
20. Houtkooper, R.H., et al., *Mitonuclear protein imbalance as a conserved longevity mechanism*. Nature, 2013. **497**(7450): p. 451-7.
21. Murphy, M.P., *How mitochondria produce reactive oxygen species*. The Biochemical journal, 2009. **417**(1): p. 1-13.
22. Han, D., E. Williams, and E. Cadenas, *Mitochondrial respiratory chain-dependent generation of superoxide anion and its release into the intermembrane space*. Biochem J, 2001. **353**(Pt 2): p. 411-6.
23. Yakes, F.M. and B. Van Houten, *Mitochondrial DNA damage is more extensive and persists longer than nuclear DNA damage in human cells following oxidative stress*. Proceedings of the National Academy of Sciences of the United States of America, 1997. **94**(2): p. 514-9.
24. Cooke, M.S., et al., *Oxidative DNA damage: mechanisms, mutation, and disease*. FASEB J, 2003. **17**(10): p. 1195-214.

25. Berlett, B.S. and E.R. Stadtman, *Protein oxidation in aging, disease, and oxidative stress*. J Biol Chem, 1997. **272**(33): p. 20313-6.
26. Halliwell, B. and S. Chirico, *Lipid peroxidation: its mechanism, measurement, and significance*. Am J Clin Nutr, 1993. **57**(5 Suppl): p. 715S-724S; discussion 724S-725S.
27. Wei, Y.H. and H.C. Lee, *Oxidative stress, mitochondrial DNA mutation, and impairment of antioxidant enzymes in aging*. Experimental biology and medicine, 2002. **227**(9): p. 671-82.
28. Andreyev, A.Y., Y.E. Kushnareva, and A.A. Starkov, *Mitochondrial metabolism of reactive oxygen species*. Biochemistry (Mosc), 2005. **70**(2): p. 200-14.
29. Liochev, S.I., *Reactive oxygen species and the free radical theory of aging*. Free Radic Biol Med, 2013. **60**: p. 1-4.
30. McCord, J.M. and I. Fridovich, *Superoxide dismutase. An enzymic function for erythrocuprein (hemocuprein)*. J Biol Chem, 1969. **244**(22): p. 6049-55.
31. Harman, D., *Aging: a theory based on free radical and radiation chemistry*. J Gerontol, 1956. **11**(3): p. 298-300.
32. Lapointe, J. and S. Hekimi, *When a theory of aging ages badly*. Cell Mol Life Sci, 2010. **67**(1): p. 1-8.
33. Hekimi, S., J. Lapointe, and Y. Wen, *Taking a "good" look at free radicals in the aging process*. Trends Cell Biol, 2011. **21**(10): p. 569-76.
34. Van Raamsdonk, J.M. and S. Hekimi, *Deletion of the mitochondrial superoxide dismutase sod-2 extends lifespan in Caenorhabditis elegans*. PLoS Genet, 2009. **5**(2): p. e1000361.
35. Doonan, R., et al., *Against the oxidative damage theory of aging: superoxide dismutases protect against oxidative stress but have little or no effect on life span in Caenorhabditis elegans*. Genes Dev, 2008. **22**(23): p. 3236-41.
36. Lee, S.J., A.B. Hwang, and C. Kenyon, *Inhibition of respiration extends C. elegans life span via reactive oxygen species that increase HIF-1 activity*. Curr Biol, 2010. **20**(23): p. 2131-6.

37. Storz, P., *Reactive oxygen species-mediated mitochondria-to-nucleus signaling: a key to aging and radical-caused diseases*. Science's STKE : signal transduction knowledge environment, 2006. **2006**(332): p. re3.
38. Raineri, I., et al., *Strain-dependent high-level expression of a transgene for manganese superoxide dismutase is associated with growth retardation and decreased fertility*. Free Radic Biol Med, 2001. **31**(8): p. 1018-30.
39. Hernandez-Garcia, D., et al., *Reactive oxygen species: A radical role in development?* Free Radic Biol Med, 2010. **49**(2): p. 130-43.
40. Cree, L.M., et al., *A reduction of mitochondrial DNA molecules during embryogenesis explains the rapid segregation of genotypes*. Nature genetics, 2008. **40**(2): p. 249-54.
41. Sato, M. and K. Sato, *Degradation of paternal mitochondria by fertilization-triggered autophagy in C. elegans embryos*. Science, 2011. **334**(6059): p. 1141-4.
42. Sato, M. and K. Sato, *Maternal inheritance of mitochondrial DNA: degradation of paternal mitochondria by allogeneic organelle autophagy, allophagy*. Autophagy, 2012. **8**(3): p. 424-5.
43. Kukat, C., et al., *Super-resolution microscopy reveals that mammalian mitochondrial nucleoids have a uniform size and frequently contain a single copy of mtDNA*. Proceedings of the National Academy of Sciences of the United States of America, 2011. **108**(33): p. 13534-9.
44. Alam, T.I., et al., *Human mitochondrial DNA is packaged with TFAM*. Nucleic acids research, 2003. **31**(6): p. 1640-5.
45. Parisi, M.A. and D.A. Clayton, *Similarity of human mitochondrial transcription factor 1 to high mobility group proteins*. Science, 1991. **252**(5008): p. 965-9.
46. Shi, Y., et al., *Mammalian transcription factor A is a core component of the mitochondrial transcription machinery*. Proc Natl Acad Sci U S A, 2012. **109**(41): p. 16510-5.
47. Sumitani, M., et al., *Biochemical properties of Caenorhabditis elegans HMG-5, a regulator of mitochondrial DNA*. J Biochem, 2011. **149**(5): p. 581-9.
48. Wallace, D.C., *Mitochondrial diseases in man and mouse*. Science, 1999. **283**(5407): p. 1482-8.

49. Yu, M., *Generation, function and diagnostic value of mitochondrial DNA copy number alterations in human cancers*. Life Sci, 2011. **89**(3-4): p. 65-71.
50. Rolo, A.P. and C.M. Palmeira, *Diabetes and mitochondrial function: role of hyperglycemia and oxidative stress*. Toxicol Appl Pharmacol, 2006. **212**(2): p. 167-78.
51. Ballinger, S.W., *Mitochondrial dysfunction in cardiovascular disease*. Free Radic Biol Med, 2005. **38**(10): p. 1278-95.
52. Coskun, P., et al., *A mitochondrial etiology of Alzheimer and Parkinson disease*. Biochim Biophys Acta, 2012. **1820**(5): p. 553-64.
53. Vander Heiden, M.G., L.C. Cantley, and C.B. Thompson, *Understanding the Warburg effect: the metabolic requirements of cell proliferation*. Science, 2009. **324**(5930): p. 1029-33.
54. Wallace, D.C., *Mitochondria and cancer*. Nat Rev Cancer, 2012. **12**(10): p. 685-98.
55. Wallace, D.C., et al., *Mitochondrial DNA mutation associated with Leber's hereditary optic neuropathy*. Science, 1988. **242**(4884): p. 1427-30.
56. Holt, I.J., A.E. Harding, and J.A. Morgan-Hughes, *Deletions of muscle mitochondrial DNA in patients with mitochondrial myopathies*. Nature, 1988. **331**(6158): p. 717-9.
57. Park, C.B. and N.G. Larsson, *Mitochondrial DNA mutations in disease and aging*. J Cell Biol, 2011. **193**(5): p. 809-18.
58. Lee, H.K., et al., *Mitochondrial dysfunction and metabolic syndrome-looking for environmental factors*. Biochimica et biophysica acta, 2010. **1800**(3): p. 282-9.
59. Lusic, A.J., A.D. Attie, and K. Reue, *Metabolic syndrome: from epidemiology to systems biology*. Nature reviews. Genetics, 2008. **9**(11): p. 819-30.
60. Chan, D.C., *Mitochondria: dynamic organelles in disease, aging, and development*. Cell, 2006. **125**(7): p. 1241-52.
61. Copeland, W.C., *Defects in mitochondrial DNA replication and human disease*. Critical reviews in biochemistry and molecular biology, 2012. **47**(1): p. 64-74.
62. Zuchner, S., et al., *Mutations in the mitochondrial GTPase mitofusin 2 cause Charcot-Marie-Tooth neuropathy type 2A*. Nature genetics, 2004. **36**(5): p. 449-51.

63. Alexander, C., et al., *OPA1, encoding a dynamin-related GTPase, is mutated in autosomal dominant optic atrophy linked to chromosome 3q28*. *Nature genetics*, 2000. **26**(2): p. 211-5.
64. Suomalainen, A. and P. Isohanni, *Mitochondrial DNA depletion syndromes--many genes, common mechanisms*. *Neuromuscular disorders : NMD*, 2010. **20**(7): p. 429-37.
65. Kraytsberg, Y., et al., *Mitochondrial DNA deletions are abundant and cause functional impairment in aged human substantia nigra neurons*. *Nat Genet*, 2006. **38**(5): p. 518-20.
66. Bender, A., et al., *High levels of mitochondrial DNA deletions in substantia nigra neurons in aging and Parkinson disease*. *Nat Genet*, 2006. **38**(5): p. 515-7.
67. Meyer, J.N., et al., *Mitochondria as a target of environmental toxicants*. *Toxicological sciences : an official journal of the Society of Toxicology*, 2013. **134**(1): p. 1-17.
68. Berneburg, M., et al., *'To repair or not to repair - no longer a question': repair of mitochondrial DNA shielding against age and cancer*. *Exp Dermatol*, 2006. **15**(12): p. 1005-15.
69. Larsen, N.B., M. Rasmussen, and L.J. Rasmussen, *Nuclear and mitochondrial DNA repair: similar pathways?* *Mitochondrion*, 2005. **5**(2): p. 89-108.
70. Clayton, D.A., J.N. Doda, and E.C. Friedberg, *The absence of a pyrimidine dimer repair mechanism in mammalian mitochondria*. *Proc Natl Acad Sci U S A*, 1974. **71**(7): p. 2777-81.
71. Backer, J.M. and I.B. Weinstein, *Mitochondrial DNA is a major cellular target for a dihydrodiol-epoxide derivative of benzo[a]pyrene*. *Science*, 1980. **209**(4453): p. 297-9.
72. Jung, D., et al., *Effects of benzo[a]pyrene on mitochondrial and nuclear DNA damage in Atlantic killifish (*Fundulus heteroclitus*) from a creosote-contaminated and reference site*. *Aquat Toxicol*, 2009. **95**(1): p. 44-51.
73. Lewis, W. and M.C. Dalakas, *Mitochondrial toxicity of antiviral drugs*. *Nat Med*, 1995. **1**(5): p. 417-22.
74. Kohler, J.J. and W. Lewis, *A brief overview of mechanisms of mitochondrial toxicity from NRTIs*. *Environ Mol Mutagen*, 2007. **48**(3-4): p. 166-72.

75. Lewis, W., B.J. Day, and W.C. Copeland, *Mitochondrial toxicity of NRTI antiviral drugs: an integrated cellular perspective*. *Nat Rev Drug Discov*, 2003. **2**(10): p. 812-22.
76. Martin, A.M., et al., *Accumulation of mitochondrial DNA mutations in human immunodeficiency virus-infected patients treated with nucleoside-analogue reverse-transcriptase inhibitors*. *Am J Hum Genet*, 2003. **72**(3): p. 549-60.
77. Blanche, S., et al., *Persistent mitochondrial dysfunction and perinatal exposure to antiretroviral nucleoside analogues*. *Lancet*, 1999. **354**(9184): p. 1084-9.
78. Poirier, M.C., et al., *Fetal consequences of maternal antiretroviral nucleoside reverse transcriptase inhibitor use in human and nonhuman primate pregnancy*. *Curr Opin Pediatr*, 2015. **27**(2): p. 233-9.
79. Johnson, R.F., et al., *Genetic mutations and aminoglycoside-induced ototoxicity in neonates*. *Otolaryngology--head and neck surgery : official journal of American Academy of Otolaryngology-Head and Neck Surgery*, 2010. **142**(5): p. 704-7.
80. Guan, M.X., *Mitochondrial 12S rRNA mutations associated with aminoglycoside ototoxicity*. *Mitochondrion*, 2011. **11**(2): p. 237-45.
81. Kirkman, M.A., et al., *Gene-environment interactions in Leber hereditary optic neuropathy*. *Brain : a journal of neurology*, 2009. **132**(Pt 9): p. 2317-26.
82. Cline, S.D., *Mitochondrial DNA damage and its consequences for mitochondrial gene expression*. *Biochimica et biophysica acta*, 2012. **1819**(9-10): p. 979-91.
83. Graziewicz, M.A., et al., *Nucleotide incorporation by human DNA polymerase gamma opposite benzo[a]pyrene and benzo[c]phenanthrene diol epoxide adducts of deoxyguanosine and deoxyadenosine*. *Nucleic Acids Res*, 2004. **32**(1): p. 397-405.
84. Friedberg, E.C., *DNA repair and mutagenesis*. 2nd ed. 2006, Washington, D.C.: ASM Press. xxix, 1118 p.
85. Lagido, C., et al., *Bridging the phenotypic gap: real-time assessment of mitochondrial function and metabolism of the nematode *Caenorhabditis elegans**. *BMC Physiol*, 2008. **8**: p. 7.
86. Dillin, A., et al., *Rates of behavior and aging specified by mitochondrial function during development*. *Science*, 2002. **298**(5602): p. 2398-401.

87. Rea, S.L., N. Ventura, and T.E. Johnson, *Relationship between mitochondrial electron transport chain dysfunction, development, and life extension in Caenorhabditis elegans*. PLoS biology, 2007. 5(10): p. e259.
88. Tsang, W.Y. and B.D. Lemire, *Mitochondrial ATP synthase controls larval development cell nonautonomously in Caenorhabditis elegans*. Developmental dynamics : an official publication of the American Association of Anatomists, 2003. 226(4): p. 719-26.
89. Durieux, J., S. Wolff, and A. Dillin, *The cell-non-autonomous nature of electron transport chain-mediated longevity*. Cell, 2011. 144(1): p. 79-91.
90. Yoneda, T., et al., *Compartment-specific perturbation of protein handling activates genes encoding mitochondrial chaperones*. Journal of cell science, 2004. 117(Pt 18): p. 4055-66.
91. Martinus, R.D., et al., *Selective induction of mitochondrial chaperones in response to loss of the mitochondrial genome*. European journal of biochemistry / FEBS, 1996. 240(1): p. 98-103.
92. Zuryn, S., et al., *Mitochondrial dysfunction in Caenorhabditis elegans causes metabolic restructuring, but this is not linked to longevity*. Mechanisms of ageing and development, 2010. 131(9): p. 554-61.
93. Kuang, J. and P.R. Ebert, *The failure to extend lifespan via disruption of complex II is linked to preservation of dynamic control of energy metabolism*. Mitochondrion, 2012. 12(2): p. 280-7.
94. Yang, W. and S. Hekimi, *Two modes of mitochondrial dysfunction lead independently to lifespan extension in Caenorhabditis elegans*. Aging cell, 2010. 9(3): p. 433-47.
95. Barker, D.J., *The fetal and infant origins of adult disease*. BMJ, 1990. 301(6761): p. 1111.
96. Ravelli, G.P., Z.A. Stein, and M.W. Susser, *Obesity in young men after famine exposure in utero and early infancy*. N Engl J Med, 1976. 295(7): p. 349-53.
97. Barker, D.J., *Sir Richard Doll Lecture. Developmental origins of chronic disease*. Public Health, 2012. 126(3): p. 185-9.
98. Feil, R. and M.F. Fraga, *Epigenetics and the environment: emerging patterns and implications*. Nat Rev Genet, 2011. 13(2): p. 97-109.

99. Kiontke, K. and W. Sudhaus, *Ecology of Caenorhabditis species*. WormBook : the online review of *C. elegans* biology, 2006: p. 1-14.
100. Brenner, S., *The genetics of Caenorhabditis elegans*. Genetics, 1974. **77**(1): p. 71-94.
101. Lai, C.H., et al., *Identification of novel human genes evolutionarily conserved in Caenorhabditis elegans by comparative proteomics*. Genome research, 2000. **10**(5): p. 703-13.
102. Sulston, J.E., et al., *The embryonic cell lineage of the nematode Caenorhabditis elegans*. Developmental biology, 1983. **100**(1): p. 64-119.
103. Rea, S.L., et al., *Bacteria, yeast, worms, and flies: exploiting simple model organisms to investigate human mitochondrial diseases*. Developmental disabilities research reviews, 2010. **16**(2): p. 200-18.
104. Tsang, W.Y. and B.D. Lemire, *The role of mitochondria in the life of the nematode, Caenorhabditis elegans*. Biochimica et biophysica acta, 2003. **1638**(2): p. 91-105.
105. Breton, S., D.T. Stewart, and W.R. Hoeh, *Characterization of a mitochondrial ORF from the gender-associated mtDNAs of Mytilus spp. (Bivalvia: Mytilidae): identification of the "missing" ATPase 8 gene*. Marine genomics, 2010. **3**(1): p. 11-8.
106. Benedetti, C., et al., *Ubiquitin-like protein 5 positively regulates chaperone gene expression in the mitochondrial unfolded protein response*. Genetics, 2006. **174**(1): p. 229-39.
107. Lagido, C., et al., *Bridging the phenotypic gap: real-time assessment of mitochondrial function and metabolism of the nematode Caenorhabditis elegans*. BMC physiology, 2008. **8**: p. 7.
108. Gogvadze, V., B. Zhivotovsky, and S. Orrenius, *The Warburg effect and mitochondrial stability in cancer cells*. Molecular aspects of medicine, 2010. **31**(1): p. 60-74.
109. Reitzer, L.J., B.M. Wice, and D. Kennell, *Evidence that glutamine, not sugar, is the major energy source for cultured HeLa cells*. The Journal of biological chemistry, 1979. **254**(8): p. 2669-76.
110. Van Laar, V.S., et al., *Bioenergetics of neurons inhibit the translocation response of Parkin following rapid mitochondrial depolarization*. Human molecular genetics, 2011. **20**(5): p. 927-40.

111. King, M.P. and G. Attardi, *Human cells lacking mtDNA: repopulation with exogenous mitochondria by complementation*. *Science*, 1989. **246**(4929): p. 500-3.
112. Chandel, N.S. and P.T. Schumacker, *Cells depleted of mitochondrial DNA (rho0) yield insight into physiological mechanisms*. *FEBS Lett*, 1999. **454**(3): p. 173-6.
113. Marroquin, L.D., et al., *Circumventing the Crabtree effect: replacing media glucose with galactose increases susceptibility of HepG2 cells to mitochondrial toxicants*. *Toxicol Sci*, 2007. **97**(2): p. 539-47.
114. Tsang, W.Y. and B.D. Lemire, *Mitochondrial genome content is regulated during nematode development*. *Biochemical and Biophysical Research Communications*, 2002. **291**(1): p. 8-16.
115. Wallace, K.B., *Doxorubicin-induced cardiac mitochondrionopathy*. *Pharmacol Toxicol*, 2003. **93**(3): p. 105-15.
116. Wood, C.E., et al., *Latent carcinogenicity of early-life exposure to dichloroacetic acid in mice*. *Carcinogenesis*, 2015.
117. Hudson, M.M., et al., *Clinical ascertainment of health outcomes among adults treated for childhood cancer*. *JAMA*, 2013. **309**(22): p. 2371-81.
118. Rea, S.L., N. Ventura, and T.E. Johnson, *Relationship between mitochondrial electron transport chain dysfunction, development, and life extension in *Caenorhabditis elegans**. *PLoS Biol*, 2007. **5**(10): p. e259.
119. Mouchiroud, L., et al., *The NAD(+)/Sirtuin Pathway Modulates Longevity through Activation of Mitochondrial UPR and FOXO Signaling*. *Cell*, 2013. **154**(2): p. 430-41.
120. Rooney, J.P., et al., *Effects of 5'-fluoro-2-deoxyuridine on mitochondrial biology in *Caenorhabditis elegans**. *Exp Gerontol*, 2014. **56**: p. 69-76.
121. Lemire, B., *Mitochondrial genetics*. *WormBook : the online review of *C. elegans* biology*, 2005: p. 1-10.
122. Braeckman, B.P., et al., *Assaying metabolic activity in ageing *Caenorhabditis elegans**. *Mech Ageing Dev*, 2002. **123**(2-3): p. 105-19.
123. AG, D., *Oxidation of cytosolic NADH formed during aerobic metabolism in mammalian cells*. *Trends Biochem Sci.*, 1979. **4**: p. 171-176.

124. Tsang, W.Y., et al., *Mitochondrial respiratory chain deficiency in Caenorhabditis elegans results in developmental arrest and increased life span*. J Biol Chem, 2001. **276**(34): p. 32240-6.
125. Giglio, M.P., et al., *The manganese superoxide dismutase gene of Caenorhabditis elegans*. Biochem Mol Biol Int, 1994. **33**(1): p. 37-40.
126. Suzuki, N., et al., *Cloning, sequencing and mapping of a manganese superoxide dismutase gene of the nematode Caenorhabditis elegans*. DNA Res, 1996. **3**(3): p. 171-4.
127. Hunter, T., W.H. Bannister, and G.J. Hunter, *Cloning, expression, and characterization of two manganese superoxide dismutases from Caenorhabditis elegans*. J Biol Chem, 1997. **272**(45): p. 28652-9.
128. Larsen, P.L., *Aging and resistance to oxidative damage in Caenorhabditis elegans*. Proc Natl Acad Sci U S A, 1993. **90**(19): p. 8905-9.
129. Fujii, M., et al., *A novel superoxide dismutase gene encoding membrane-bound and extracellular isoforms by alternative splicing in Caenorhabditis elegans*. DNA Res, 1998. **5**(1): p. 25-30.
130. Donoghue, L., *Consequences of Persistent Mitochondrial DNA Damage Under Conditions of Increased Oxidative Stress in Department of Environmental Sciences and Engineering*. 2014, Gillings School of Global Public Health at the University of North Carolina at Chapel Hill.
131. Kayser, E.B., et al., *Mitochondrial expression and function of GAS-1 in Caenorhabditis elegans*. J Biol Chem, 2001. **276**(23): p. 20551-8.
132. Kayser, E.B., M.M. Sedensky, and P.G. Morgan, *The effects of complex I function and oxidative damage on lifespan and anesthetic sensitivity in Caenorhabditis elegans*. Mech Ageing Dev, 2004. **125**(6): p. 455-64.
133. Ishii, N., et al., *A mutation in succinate dehydrogenase cytochrome b causes oxidative stress and ageing in nematodes*. Nature, 1998. **394**(6694): p. 694-7.
134. Ishii, N., et al., *A methyl viologen-sensitive mutant of the nematode Caenorhabditis elegans*. Mutat Res, 1990. **237**(3-4): p. 165-71.
135. An, J.H. and T.K. Blackwell, *SKN-1 links C. elegans mesendodermal specification to a conserved oxidative stress response*. Genes Dev, 2003. **17**(15): p. 1882-93.

136. Lin, K., et al., *daf-16: An HNF-3/forkhead family member that can function to double the life-span of Caenorhabditis elegans*. Science, 1997. **278**(5341): p. 1319-22.
137. Murphy, C.T., et al., *Genes that act downstream of DAF-16 to influence the lifespan of Caenorhabditis elegans*. Nature, 2003. **424**(6946): p. 277-83.
138. Ogg, S., et al., *The Fork head transcription factor DAF-16 transduces insulin-like metabolic and longevity signals in C. elegans*. Nature, 1997. **389**(6654): p. 994-9.
139. Castello, P.R., D.A. Drechsel, and M. Patel, *Mitochondria are a major source of paraquat-induced reactive oxygen species production in the brain*. J Biol Chem, 2007. **282**(19): p. 14186-93.
140. Sohal, R.S. and R. Weindruch, *Oxidative stress, caloric restriction, and aging*. Science, 1996. **273**(5271): p. 59-63.
141. Schmitt, M.W., et al., *Detection of ultra-rare mutations by next-generation sequencing*. Proc Natl Acad Sci U S A, 2012. **109**(36): p. 14508-13.
142. Kennedy, S.R., et al., *Ultra-sensitive sequencing reveals an age-related increase in somatic mitochondrial mutations that are inconsistent with oxidative damage*. PLoS Genet, 2013. **9**(9): p. e1003794.
143. Vafai, S.B. and V.K. Mootha, *Mitochondrial disorders as windows into an ancient organelle*. Nature, 2012. **491**(7424): p. 374-83.
144. Menzies, R.A. and P.H. Gold, *The turnover of mitochondria in a variety of tissues of young adult and aged rats*. J Biol Chem, 1971. **246**(8): p. 2425-9.
145. Lipsky, N.G. and P.L. Pedersen, *Mitochondrial turnover in animal cells. Half-lives of mitochondria and mitochondrial subfractions of rat liver based on [¹⁴C]bicarbonate incorporation*. J Biol Chem, 1981. **256**(16): p. 8652-7.
146. Kai, Y., et al., *Rapid and random turnover of mitochondrial DNA in rat hepatocytes of primary culture*. Mitochondrion, 2006. **6**(6): p. 299-304.
147. Shokolenko, I., et al., *Oxidative stress induces degradation of mitochondrial DNA*. Nucleic Acids Res, 2009. **37**(8): p. 2539-48.
148. Brand, M.D., *The proton leak across the mitochondrial inner membrane*. Biochim Biophys Acta, 1990. **1018**(2-3): p. 128-33.

149. Enerback, S., et al., *Mice lacking mitochondrial uncoupling protein are cold-sensitive but not obese*. *Nature*, 1997. **387**(6628): p. 90-4.
150. Brand, M.D., *Uncoupling to survive? The role of mitochondrial inefficiency in ageing*. *Exp Gerontol*, 2000. **35**(6-7): p. 811-20.
151. Pfeiffer, M., et al., *Caenorhabditis elegans UCP4 protein controls complex II-mediated oxidative phosphorylation through succinate transport*. *J Biol Chem*, 2011. **286**(43): p. 37712-20.
152. Echtay, K.S., et al., *Superoxide activates mitochondrial uncoupling proteins*. *Nature*, 2002. **415**(6867): p. 96-9.
153. Jastroch, M., et al., *Mitochondrial proton and electron leaks*. *Essays Biochem*, 2010. **47**: p. 53-67.
154. Lemire, B.D., et al., *C. elegans longevity pathways converge to decrease mitochondrial membrane potential*. *Mech Ageing Dev*, 2009. **130**(7): p. 461-5.
155. Brand, M.D., et al., *The basal proton conductance of mitochondria depends on adenine nucleotide translocase content*. *Biochem J*, 2005. **392**(Pt 2): p. 353-62.
156. Rydstrom, J., *Evidence for a proton-dependent regulation of mitochondrial nicotinamide-nucleotide transhydrogenase*. *Eur J Biochem*, 1974. **45**(1): p. 67-76.
157. Meredith, M.J. and D.J. Reed, *Status of the mitochondrial pool of glutathione in the isolated hepatocyte*. *J Biol Chem*, 1982. **257**(7): p. 3747-53.
158. Kumsta, C., M. Thamsen, and U. Jakob, *Effects of oxidative stress on behavior, physiology, and the redox thiol proteome of Caenorhabditis elegans*. *Antioxid Redox Signal*, 2011. **14**(6): p. 1023-37.
159. Waterland, R.A. and K.B. Michels, *Epigenetic epidemiology of the developmental origins hypothesis*. *Annu Rev Nutr*, 2007. **27**: p. 363-88.
160. Simpson, V.J., T.E. Johnson, and R.F. Hammen, *Caenorhabditis elegans DNA does not contain 5-methylcytosine at any time during development or aging*. *Nucleic Acids Res*, 1986. **14**(16): p. 6711-9.
161. Greer, E.L., et al., *DNA Methylation on N(6)-Adenine in C. elegans*. *Cell*, 2015. **161**(4): p. 868-78.

162. Riedel, C.G., et al., *DAF-16 employs the chromatin remodeller SWI/SNF to promote stress resistance and longevity*. *Nat Cell Biol*, 2013. **15**(5): p. 491-501.
163. Rauthan, M., et al., *A Mutation in Caenorhabditis elegans NDUF-7 Activates the Mitochondrial Stress Response, and Prolongs Lifespan via ROS and CED-4*. G3 (Bethesda), 2015.
164. O'Rourke, E.J., et al., *C. elegans major fats are stored in vesicles distinct from lysosome-related organelles*. *Cell Metab*, 2009. **10**(5): p. 430-5.
165. Hunter, S.E., et al., *The QPCR assay for analysis of mitochondrial DNA damage, repair, and relative copy number*. *Methods*, 2010. **51**(4): p. 444-51.
166. Meyer, J.N., *QPCR: a tool for analysis of mitochondrial and nuclear DNA damage in ecotoxicology*. *Ecotoxicology*, 2010. **19**(4): p. 804-11.
167. Furda, A.M., et al., *Analysis of DNA damage and repair in nuclear and mitochondrial DNA of animal cells using quantitative PCR*. *Methods in molecular biology*, 2012. **920**: p. 111-32.
168. Bratic, I., et al., *Mitochondrial DNA level, but not active replicase, is essential for Caenorhabditis elegans development*. *Nucleic Acids Res*, 2009. **37**(6): p. 1817-28.
169. Brys, K., et al., *Disruption of insulin signalling preserves bioenergetic competence of mitochondria in ageing Caenorhabditis elegans*. *BMC Biol*, 2010. **8**: p. 91.
170. Lagido, C., et al., *Rapid sublethal toxicity assessment using bioluminescent Caenorhabditis elegans, a novel whole-animal metabolic biosensor*. *Toxicol Sci*, 2009. **109**(1): p. 88-95.
171. Robida-Stubbs, S., et al., *TOR signaling and rapamycin influence longevity by regulating SKN-1/Nrf and DAF-16/FoxO*. *Cell Metab*, 2012. **15**(5): p. 713-24.
172. Bratic, I., et al., *Mitochondrial DNA level, but not active replicase, is essential for Caenorhabditis elegans development*. *Nucleic acids research*, 2009. **37**(6): p. 1817-28.
173. Rooney, J.P., et al., *PCR based determination of mitochondrial DNA copy number in multiple species*. *Methods Mol Biol*, 2015. **1241**: p. 23-38.
174. Holt, I.J., *Zen and the art of mitochondrial DNA maintenance*. *Trends Genet*, 2010. **26**(3): p. 103-9.

175. Copeland, W.C., *The mitochondrial DNA polymerase in health and disease*. Subcell Biochem, 2010. **50**: p. 211-22.
176. Stumpf, J.D. and W.C. Copeland, *Mitochondrial DNA replication and disease: insights from DNA polymerase gamma mutations*. Cell Mol Life Sci, 2011. **68**(2): p. 219-33.
177. Stumpf, J.D. and W.C. Copeland, *MMS exposure promotes increased MtdNA mutagenesis in the presence of replication-defective disease-associated DNA polymerase gamma variants*. PLoS Genet, 2014. **10**(10): p. e1004748.
178. Detmer, S.A. and D.C. Chan, *Functions and dysfunctions of mitochondrial dynamics*. Nat Rev Mol Cell Biol, 2007. **8**(11): p. 870-9.
179. Yu-Wai-Man, P., et al., *Multi-system neurological disease is common in patients with OPA1 mutations*. Brain : a journal of neurology, 2010. **133**(Pt 3): p. 771-86.
180. Waterham, H.R., et al., *A lethal defect of mitochondrial and peroxisomal fission*. The New England journal of medicine, 2007. **356**(17): p. 1736-41.
181. Kim, I., S. Rodriguez-Enriquez, and J.J. Lemasters, *Selective degradation of mitochondria by mitophagy*. Arch Biochem Biophys, 2007. **462**(2): p. 245-53.
182. Valente, E.M., et al., *Hereditary early-onset Parkinson's disease caused by mutations in PINK1*. Science, 2004. **304**(5674): p. 1158-60.
183. Kitada, T., et al., *Mutations in the parkin gene cause autosomal recessive juvenile parkinsonism*. Nature, 1998. **392**(6676): p. 605-8.
184. Narendra, D., et al., *Parkin is recruited selectively to impaired mitochondria and promotes their autophagy*. The Journal of cell biology, 2008. **183**(5): p. 795-803.
185. Narendra, D.P., et al., *PINK1 is selectively stabilized on impaired mitochondria to activate Parkin*. PLoS biology, 2010. **8**(1): p. e1000298.
186. Lemasters, J.J., *Selective mitochondrial autophagy, or mitophagy, as a targeted defense against oxidative stress, mitochondrial dysfunction, and aging*. Rejuvenation Res, 2005. **8**(1): p. 3-5.
187. Rabinowitz, J.D. and E. White, *Autophagy and metabolism*. Science, 2010. **330**(6009): p. 1344-8.

188. Mizushima, N., et al., *Autophagy fights disease through cellular self-digestion*. *Nature*, 2008. **451**(7182): p. 1069-75.
189. Austin, J. and J. Kimble, *glp-1 is required in the germ line for regulation of the decision between mitosis and meiosis in C. elegans*. *Cell*, 1987. **51**(4): p. 589-99.
190. Falk, M.J., et al., *Mitochondrial complex I function modulates volatile anesthetic sensitivity in C. elegans*. *Curr Biol*, 2006. **16**(16): p. 1641-5.
191. Kennedy, S.R., et al., *Detecting ultralow-frequency mutations by Duplex Sequencing*. *Nat Protoc*, 2014. **9**(11): p. 2586-606.
192. Coskun, P.E., et al., *Systemic mitochondrial dysfunction and the etiology of Alzheimer's disease and down syndrome dementia*. *J Alzheimers Dis*, 2010. **20 Suppl 2**: p. S293-310.
193. Felix, M.A. and C. Braendle, *The natural history of Caenorhabditis elegans*. *Curr Biol*, 2010. **20**(22): p. R965-9.
194. Consortium, C.e.S., *Genome sequence of the nematode C. elegans: a platform for investigating biology*. *Science*, 1998. **282**(5396): p. 2012-8.
195. Kaletta, T. and M.O. Hengartner, *Finding function in novel targets: C. elegans as a model organism*. *Nat Rev Drug Discov*, 2006. **5**(5): p. 387-98.
196. Kenyon, C., et al., *A C. elegans mutant that lives twice as long as wild type*. *Nature*, 1993. **366**(6454): p. 461-4.
197. Walker, G., et al., *Dietary restriction in C. elegans: from rate-of-living effects to nutrient sensing pathways*. *Mech Ageing Dev*, 2005. **126**(9): p. 929-37.
198. Mitchell, D.H., et al., *Synchronous growth and aging of Caenorhabditis elegans in the presence of fluorodeoxyuridine*. *J Gerontol*, 1979. **34**(1): p. 28-36.
199. Cohen, S.S., et al., *The Mode of Action of 5-Fluorouracil and Its Derivatives*. *Proc Natl Acad Sci U S A*, 1958. **44**(10): p. 1004-12.
200. Bell, S. and S. Wolff, *Studies on the Mechanism of the Effect of Fluorodeoxyuridine on Chromosomes*. *Proc Natl Acad Sci U S A*, 1964. **51**: p. 195-202.
201. Hosono, R., et al., *Life span of the wild and mutant nematode Caenorhabditis elegans. Effects of sex, sterilization, and temperature*. *Exp Gerontol*, 1982. **17**(2): p. 163-72.

202. Gandhi, S., et al., *A simple method for maintaining large, aging populations of Caenorhabditis elegans*. Mech Ageing Dev, 1980. **12**(2): p. 137-50.
203. Aitlhadj, L. and S.R. Sturzenbaum, *The use of FUDR can cause prolonged longevity in mutant nematodes*. Mech Ageing Dev, 2010. **131**(5): p. 364-5.
204. Van Raamsdonk, J.M. and S. Hekimi, *FUDR causes a twofold increase in the lifespan of the mitochondrial mutant gas-1*. Mech Ageing Dev, 2011. **132**(10): p. 519-21.
205. Davies, S.K., A.M. Leroi, and J.G. Bundy, *Fluorodeoxyuridine affects the identification of metabolic responses to daf-2 status in Caenorhabditis elegans*. Mech Ageing Dev, 2012. **133**(1): p. 46-9.
206. Petes, T.D. and W.L. Fangman, *Preferential synthesis of yeast mitochondrial DNA in alpha factor-arrested cells*. Biochem Biophys Res Commun, 1973. **55**(3): p. 603-9.
207. Vanfleteren, J.R. and A. De Vreese, *The gerontogenes age-1 and daf-2 determine metabolic rate potential in aging Caenorhabditis elegans*. FASEB J, 1995. **9**(13): p. 1355-61.
208. Curbo, S., M. Johansson, and A. Karlsson, *5-Fluoro-2'-deoxyuridine has effects on mitochondria in CEM T-lymphoblast cells*. Nucleosides Nucleotides Nucleic Acids, 2004. **23**(8-9): p. 1495-8.
209. Barclay, B.J., et al., *A rapid assay for mitochondrial DNA damage and respiratory chain inhibition in the yeast Saccharomyces cerevisiae*. Environ Mol Mutagen, 2001. **38**(2-3): p. 153-8.
210. Mattoccia, L.P. and S. Roberti, *Effect of specific inhibitors on mitochondrial DNA replication in HeLa cells*. Biochem Biophys Res Commun, 1974. **60**(3): p. 875-81.
211. Singh, G., S.M. Sharkey, and R. Moorehead, *Mitochondrial DNA damage by anticancer agents*. Pharmacol Ther, 1992. **54**(2): p. 217-30.
212. Lewis, J.A. and J.T. Fleming, *Basic culture methods*. Methods Cell Biol, 1995. **48**: p. 3-29.
213. Breton, S., D.T. Stewart, and W.R. Hoeh, *Characterization of a mitochondrial ORF from the gender-associated mtDNAs of Mytilus spp. (Bivalvia: Mytilidae): identification of the "missing" ATPase 8 gene*. Mar Genomics, 2010. **3**(1): p. 11-8.

214. Golden, T.R., et al., *Dramatic age-related changes in nuclear and genome copy number in the nematode Caenorhabditis elegans*. *Aging Cell*, 2007. **6**(2): p. 179-88.
215. Wood, W.B., *The Nematode Caenorhabditis elegans*. Cold Spring Harbor monograph series. 1988, Cold Spring Harbor, N.Y.: Cold Spring Harbor Laboratory. xiii, 667 p.
216. Twig, G., et al., *Fission and selective fusion govern mitochondrial segregation and elimination by autophagy*. *EMBO J*, 2008. **27**(2): p. 433-46.
217. Batista, P.J., et al., *PRG-1 and 21U-RNAs interact to form the piRNA complex required for fertility in C. elegans*. *Mol Cell*, 2008. **31**(1): p. 67-78.
218. Das, P.P., et al., *Piwi and piRNAs act upstream of an endogenous siRNA pathway to suppress Tc3 transposon mobility in the Caenorhabditis elegans germline*. *Mol Cell*, 2008. **31**(1): p. 79-90.
219. Hsin, H. and C. Kenyon, *Signals from the reproductive system regulate the lifespan of C. elegans*. *Nature*, 1999. **399**(6734): p. 362-6.
220. Arantes-Oliveira, N., et al., *Regulation of life-span by germ-line stem cells in Caenorhabditis elegans*. *Science*, 2002. **295**(5554): p. 502-5.
221. Mendenhall, A.R., et al., *Reduction in ovulation or male sex phenotype increases long-term anoxia survival in a daf-16-independent manner in Caenorhabditis elegans*. *Physiol Genomics*, 2009. **36**(3): p. 167-78.
222. Angeli, S., et al., *A DNA synthesis inhibitor is protective against proteotoxic stressors via modulation of fertility pathways in Caenorhabditis elegans*. *Aging (Albany NY)*, 2013. **5**(10): p. 759-69.
223. Bogenhagen, D. and D.A. Clayton, *Thymidylate nucleotide supply for mitochondrial DNA synthesis in mouse L-cells. Effect of 5-fluorodeoxyuridine and methotrexate in thymidine kinase plus and thymidine kinase minus cells*. *J Biol Chem*, 1976. **251**(10): p. 2938-44.
224. Bestwick, R.K., G.L. Moffett, and C.K. Mathews, *Selective expansion of mitochondrial nucleoside triphosphate pools in antimetabolite-treated HeLa cells*. *J Biol Chem*, 1982. **257**(16): p. 9300-4.

225. Gross, N.J., G.S. Getz, and M. Rabinowitz, *Apparent turnover of mitochondrial deoxyribonucleic acid and mitochondrial phospholipids in the tissues of the rat*. J Biol Chem, 1969. **244**(6): p. 1552-62.
226. Kim, T.Y., et al., *Metabolic labeling reveals proteome dynamics of mouse mitochondria*. Mol Cell Proteomics, 2012. **11**(12): p. 1586-94.
227. Boyd, W.A., et al., *Nucleotide excision repair genes are expressed at low levels and are not detectably inducible in Caenorhabditis elegans somatic tissues, but their function is required for normal adult life after UVC exposure*. Mutat Res, 2010. **683**(1-2): p. 57-67.
228. Ono, T., et al., *Human cells are protected from mitochondrial dysfunction by complementation of DNA products in fused mitochondria*. Nat Genet, 2001. **28**(3): p. 272-5.
229. Meyer, J.N., et al., *Decline of nucleotide excision repair capacity in aging Caenorhabditis elegans*. Genome Biol, 2007. **8**(5): p. R70.
230. Ermolaeva, M.A., et al., *DNA damage in germ cells induces an innate immune response that triggers systemic stress resistance*. Nature, 2013. **501**(7467): p. 416-20.
231. Lapiere, L.R., et al., *Autophagy genes are required for normal lipid levels in C. elegans*. Autophagy, 2013. **9**(3): p. 278-86.
232. Alper, S., et al., *The Caenorhabditis elegans germ line regulates distinct signaling pathways to control lifespan and innate immunity*. J Biol Chem, 2010. **285**(3): p. 1822-8.
233. Wang, M.C., E.J. O'Rourke, and G. Ruvkun, *Fat metabolism links germline stem cells and longevity in C. elegans*. Science, 2008. **322**(5903): p. 957-60.

Biography

John Patrick Rooney was born in Ballston Spa, NY, to Kathleen and Lawrence Rooney on March 17th, 1981. He received his Bachelor of Science degree, with high honors, from Rochester Institute of Technology in May of 2003.

Publications:

Gonzalez-Hunt, C, **Rooney, JP**, Ryde, IT, Anbalagan, C, Meyer, JN. PCR-based analysis of mitochondrial DNA copy number, mitochondrial DNA damage, and nuclear DNA damage. *Current Protocols*. Submitted.

Luz, AL, Smith, LL, **Rooney, JP**, Meyer, JN. Seahorse Xfe24 Extracellular Flux Analyzer-based analysis of cellular respiration in *Caenorhabditis elegans*. *Current Protocols*. Submitted.

Luz AL, **Rooney JP**, Kubik LL, Gonzalez CP, Song DH, Meyer JN. **2015**. Mitochondrial Morphology and Fundamental Parameters of the Mitochondrial Respiratory Chain Are Altered in *Caenorhabditis elegans* Strains Deficient in Mitochondrial Dynamics and Homeostasis Processes. *PLoS One* **10**(6):e0130940. PMID: 26106885

Rooney, JP, Ryde IT, Sanders LH, Howlett EH, Colton MD, Germ KE, Mayer GD, Greenamyre JT and Meyer JN. **2015**. PCR based determination of mitochondrial DNA copy number in multiple species. Methods Molecular Biology: Mitochondrial Regulation: Methods and Protocols 1241: 23-38. PMID: 25308485

Rooney, JP, Luz AL, Gonzalez-Hunt CP, Bodhicharla R, Ryde IT, Anbalagan C and Meyer JN. **2014**. Effects of 5'-fluoro-2-deoxyuridine on mitochondrial biology in *Caenorhabditis elegans*. *Exp Gerontol* 56: 69-76. PMID: 24704715

Rand AA, **Rooney JP**, Butt CM, Meyer JN, Mabury SA. **2014**. Cellular toxicity associated with exposure to perfluorinated carboxylates (PFCAs) and their metabolic precursors. *Chem Res Toxicol*. 27(1):42-50. PMID: 24299273

Meyer JN, Leung MC, **Rooney JP**, Sendoel A, Hengartner MO, Kisby GE, Bess AS. **2013**. Mitochondria as a target of environmental toxicants. *Toxicol Sci* 134(1):1-17. PMCID: PMC3693132

Leung MC, **Rooney JP**, Ryde IT, Bernal AJ, Bess AS, Crocker TL, Ji AQ, Meyer JN. **2013**. Effects of early life exposure to ultraviolet C radiation on mitochondrial DNA content, transcription, ATP production, and oxygen consumption in developing *Caenorhabditis elegans*. *BMC Pharmacol Toxicol.* 4;14:9. PMID: PMC3621653

Bess AS, Leung MC, Ryde IT, **Rooney JP**, Hinton DE, Meyer JN. **2013**. Effects of mutations in mitochondrial dynamics-related genes on the mitochondrial response to ultraviolet C radiation in developing *Caenorhabditis elegans*. *Worm.* 1;2(1):e23763. PMID: PMC3670464

Patil A, Dyavaiah M, Joseph F, **Rooney JP**, Chan CT, Dedon PC, Begley TJ. **2012**. Increased tRNA Modification and Gene-Specific Codon Usage Regulate Cell Cycle Progression During the DNA Damage Response. *Cell Cycle.*11(19):3656-65. PMID: PMC3478316

Patil A, Chan CT, Dyavaiah M, **Rooney JP**, Dedon PC, Begley TJ. **2012**. Translational Infidelity-Induced Protein Stress Results from a Deficiency in Trm9-Catalyzed tRNA Modifications. *RNA Biol.* 9(7):990-1001. PMID: PMC3495739

Dyavaiah M, **Rooney JP**, Chittur SV, Lin Q, Begley TJ. **2011**. Autophagy-Dependent Regulation of the DNA Damage Response Protein Ribonucleotide Reductase 1. *Mol Cancer Res.* (4):462-75. PMID: 21343333

Rooney JP, Patil A, Joseph F, Endres L, Begley U, Zappala M, Cunningham RP, Begley TJ. **2011**. Cross-species Functionome analysis identifies proteins associated with DNA repair, translation and aerobic respiration as conserved modulators of UV-toxicity. *Genomics.* 97(3):133-147. PMID: PMC3053583

Arita A, Zhou X, Ellen TP, Liu X, Bai J, **Rooney JP**, Kurtz A, Klein CB, Dai W, Begley TJ, Costa M. **2009**. A genome-wide deletion mutant screen identifies pathways affected by nickel sulfate in *Saccharomyces cerevisiae*. *BMC Genomics.* 15;10:524. PMID: PMC2784802

Zhou X, Arita A, Ellen TP, Liu X, Bai J, **Rooney JP**, Kurtz AD, Klein CB, Dai W, Begley TJ, Costa M. **2009**. A Genome-Wide Screen in *Saccharomyces cerevisiae* Reveals Pathways Affected by Arsenic Toxicity. *Genomics.* 94(5):294-307. PMID: PMC2763962

Rooney JP, George AD, Patil A, Begley U, Bessette E, Zappala MR, Huang X, Conklin DS, Cunningham RP, Begley TJ. **2009**. Systems Based Mapping Demonstrates

that Recovery From Alkylation Damage Requires DNA Repair, RNA Processing, and Translation Associated Networks. *Genomics*. 93(1):42-51. PMID: PMC2633870

Rooney JP, Patil A, Zappala MR, Conklin DS, Cunningham RP, Begley TJ. **2008**. A Molecular Bar-Coded DNA Repair Resource for Pooled Toxicogenomic Screens. *DNA Repair (Amst)* 7(11): 1855-68. PMID: PMC2613943

Begley U, Dyavaiah M, Patil A, **Rooney JP**, Drenzo D, Young CM, Conklin DS, Zitomer RS, Begley TJ. **2007**. Trm9-Catalyzed tRNA Modifications Link Translation to the DNA Damage Response. *Mol. Cell*. 28(5): 860-870. PMID: PMC2211415

Higgins JJ, Lombardi RQ, Pucilowska J, Jankovic J, Tan EK, **Rooney JP**. **2005**. A Variant in the HS1-BP3 Gene is Associated With Familial Essential Tremor. *Neurology* 64(3):417-21. PMID: PMC1201396

Higgins JJ, Pucilowska J, Lombardi RQ, **Rooney JP**. **2004**. A Mutation in a Novel ATP-Dependent Lon Protease Gene in a Kindred With Mild Mental Retardation. *Neurology* 63(10):1927-31. PMID: PMC1201536

Higgins JJ, Lombardi RQ, Tan EK, Jankovic J, Pucilowska J, **Rooney JP**. **2004**. Haplotype Analysis at the *ETM2* locus in a Singaporean sample with Familial Essential Tremor. *Clin Genet* 66(4):353-7. PMID: 15355439

Higgins JJ, Pucilowska J, Lombardi RQ, **Rooney JP**. **2004**. Candidate Genes for Recessive Non-Syndromic Mental Retardation on Chromosome 3p. (*MRT2A*) *Clin Genet* 65:496-500. PMID: 15151510

Higgins JJ, Jankovic J, Lombardi RQ, Pucilowska J, Tan EK, Ashizawa T, **Rooney JP**. **2004**. Haplotype Analysis at the *ETM2* Locus in American and Singaporean populations with Familial Essential Tremor. *Neurology* 62(suppl 5):A27.

Honors and Awards:

Duke University Graduate School Travel Award, 2015

Nicholas School of the Environment Student Travel Award, 2015

Duke University Chancellor's Scholarship, 2010